RAPID DETECTION OF PATHOGENS AND THEIR ANTIBIOTIC SUSCEPTIBILITY USING SIMPLE MICROFLUIDICS AND CCD IMAGING

By

Farhan Ahmad

A DISSERTATION

Submitted to
Michigan State University
in partial fulfillment of the requirements
for the degree of

DOCTOR OF PHILOSOPHY

Environmental Engineering

2011

ABSTRACT

RAPID DETECTION OF PATHOGENS AND THEIR ANTIBIOTIC SUSCEPTIBILITY USING SIMPLE MICROFLUIDICS AND CCD IMAGING

By

Farhan Ahmad

Emergence of virulent and antibiotic resistant bacterial strains is posing a serious threat to human health. In developing countries, deaths associated with infectious diseases (e.g., diarrheal pathogens) are often due to the delayed diagnostics rather than effective and economical treatment options. Gold standard methods for pathogen/resistance identification rely on either polymerase chain reaction (PCR) or culture-based approaches, which are time consuming and require either manual intervention(s) or expensive instrumentation. Microfluidic PCR-based diagnostic systems require dedicated sample processing steps, thermal cycling, and sophisticated microfabrication processes, thus are slow and expensive. Microfluidic loop-mediated isothermal amplification (LAMP) is a promising alternative as it requires simpler instrumentation and inexpensive detector due to its isothermal character and high amplicon yield. Therefore, for this dissertation, novel fluorogenic dyes were applied to isothermal genetic and cellular assays for rapid and real-time detection of pathogens and their antibiotic susceptibility by using simple microfluidics and charge-coupled device (CCD) imaging.

A critical and quantitative review on miniaturized nucleic acid amplification systems was performed for the selection of an appropriate molecular assay, low cost material for microchip, detection system, and parameters that influence the gene amplification time. Real-time fluorescence LAMP (microRT$_f$-LAMP) assays of 12 virulence genes of 6 diarrheal pathogens were performed in cyclic olefin copolymer microchips and monitored by a $1000 CCD-based

fluorescence imaging system. Application of a highly fluorogenic Syto-82 dye and CCD exposure control to microRT$_f$-LAMP assays, increased their signal-to-noise ratios by 10-fold and reduced their threshold times to 10-50-fold, providing the single DNA copy level sensitivity. A novel digital LAMP method to track the *in situ* bacterial growth by gene amplification directly from gram-negative (*Escherichia coli*) and gram positive (*Enterococcus faecalis*) bacterial cells was developed. Propidium monoazide-based LAMP assay was performed to confirm the gene amplification was only from viable cells. Digital LAMP assays were rapid (20 min) and sensitive to single cell. Cost reduction of 50-fold was achieved by using polyester material for digital LAMP assays. To reduce the time of antibiotic susceptibility testing (AST), a microchip-based dynamic method for *E. coli* growth monitoring in the presence of a membrane intercalating fluorogenic dye (FM5-95) was developed. A variety of dye concentrations and CCD exposure times were tested. A combination of 20 µg/mL FM5-95 dye and 10 s of CCD exposure provided the detection of 1×10^4 *E. coli* cells in only 60 min. MicroAST of ampicillin and tetracycline on *E. coli* strain provided the minimum inhibitory concentration (MIC) of 16 µg/mL and 1.6 µg/mL respectively, which were consistent with the MIC values reported in literature.

The methods developed for this dissertation would eliminate the requirement of complex sample preparation steps, facilitating the development of sensitive, rapid, low-cost, and integrated diagnostic systems. The methods developed here for digital LAMP and microAST when integrated on a single microfluidic chip will enable faster detection of AST in clinical settings. The overall approach of faster detection of pathogens and their antibiotic resistance based on pathogen growth in the presence of antibiotic(s) using digital LAMP directly on cells can be extended to many different fields.

ACKNOWLEDGEMENTS

I feel surprised and the same time very grateful for everything I have received in my professional life. Looking back at the past five years, they have been tough but shaped me as a different person. The perspectives and skill sets, I have developed during this training period, would certainly be useful for my future career and goals.

Any of my accomplishments during PhD would not have been possible without the help and support of my advisor, Dr. Syed A. Hashsham. I believe that thanks would not be enough for his mentorship. But still, I would like to thank him for having the confidence in me to do this work. I still remember my first oral presentation in our group meeting and the critiques that I had received from my advisor. It was due to his dedication and mentorship that helped me to grow up as a scientist and have my own vision for research. I also truly appreciate his patience and tolerance. He was always there whenever I needed him. I also thank my committee members Dr. James Tiedje, Dr. Alison Cupples and Dr. Irene Xagoraraki for their valuable suggestions and insights. I was fortunate enough to have them as my teachers. Their dedication and passion towards teaching, research, and outreach services had always motivated me. Also, my special thanks to other scientists and most importantly the best teachers, I have had at Michigan State University, Dr. Terence Marsh, Dr. Volodymyr Tarabara, Dr. Thomas Voice, Dr. Phanikumar Mantha, Dr. Jay Lennon, Dr. Edward Walker, and Dr. Russell Freed.

I would also like to thank for the all the support from Department of Civil and Environmental Engineering and Graduate School at Michigan State University for the fellowships and teaching assistantships during my PhD.

It was a pleasure to share my doctoral studies and time with wonderful people like Bob, Greg, Tiffany, Dieter, Prianca, Amanda, Maggie, Erick, Tim, and Aaron, who are very close friends now. I would specially like to thank Bob for helping me in research, Dieter for his critical comments, and Erick and Tim for useful discussions about antibiotic resistance and gene sequencing. My days in East Lansing would not have been as enjoyable without some good friends, including Rehan Baqri, Abu Hassan, Basir Ahmad, Pramod Thupaki, Kashi Telsang, Indumathy Jayamani, and Weimin Sun. I would also like to acknowledge the help of the staff in the CEE and CME office including Lori Larner, Margaret Conner, Laura Taylor, Yanlyang Pan, Joseph Nguyen, and Maryam Thompson.

Finally, and importantly, I thank my family for their selfless support. I cannot imagine going through this journey without the love and support of my wife Shazia, who has always stood beside me in sharing my difficulties and celebrating my achievements.

TABLE OF CONTENTS

LIST OF TABLES

LIST OF FIGURES

CHAPTER I

1. INTRODUCTION

1.1 Emergence of pathogens with antibiotic resistance

Emergence of virulent and antibiotic resistant (AR) bacterial strains is posing a serious threat to human health (Soto 2009; Allen et al. 2010). According to the National Institute of Allergy and Infectious Diseases, the annual treatment costs of AR infections in the U.S are $5 billon. The death rates by some of the major drug-resistant pathogens like tetracycline and methicillin-resistant *Staphylococcus aureus* (MRSA), penicillin-resistant *Streptococcus pneumoniae*, vancomycin-resistant *Enterococcus* spp., and multidrug-resistant *Mycobacterium tuberculosis* have risen drastically. Due to the consistent and excessive use of antibiotics in clinical, agricultural, and livestock settings, targeted bacterial strains have evolved novel genetic mechanisms to combat the actions of antibiotics (Nikaido 2009). Once acquired, antibiotic resistance genes (ARGs) can be transferred vertically through host cell division and horizontally to other bacterial species by transduction, conjugation, or transformation. These AR traits are not only been transferred to bacterial species in local environment but also crossing global boundaries. An example is the recent discovery of carbapenem-resistance gene (blaNDM-1) in *Klebsiella pneumoniae* and *Escherichia. coli* strains which were imported into the UK and Kenya by patients returning from the Indian subcontinent (Kumarasamy et al. 2010; Poirel et al. 2011). Another major problem is diarrheal diseases, which are the second leading cause of death, killing approximately 2.2 million people worldwide, according to World Health Organization (Craun et al. 2010a). Most of the cases of diarrheal diseases are confined to underdeveloped nations due to contamination of food/water, lack of improper sanitation and late treatment, and

poverty. Approximately 60% of diarrheal diseases are caused by pathogenic bacteria and protozoan including, *Campylobacter*, *Salmonella*, *Shigella*, *E. coli* O157:H7, *Giardia*, and *Cryptosporidium*. Emergence of ARGs in these pathogens is posing additional challenges related to their treatment (Sack et al. 1997). In many cases, deaths due to infectious diseases are because of the lack of appropriate diagnosis rather than availability of effective and economical prevention and treatment options (Yager et al. 2008). A recent estimation showed that a 100% accurate diagnostic test for tuberculosis could save at least 625,000 lives per year globally (McNerney and Daley 2011).

1.2 Gold standard methods for pathogen/resistance diagnosis

Gold standard methods for antibiotic susceptibility testing (AST) and pathogen identification rely upon culture-based approaches, e.g., broth or agar dilution, and disk diffusion, which are simple and inexpensive (Bauer et al. 1966; Stalons and Thornsberry 1975). However, they are also selective and time consuming to permit same-day diagnosis and this delays treatment and increase the risk of inappropriate use of antibiotics. Cell growth in conventional culture methods has longer lag-phase (6 h for *E. coli* by absorbance measurement) and is often limited by the depletion of nutrients and accumulation of metabolites (Groisman et al. 2005; Arora et al. 2009). Towards the goal of achieving faster AST there is a need for improvement in optical methods and development of microchip-based platforms to detect cell growth (Boedicker et al. 2008; Chen et al. 2010). Relatively faster genetic methods such as polymerase chain reaction (PCR) and loop-mediated isothermal amplification (LAMP) have been extensively applied for the detection of pathogenic microorganisms and genetic markers for resistance (Seyrig et al. 2010). However, these methods only provide the genetic profiles of the pathogens and lack the ability to confirm the phenotypic functions such as susceptibility to antibiotics.

Additionally, AR trait will only be present upon the expression of ARG(s) in the AR pathogen. Commercial instruments for AST and nucleic acid amplification/detection are highly expensive. For example, turbidity-based VITEK® 2 (Biomerieux) and fluorescence-based autoSCAN® 4 (Siemens) for AST have detection time of 24 h and costs around $70,000. Commercial PCR instruments like RAPID® System (Idaho Technologies) and RAZOR EX® Instrument (Smith Detection) takes 1-2 h and costs in the range from $30,000 to $50,000. Also the cost per assay range from $10 to $50 or higher depending on the reaction chemistry. The need for expensive instrumentation and highly trained personnel, however, currently limits their widespread use, especially in resource-poor settings.

1.3 Microfluidic-based molecular diagnostic tools

In resource-limited settings, molecular tests are commonly performed in centralized laboratories. Applications where a point-of-care (POC) genetic analysis system will provide superior capabilities compared to centralized screening are numerous. Examples include quantitative detection of viral load for human immune deficiency syndrome (Richman et al. 2009), genotyping of influenza (Van Kerkhove et al. 2011), *M. tuberculosis* with capabilities to detect drug resistance (McNerney and Daley 2011), MRSA (Klevens et al. 2007), malaria (*Plasmodium spp.*) (Feachem et al. 2010), dengue (Guzman et al. 2010), genotyping for *E. coli* O157:H7 (Craun et al. 2010b). Many of these applications also require screening for multiple agents simultaneously. In resource-limited settings, immunoassay-based diagnostic tests for these infectious agents are commonly performed due to their speed, simplicity, and low-cost, albeit having lower sensitivity than culture methods and nucleic acid-based assays. For molecular assays to become more easily accessible outside of laboratory settings, detection time, complexity of the test, instrumentation cost, and cost-per assay must be reduced.

Early on, semiconductor manufacturing technology played a significant role in the development of microchips made of silicon or glass for nucleic acid amplification. However, because silicon wafers need for sophisticated fabrication facility, high turn-around time, and are expensive, more recent efforts have shifted to a variety of polymeric materials (Fiorini and Chiu 2005; Bhattacharyya and Klapperich 2006; Tsao and DeVoe 2009; Ahmad et al. 2011; Chantiwas et al. 2011). Application of polymers in DNA amplification microchips drastically reduces the turnaround time from days to hours and cost of disposable microchips from dollars to cents. Towards the development of miniaturized nucleic acid analysis systems for the automation of steps from sample preparation through amplification reaction to result, microchips are being integrated with additional components such as pumps, valves, and detectors (Zhang et al. 2007; Liu et al. 2010). Partially integrated nucleic acid analysis systems with amplification and detection modules, based on PCR and isothermal nucleic acid amplification assays (e.g., loop-mediated isothermal amplification, LAMP) with nucleic acids as the starting material, has been extensively reported (Zhang et al. 2006; Zhang and Da 2010; Asiello and Baeumner 2011). However, seamless integration of all the analytical steps, including the onchip sample processing from pathogenic bacterial/viral cells (e.g., cell lysis, DNA extraction and purification) is only beginning to emerge (Chen et al. 2007; Park et al. 2011). Complete integration of all the analytical processes in miniaturized nucleic acid analysis systems is must for a successful POC genetic analysis device disease diagnostics (Lee et al. 2010; Chin et al. 2011; Niemz et al. 2011). MicroPCR systems required dedicated nucleic acid processing modules due to possibility of reaction inhibition by a variety of components present in raw samples. Thermal cycling time of microPCR system is dependent on thermal mass of the system, which if reduced could lead to faster gene amplification. For example, nucleic acid amplification on microPCR systems could

be performed from 90 s for a flow-through system (Kopp et al. 1998) to 6 min for a miniaturized silicon integrated heater (Neuzil et al. 2006). On the other hand microLAMP system uses simpler instrumentation due to its isothermal character and inexpensive detector due to high amplicon yield (Seyrig et al. 2010; Ahmad et al. 2011). Translation of these characteristics on microchip-based platforms is expected to lead to low-cost miniaturized molecular devices for rapid pathogen diagnosis. Development of molecular diagnostic devices for POC settings requires an approach with a goal towards speed, sensitivity, specificity, user-friendliness, robustness, and low cost.

Monitoring of nucleic acid amplification assays (e.g., PCR or isothermal variants) in microchips are commonly performed by optical detection strategies, including absorbance, fluorescence, interferometry, chemiluminescence, and surface plasmon resonance (Kuswandi et al. 2007; Myers and Lee 2008). Fluorescence sensing is most common due to its high sensitivity and selectivity as well as the commercial availability of well-established fluorophores (Schulze et al. 2009) and because fluorescence forms the cornerstone for many molecular diagnostic assays (Niemz et al. 2011). Sensitivity of optical devices is influenced by multiple parameters, including intensity of light source, fluorescence light collection efficiency, and background signal and noise. Fluorescence light collection efficiency is dependent on the light channeling components (optical fibers, filters), light collection components (lens, detector) and their assembly in the device. Inexpensive, compact and robust optical devices require low-cost, small and durable light sources. Light emitting diodes (LEDs) meet these criteria and are very well suited for diagnostic devices (Moe et al. 2005). LEDs are increasingly being used to replace conventional light sources such as lasers, and mercury and tungsten-halogen lamps. Important requirements from photon detectors are high sensitivity and signal-to-noise ratio (SNR), low

cost, and compactness. Photon detectors such as solid state photodiodes, vacuum-based photomultiplier tubes, charge-coupled devices (CCDs) are used in conventional and microchip-based optical systems (Yotter and Wilson 2003). For portable microchip-based devices, integration of intense light sources and sensitive photon detectors is critical, especially considering the minute sample volumes. This is because reduced sample volumes in the micro- to nanoliter range also translate into smaller detection volumes and a decrease in the number of analytes available for detection. The challenge in developing microchip-based detection systems is the miniaturization of the optical hardware at low cost while still maintaining the sensitivity and specificity required for interrogating molecular assays. Drastic improvements in these systems can be realized with the improvement in the quality of light sources and photon detectors and the availability of low-cost optical components. Leveraging these off-the-shelf technologies may be one of the keys to realizing POC diagnostic devices.

1.4 CCD-based imaging

Compared to spot detectors such as photodiode and photomultiplier tube, CCD has wider field-of-view, thus suitable for high throughput fluorescence imaging applications (Salmon and Waters 2011). Also due to exposure control features in CCDs, they provide more sensitive detection than simple photodiodes. CCD camera was invented at AT&T Bell Labs by Willard Boyle and George E. Smith in 1969 (Boyle and Smith 1970). A CCD is an array of light-sensing elements (pixels) arranged on a silicon substrate. The semiconductor properties of silicon allow the light sensor to trap and hold photon-induced charge carriers (photoelectrons) under appropriate electrical bias conditions. The basic light-sensing unit of the CCD is a photodiode attached with a storage area for photoelectrons (potential well). Photodiode elements of the CCD absorb the energy from incoming photons resulting into liberation of photoelectrons, and the

formation of holes within the silicon crystal lattice. A single electron-hole pair is generated from each absorbed photon. The numbers of photoelectrons generated at a particular pixel is directly proportional to the incoming light intensity. Each pixel in the sensor accumulates these charges during the imaging process. During readout, these collected charges are subsequently shifted along the transfer channels under the influence of applied voltages. Finally, an analog to digital convertor assigns a digital value to each pixel according to its voltage amplitude, creating a digital image.

Characteristics of CCD camera such as sensor architecture, spatial resolution, dynamic range, quantum efficiency, exposure time, and noise factor are the critical determinants of the quality of digital image and the resulting SNR, and detection sensitivity (Hiraoka et al. 1987; Salmon and Waters 2011). Spatial resolution of a CCD sensor is a function of the number of pixels and their size. Spatial resolution is also affected by the quality of the lens and imaging optics. Readout noise is associated with individual pixel. The total readout noise will be dependent on the total number of pixels on the CCD sensor. Therefore, the readout noise will be higher for relatively high numbers of smaller-sized pixels than low numbers of relatively larger pixels. A proper balance is needed between the required resolution and the SNR. Binning is commonly performed to increase the SNR by compromising with the spatial resolution. Binning is the process of combining pixels to form a super pixel. A binning of 2×2 means that an area of 4 adjacent pixels is combined into one larger pixel. In this case, the SNR will increase by 4 times and the resolution of the image will be reduced by half. CCDs are available with a range of pixel sizes (1.4 µm-30 µm) and pixel numbers (1-50 megapixels). For example, Kodak recently launched a full frame CCD sensor (KAF-50100) with highest number of pixels (50 megapixels) with unit pixel dimension of 6 µm × 6 µm. Sony has a 14 megapixel interline CCD sensor

(ICX681SQW) with smallest pixel dimension of 1.43 µm × 1.43 µm. Dynamic range of a CCD is a measure of two properties; i) the difference between the highest and lowest signal values, and ii) the number of steps captured between the highest and lowest values. A CCD sensor with larger dynamic range can capture faint signal without distorting its highlights in the image. Dynamic range is calculated by dividing the full well electron capacity by the readout noise. Full well electron capacity is number of total photoelectrons a pixel can hold before saturation. For example, a CCD with full well electron capacity of 55,000 per pixel and readout noise of 8 e^- will have a dynamic range of 6875. The signals lower than the readout noise (<5 e^-) will be buried in the noise, thus readout noise represents the smallest possible signal this CCD can capture. Dynamic range also represents the number of steps the CCD is capable of recording above the noise. Bit depth, which is the property of CCD's analog to digital converter, transforms those captured steps into digital format. Conversion of all the captured steps in the digital format allows the image to have clear signal. For example, a CCD with 12 bit depth and 16 bit depth will have 2^{12} (4,096) and 2^{16} (65,536) digital steps respectively. CCD with higher bit depth will capture more variations or shades in the image. CCD with 12 bit depth (4,096 digital steps) will not utilize the available dynamic range of 6875. However, a CCD with 16 bit depth (65,536 digital steps) will take full advantage of the available dynamic range. Therefore, CCD with high dynamic range is needed to capture fine gradations of intensity steps in the image. At the same time, a high bit depth is needed to convert all of those captured steps into a usable digital output. Quantum efficiency is the ability of the CCD to convert incoming photons into signal output. It is defined as the ratio of incoming photons to those actually detected in the device. Silicon has band gap energy of 1.14 electron volts. It can absorb the photons with wavelengths ranging from 400 nm-1100 nm. Silicon will be transparent to the wavelengths lower

than 400 nm (absorption by gate structures) and higher than 1100 nm (low energy for electron-hole generation). Quantum efficiency is measured over a range of different wavelengths to characterize the CCD efficiency at different photon energies. Quantum efficiency of commercially available CCDs lies between 40-50%. Exposure/integration time is directly related to the measured signal from a CCD. Scientific CCDs have exposure times from milliseconds to hours. Emission light from low sample volumes is also very low (100-1000 photons). In order to image the low signals, a high exposure is needed. It has been demonstrated that increasing the exposure time increases the SNR. However, increasing the exposure time will also increase the background signal and dark current along with the fluorescence signal. It is suggested to cool the CCD sensor for exposure time higher than 1 second. Cooled CCDs have successfully been applied to detect microchip-based chemiluminescence assays with an exposure time of 20 min (Yang et al. 2008, 2009). Noise factors are introduced during the integration and read out of an image from a CCD. Three major noise factors are shot noise, read noise and dark current (Robbins and Hadwen 2003). CCD manufactures report these noise factors as electrons root mean square or number of electrons per pixel. Shot noise is inherent to light characteristics and results from the statistical variation in the arrival rate of photons on CCD. The probability of photon arrival on a pixel is predicted by Poisson distribution. Shot noise is directly proportional to the square root of signal value. It is more apparent for low light conditions. It can be reduced by either collecting more photons (increase in exposure time) or by combining multiple frames. Readout noise is a form of electronic noise added to the final signal upon readout of the device, is independent of exposure time. Read out noise can be suppressed by binning the pixels. Dark current is a multiplicative form of noise, which is proportional to the length of the exposure time. It is caused by thermally generated electrons that build up in the pixels and depends on the

exposure time and temperature of the CCD sensor. It is the square root of the number of thermal electrons multiplied by the exposure time. It has been reported that for cooling the CCD for every 6°C will reduce the dark current by half. MEADE DSI Pro II applies a unique concept of dark frame subtraction to reduce the dark current. Dark frames are the images taken in the dark with different exposure times. During imaging, this dark frame is automatically subtracted from an image by matching the imaging exposure time with the exposure time of the stored dark frame.

Table 1.1 Comparison of the parameters of monochrome CCD cameras

Parameter	Non-cooled CCD	Cooled CCD	EMCCD
Company	Meade™	ATIK™	Proxitronic™
Model	DSI Pro	16 IC-HS	Proxi eCam 200
Sensor	Sony ICX429ALL	Sony ICX424AL	TI TC247SPD
CCD type	Interline	Interline	Interline
Pixels	752 × 582	659 × 494	658 × 496
Pixel size (µm)	8.3 × 8.6	7.4 ×7.4	10 ×10
Full well capacity (e/p)	50,000	30,000	-
ADC (bit)	16	16	14
Exposure time (ms-h)	0.1 - 1	1 - 1	0.5 - 0.04
Read noise (e)	15	7	≤ 1
Cooling (°C)	none	-20	-20
Weight (g)	283	350	500
EM gain	-	-	2000
Cost ($)	399	495	11,000

DSI Pro (MEADE™) and 16 IC-HS (ATIK™) cameras were is very similar in terms of the given specifications expect the peltier cooling in 16 IC-HS, which reduced the noise factors to half but increased the cost by $100 (Table 1.1). Another difference was the better dynamic range (4286) of 16 IC-HS than DSI Pro (3333). Electron multiplying CCD (Proxi eCam 200) was 25-times expensive than DSI Pro and 16 IC-HS. DSI Pro and 16 IC-HS were applied to

image PCR and chemiluminescence assays in microfluidic chips (Kaigala et al. 2008; Yang et al. 2008, 2009). Also, the effect of CCD exposure time on increasing SNR was demonstrated. However, these low-cost CCDs were not yet applied for monitoring microRT$_f$-LAMP assays. Therefore, we selected DSI Pro CCD to evaluate the effect of exposure time on SNR and threshold time (Tt) of microRT$_f$-LAMP assays (Ahmad et al. 2011).

1.5 Objectives

The overall goal of this dissertation research was to develop a simple platform for rapid detection of pathogens and their antibiotic susceptibility. The specific objectives are discussed below;

Objective 1: To reduce Tt of microRT$_f$-LAMP by 40% as compared to real-time PCR instrument by using a novel DNA intercalating dye and a low-cost CCD imaging system.

Hypothesis: Application of CCD exposure control to Syto-82-based microRT$_f$-LAMP may reduce Tt due to increase in the SNR by high fluorescence of Syto-82 dye and with increasing CCD exposure time (as already been shown for PCR and chemiluminescence assays).

Objective 2: To develop digital LAMP method for amplifying genetic sequences directly from bacterial cells without any processing at a moderate temperature of 63 ^{o}C.

Increase in the temperature about 50 ^{o}C slightly increases the membrane permeability of gram-negative and gram-positive bacterial cells.

Hypothesis: *In situ* LAMP may be performed, considering the successful inclusion of LAMP reaction components inside the bacterial cell even with a slight change in membrane permeability at 63 ^{o}C.

Objective 3: To develop a dynamic method of measuring cell growth/ antibiotic susceptibility and reduce the Tt to 1-2 h by using a novel cell membrane intercalating dye and low-cost CCD imaging system.

Hypothesis: Application of CCD exposure control to FM5-95-based microAST may reduce Tt due to increase in the SNR by high fluorescence of FM5-95 dye and with increasing CCD exposure time.

1.6 Organization

This dissertation is organized into six chapters focusing on various aspects of the overall project. Chapter I introduces the needs and requirements for rapid, low-cost, and simplified miniaturized systems for the diagnosis of pathogens and their antibiotic susceptibility. Chapter II presents an extensive critical review on the miniaturized molecular diagnostic systems such as microPCR and microLAMP. The main aim of this review is to understand the effect of various parameters (e.g., thermal mass and conductivity, heating/cooling rate) of the nucleic acid amplification time and the current state of these systems in terms of their advantages and limitations for POC diagnostics. This quantitative comparison of miniaturized molecular diagnostic systems is used for the selection of an appropriate nucleic acid amplification assay, microchip material, and detection system for this project. Chapter III (published) presents the development of Syto-82 dye-based LAMP assays for 12 virulence genes of 6 diarrheal pathogens, translation of these assays on microfluidic chips, and evaluation of CCD exposure

time on the SNR and threshold time of microLAMP assays. Chapter IV presents the development of novel microLAMP assays, "digital LAMP", for the genetic amplification from *E. coli* (uidA gene) and *E. faecalis* (gelE gene) cells at 63 ^{o}C without any sample processing. Chapter V evaluates a membrane intercalating dye, FM-5-95 and CCD exposure time, for the rapid detection of *E. coli* growth on microchip. The concept is also extended for the rapid testing of antibiotic sensitivity (ampicillin and tetracycline) on *E. coli*. Finally, Chapter VI presents the conclusions and future directions. The designed LAMP primer sequences are provided in the appendix at the end. Brief summary of these chapters is provided below.

Chapter II Critical evaluation of miniaturized nucleic acid amplification systems for POC diagnostics: POC genetic diagnostics critically depends on miniaturization of amplification, detection, and sequencing techniques. Isothermal amplification techniques, which are still emerging, have a better potential for POC diagnostics. Isothermal amplification techniques (e.g., LAMP) are promising for the low-cost and integrated nucleic acid analysis due to i) moderate incubation temperature leading to simplified heating and low power consumption, ii) high amount of amplification products, which can be detected visually or by simple detectors, iii) direct genetic amplification from bacterial cells due to the superior tolerance to substances that typically inhibit PCR, iv) high specificity, sensitivity up to single copy, and rapid detection in 10-20 min. LAMP assays on microfluidic chips (microLAMP) were evaluated under the World Health Organization's guidelines of POC diagnostic systems towards elimination of any instrumentation and integration of sample processing step in future. Microfluidic chips for microPCR with different materials and designs have been reported. Temperature cycling systems with varying thermal masses and conductivities, thermal cycling times, flow-rates, and cross-sectional areas, have also been developed to reduce the nucleic acid amplification time. A

quantitative critical evaluation of these factors in relation to time taken to amplify nucleic acid was not available in the current literature. An in-depth analysis of the parameters responsible for rapid nucleic acid amplification in two major types of microPCR systems (static chamber and flow-through) along with their integration with sample processing steps for sample-in-answer-out capability was presented. The major aim was to provide a better understanding of the advantages and limitations of microPCR and microLAMP systems for POC diagnostics.

Chapter III A CCD-based fluorescence imaging system for real-time loop-mediated isothermal amplification-based rapid and sensitive detection of waterborne pathogens on microchips: Rapid, sensitive, and low-cost pathogen diagnostic systems are needed for early disease diagnosis and treatment, especially in resource-limited settings. This study reports a low-cost CCD-based imaging system for rapid detection of waterborne pathogens by isothermal gene amplification in disposable microchips. Fluorescence imaging capability of this monochromatic CCD camera was evaluated by optimizing the gain, offset, and exposure time. This imaging system was validated for 12 virulence genes of major waterborne pathogens on cyclic olefin copolymer microchips, using Syto-82 dye and real-time fluorescence LAMP referred here as microRT$_f$-LAMP. SNR and Tt values of microRT$_f$-LAMP assays were compared with those from a commercial real-time polymerase chain reaction (PCR) instrument. Applying a CCD exposure of 5 s to 10^5 starting DNA copies of microRT$_f$-LAMP assays increased the SNR by 8-fold and reduced the Tt by 9.8 min in comparison to a commercial real-time PCR instrument. Additionally, single copy level sensitivity for *Campylobacter jejuni* 0414 gene was obtained for microRT$_f$-LAMP with a Tt of 19 min, which was half the time of the real-time PCR instrument. Due to the control over the exposure time and the wide field imaging capability of CCD, this

low-cost fluorescence imaging system has the potential for rapid and parallel detection of pathogenic microorganisms in high throughput microfluidic chips.

Chapter IV Digital LAMP for rapid and sensitive genetic amplification of gram-negative and gram-positive bacteria with no sample processing: An isothermal method for gene amplification directly from gram-negative (*Escherichia coli*) and gram positive (*Enterococcus faecalis*) bacterial cells at 63 ^{o}C with most probable number (MPN) approach leading to the concept of "digital LAMP" is reported. RT_f-LAMP assays (from 10^5 cells to single cell) of *E. coli* (uidA gene) and *E. faecalis* (gelE gene) were successfully performed by directly incubating the cells at 63 ^{0}C (without any prior processing) on a commercial PCR instrument. Threshold time values of RT_f-LAMP assays of bacterial cells, heat treated bacterial cells (95 ^{o}C for 5 min), and their purified genomic DNA templates were similar, implying that DNA could be amplified either by lysis or permeabilization of bacterial cells at 63 ^{o}C. Gene amplification from viable *E. faecalis* cells was confirmed by performing propidium monoazide (PMA)-RT_f-LAMP assays. Single cell-based RT_f-LAMP assays were also translated on polymeric microchips (microRT_f-LAMP) and monitored by a low-cost fluorescence imaging system. MicroRT_f-LAMP assays provided SNR ratio between 500- to 800, sensitivity of single cell, and detection time of approximately 20 min. Endpoint microLAMP assays were performed from 10^5 bacterial cells to 0.01 bacterial cell in digital format for MPN analysis. MPN values from digital LAMP assays confirmed the genetic amplification were from single cell. Direct gene amplification from bacterial cells at 63 ^{o}C would eliminate the requirement of complex sample preparation steps,

facilitating the development of sensitive, rapid, low-cost, and integrated POC diagnostic systems. In addition, rapid digital LAMP has the potential to replace conventional MPN method.

Chapter V Rapid and sensitive detection of the growth of *Escherichia coli* and antibiotic susceptibility testing on microchip: Real-time growth monitoring of *E. coli* at 37 ^{0}C in the presence of a membrane intercalating FM dye, by using a low-cost microchip and CCD imaging system is reported. Various concentrations of FM5-95 dye (1 µg/mL-50 µg/mL) and two different CCD exposure times (1 s and 10 s) were tested towards the rapid detection of *E. coli* growth. A combination of 20 µg/mL FM5-95 dye and 10 s of CCD exposure time provided the detection of 10^{4} *E. coli* in only 1 h. Highest concentration of FM5-95 (50 µg/mL) inhibited the *E. coli* growth. Sensitivity of the cell growth assay was tested with the dilution series of *E. coli* from 10^{4} to 1 cell. The assay was sensitive to single cell with a detection time of 5 h. Antibiotic sensitivity of ampicillin and tetracycline on this *E coli* strain was also tested. MIC values of ampicillin and tetracycline were 16 µg/mL and 1.6 µg/mL respectively, which were also consistent with the literature values. This method would be useful for high throughput, rapid and real-time monitoring of bacterial growth for their AST.

REFERENCES

1.7 References

Ahmad F, Seyrig G, Stedtfeld RD, Tourlousse DM, Tiedje JM, Hashsham SA (2011) A CCD-based fluorescence imaging system for real-time loop-mediated isothermal amplification-based rapid and sensitive detection of waterborne pathogens on microchips. Biomedical Microdevices 13:929-937

Allen HK, Donato J, Wang HH, Cloud-Hansen KA, Davies J, Handelsman J (2010) Call of the wild: antibiotic resistance genes in natural environments. Nature Reviews Microbiology 8:251-259

Arora S, Lim CS, Foo JY, Sakharkar MK, Dixit P, Liu AQ, Miao JM (2009) Microchip system for monitoring microbial physiological behaviour under drug influences. Proceedings of the Institution of Mechanical Engineers Part H-Journal of Engineering in Medicine 223:777-786

Asiello PJ, Baeumner AJ (2011) Miniaturized isothermal nucleic acid amplification, a review. Lab on a Chip 11:1420-1430

Bauer AW, Kirby WMM, Sherris JC, Turck M (1966) Antibiotic susceptibility testing by a standardized single disk method. American Journal of Clinical Pathology 45:493-496

Bhattacharyya A, Klapperich CM (2006) Thermoplastic microfluidic device for on-chip purification of nucleic acids for disposable diagnostics. Analytical Chemistry 78:788-792

Boedicker JQ, Li L, Kline TR, Ismagilov RF (2008) Detecting bacteria and determining their susceptibility to antibiotics by stochastic confinement in nanoliter droplets using plug-based microfluidics. Lab on a Chip 8:1265-1272

Boyle WS, Smith GE (1970) Charge-coupled semiconductor devices. Bell System Technology Journal 49:587–593

Chantiwas R, Park S, Soper SA, Kim BC, Takayama S, Sunkara V, Hwang H, Cho YK (2011) Flexible fabrication and applications of polymer nanochannels and nanoslits. Chemical Society Reviews 40:3677-3702

Chen CH, Lu Y, Sin MLY, Mach KE, Zhang DD, Gau V, Liao JC, Wong PK (2010) Antimicrobial susceptibility testing using high surface-to-volume ratio microchannels. Analytical Chemistry 82:1012-1019

Chen L, Manz A, Day PJR (2007) Total nucleic acid analysis integrated on microfluidic devices. Lab on a Chip 7:1413-1423

Chin CD, Laksanasopin T, Cheung YK, Steinmiller D, Linder V, Parsa H, Wang J, Moore H, Rouse R, Umviligihozo G, Karita E, Mwambarangwe L, Braunstein SL, van de Wijgert J, Sahabo R, Justman JE, El-Sadr W, Sia SK (2011) Microfluidics-based diagnostics of infectious diseases in the developing world. Nature Medicine 17:1015-U1138

Craun GF, Brunkard JM, Yoder JS, Roberts VA, Carpenter J, Wade T, Calderon RL, Roberts JM, Beach MJ, Roy SL (2010a) Causes of outbreaks associated with drinking water in the United States from 1971 to 2006. Clinical Microbiology Reviews 23:507-+

Craun GF, Brunkard JM, Yoder JS, Roberts VA, Carpenter J, Wade T, Calderon RL, Roberts JM, Beach MJ, Roy SL (2010b) Causes of outbreaks associated with drinking water in the united states from 1971 to 2006. Clinical Microbiology Reviews 23:507-528

Feachem RGA, Phillips AA, Hwang J, Cotter C, Wielgosz B, Greenwood BM, Sabot O, Rodriguez MH, Abeyasinghe RR, Ghebreyesus TA, Snow RW (2010) Shrinking the malaria map: progress and prospects. Lancet 376:1566-1578

Fiorini GS, Chiu DT (2005) Disposable microfluidic devices: fabrication, function, and application. Biotechniques 38:429-446

Groisman A, Lobo C, Cho HJ, Campbell JK, Dufour YS, Stevens AM, Levchenko A (2005) A microfluidic chemostat for experiments with bacterial and yeast cells. Nature Methods 2:685-689

Guzman MG, Halstead SB, Artsob H, Buchy P, Jeremy F, Gubler DJ, Hunsperger E, Kroeger A, Margolis HS, Martinez E, Nathan MB, Pelegrino JL, Cameron S, Yoksan S, Peeling RW (2010) Dengue: a continuing global threat. Nature Reviews Microbiology:S7-S16

Hiraoka Y, Sedat JW, Agard DA (1987) The use of a charge-coupled device for quantitative optical microscopy of biological structures. Science 238:36-41

Kaigala GV, Hoang VN, Stickel A, Lauzon J, Manage D, Pilarski LM, Backhouse CJ (2008) An inexpensive and portable microchip-based platform for integrated RT-PCR and capillary electrophoresis. Analyst 133:331-338

Klevens RM, Morrison MA, Nadle J, Petit S, Gershman K, Ray S, Harrison LH, Lynfield R, Dumyati G, Townes JM, Craig AS, Zell ER, Fosheim GE, McDougal LK, Carey RB, Fridkin SK (2007) Invasive methicillin-resistant Staphylococcus aureus infections in the United States. Jama-Journal of the American Medical Association 298:1763-1771

Kopp MU, de Mello AJ, Manz A (1998) Chemical amplification: Continuous-flow PCR on a chip. Science 280:1046-1048

Kumarasamy KK, Toleman MA, Walsh TR, Bagaria J, Butt F, Balakrishnan R, Chaudhary U, Doumith M, Giske CG, Irfan S, Krishnan P, Kumar AV, Maharjan S, Mushtaq S, Noorie T, Paterson DL, Pearson A, Perry C, Pike R, Rao B, Ray U, Sarma JB, Sharma M, Sheridan E, Thirunarayan MA, Turton J, Upadhyay S, Warner M, Welfare W, Livermore DM, Woodford N (2010) Emergence of a new antibiotic resistance mechanism in India, Pakistan, and the UK: a molecular, biological, and epidemiological study. Lancet Infectious Diseases 10:597-602

Kuswandi B, Nuriman, Huskens J, Verboom W (2007) Optical sensing systems for microfluidic devices: A review. Analytica Chimica Acta 601:141-155

Lee WG, Kim YG, Chung BG, Demirci U, Khademhosseini A (2010) Nano/Microfluidics for diagnosis of infectious diseases in developing countries. Advanced Drug Delivery Reviews 62:449-457

Liu KK, Wu RG, Chuang YJ, Khoo HS, Huang SH, Tseng FG (2010) Microfluidic Systems for Biosensing. Sensors 10:6623-6661

McNerney R, Daley P (2011) Towards a point-of-care test for active tuberculosis: obstacles and opportunities. Nature Reviews Microbiology 9:204-213

Moe AE, Marx S, Banani N, Liu M, Marquardt B, Wilson DM (2005) Improvements in LED-based fluorescence analysis systems. Sensors and Actuators B-Chemical 111:230-241

Myers FB, Lee LP (2008) Innovations in optical microfluidic technologies for point-of-care diagnostics. Lab on a Chip 8:2015-2031

Neuzil P, Zhang CY, Pipper J, Oh S, Zhuo L (2006) Ultra fast miniaturized real-time PCR: 40 cycles in less than six minutes. Nucleic Acids Research 34:e77

Niemz A, Ferguson TM, Boyle DS (2011) Point-of-care nucleic acid testing for infectious diseases. Trends in Biotechnology 29:240-250

Nikaido H (2009) Multidrug Resistance in Bacteria. Annual Review of Biochemistry 78:119-146

Park S, Zhang Y, Lin S, Wang T-H, Yang S (2011) Advances in microfluidic PCR for point-of-care infectious disease diagnostics. Biotechnology Advances 29:830-839

Poirel L, Revathi G, Bernabeu S, Nordmann P (2011) Detection of NDM-1-producing Klebsiella pneumoniae in Kenya. Antimicrobial Agents and Chemotherapy 55:934-936

Richman DD, Margolis DM, Delaney M, Greene WC, Hazuda D, Pomerantz RJ (2009) The challenge of finding a cure for HIV infection. Science 323:1304-1307

Robbins MS, Hadwen BJ (2003) The noise performance of electron multiplying charge-coupled devices. IEEE Transactions on Electron Devices 50:1227-1232

Sack RB, Rahman M, Yunus M, Khan EH (1997) Antimicrobial resistance in organisms causing diarrheal disease. Clinical Infectious Diseases 24:S102-S105

Salmon WC, Waters JC (2011). CCD cameras for fluorescence imaging of living cells. In G. e. al. (Ed.): CSHL Press, Cold Spring Harbor, NY, USA

Schulze H, Giraud G, Crain J, Bachmann TT (2009) Multiplexed optical pathogen detection with lab-on-a-chip devices. Journal of Biophotonics 2:199-211

Seyrig G, Ahmad F, Stedtfeld RD, Tourlousse DM, Hashsham SA (2010). Simple, Powerful, and Smart: Using LAMP for Low Cost Screening of Multiple Waterborne Pathogens In K. Sen & N. J. Ashbolt (Eds.), Environmental Microbiology: Current Technology and Water Applications: Caister Academic Press 103-125

Soto SM (2009) Relationship between virulence and antimicrobial resistance in bacteria. Reviews in Medical Microbiology 20:84-90

Stalons DR, Thornsberry C (1975) Broth-dilution method for determining the antibiotic susceptibility of anaerobic bacteria. Antimicrobial Agents and Chemotherapy 7:15-21

Tsao CW, DeVoe DL (2009) Bonding of thermoplastic polymer microfluidics. Microfluidics and Nanofluidics 6:1-16

Van Kerkhove MD, Mumford E, Mounts AW, Bresee J, Ly S, Bridges CB, Otte J (2011) Highly pathogenic avian influenza (H5N1): Pathways of exposure at the animal-human interface, a systematic review. Plos One 6

Yager P, Domingo GJ, Gerdes J (2008) Point-of-care diagnostics for global health. Annual Review of Biomedical Engineering 10:107-144

Yang MH, Kostov Y, Bruck HA, Rasooly A (2008) Carbon nanotubes with enhanced chemiluminescence immunoassay for CCD-based detection of Staphylococcal enterotoxin B in food. Analytical Chemistry 80:8532-8537

Yang MH, Kostov Y, Bruck HA, Rasooly A (2009) Gold nanoparticle-based enhanced chemiluminescence immunosensor for detection of Staphylococcal enterotoxin B (SEB) in food. International Journal of Food Microbiology 133:265-271

Yotter RA, Wilson DM (2003) A review of photodetectors for sensing light-emitting reporters in biological systems. IEEE Sensors Journal 3:288-303

Zhang C, Da X (2010) Single-Molecule DNA Amplification and Analysis Using Microfluidics. Chemical Reviews 110:4910-4947

Zhang CS, Xing D, Li YY (2007) Micropumps, microvalves, and micromixers within PCR microfluidic chips: Advances and trends. Biotechnology Advances 25:483-514

Zhang CS, Xu JL, Ma WL, Zheng WL (2006) PCR microfluidic devices for DNA amplification. Biotechnology Advances 24:243-284

CHAPTER II

2. CRITICAL EVALUATION OF MINITURIZED NUCLEIC ACID AMPLIFICATION SYSTEMS FOR POINT-OF-CARE DIAGNOSTICS

2.1 Introduction

Miniaturized nucleic acid amplification systems are highly needed for point-of-care (POC) diagnostic applications. For genetic testing, two key approaches, that are commonly used are polymerase chain reaction (PCR) and isothermal assay (e.g., loop-mediated isothermal amplification, LAMP) (Notomi et al. 2000b). Other approaches that are potentially useful but have received less attention include transcription-mediated amplification (Hofmann et al. 2005), helicase dependent amplification (Vincent et al. 2004), recombinase polymerase amplification (Piepenburg et al. 2006), nucleic acid sequence-based amplification (Gracias and McKillip 2007), and non-amplification-based method (Nam et al. 2004). Early studies in this direction started in 1993 with the demonstration of PCR in 50 μL silicon microchip (Northrup et al. 1993b). Over the last two decades, there has been a surge in miniaturized nucleic acid amplification systems with innovative concepts, designs, sizes, materials, modes of integration among others (Zhang et al. 2006; Zhang and Xing 2007a; Zhang and Ozdemir 2009; Park et al. 2011). Molecular assays carried out in micro/microfluidic chips typically enable shorter analysis times, reduce reagent consumption, minimize risk of sample contamination, and often enhance assay performance (except lower limit of detection due to smaller sample volume). MicroPCR/LAMP refers to microfluidic chip with micron size chamber(s) for performing single or multiple PCR or LAMP reactions (Mark et al. 2010). MicroPCR/LAMP system in its most basic form includes a microchip for confined reaction and a heater for thermal cycling. In

addition, it may also include pumps and valves for liquid handling, detection components, and interface for heater control and other parameters (Burns et al. 1998). PCR is an enzymatic process of amplifying selected regions of nucleic acid (Saiki et al. 1988). It relies on thermal cycling i.e., cycles of repeated heating and cooling of the PCR reagent mixture (target DNA, nucleotides, polymerase, primers, and buffer components). This process produces large number of copies of a specific segment of target DNA. LAMP is a promising alternative since the amplification reaction is performed at 63 ^{o}C with the strand displacement activity of polymerase (Notomi et al. 2000b). LAMP provides higher amplicon yield than PCR, thus the positivity of amplification can be detected either visually or by low-cost detectors. MicroPCR/LAMP systems have the potential of rapid amplification, multiplexing, portability, and low-cost integration for complete nucleic acid analysis.

Static chamber and flow-through microPCR systems are commonly applied for the amplification and detection of nucleic acids. Based on whether the temperature is cycled for PCR reagent mixture contained in a static chamber or it is cycled through various temperature zones, microPCR systems can be classified into two major types, static chamber type (Northrup et al. 1993a) and flow-through type (Kopp et al. 1998). Other types of microPCR systems such as convective, thermal gradient, and oscillatory are also reported. Static chamber microPCR chip is commonly fabricated in well or capillary format. Flow-through microPCR chip is fabricated in a serpentine channel format to take advantage of the three temperature zones. Certain parameters in microPCR systems like thermal mass, conductivity, flow rate, and channel cross-sectional area, which if optimized properly can lead to amplification in less than 5-10 min compared to 30 min to 2 hours in conventional PCR systems. Using the flow-through system, it can be reduced to as low as 1.5 min, albeit for large starting copy numbers (10^{8} copies) (Kopp et al. 1998).

There are a number of advantages of static chamber microPCR over the conventional PCR like rapid gene amplification, lower cost of reagents and system components, high throughput, and possibility of integration as a portable or hand-held molecular diagnostic device (Zou et al. 2002; Lee and Hsing 2006; Wang et al. 2006). Comparatively, more reports are available on static chamber microPCR systems than flow-through microPCR systems. More interest of the research community towards static chamber microPCR systems is due to: i) smaller footprint of chip, ii) possibility of high throughput, and iii) easier integration of detection step for real-time nucleic acid amplification (Xiang et al. 2005b). The concept of real-time flow-through microPCR system has been often described in literature but only one real-time flow-through microPCR system has been reported yet (Pjescic et al. 2010a).

Static chamber microPCR systems have similar working principle as commercial PCR machines in which 50-100 μl vials containing PCR reagent mixture are placed on a metallic block that can undergo through a temperature cycle causing target DNA denaturation (95 ^{o}C for 1 min), primer annealing (55 ^{o}C for 1 min), and copying or extension (72 ^{o}C for 2 min). This cycle is repeated 30 to 35 times, which takes around 2 h for complete nucleic acid amplification. During this process, time is required for bringing the temperature of the heating block to the cycle equilibrium temperature and to transfer heat to the PCR reagent mixture. Due to the high mass and limited response time of the heating blocks in commercial PCR machines, until recently very slow heating and cooling rates (1-2 ^{o}C /s) were employed. This, however, is changing with systems that now have 10-20 ^{o}C /s of heating and cooling rates requiring only 20-30 minutes for nucleic acid amplification. In both the cases, a major fraction (>90%) of the total time is needed due to ramping up and down of the heating block rather than the amplification

process. It has been shown that DNA denaturation and primer annealing are almost instantaneous (< 1 s) once the PCR reagent mixture reaches to appropriate temperature (Saiki et al. 1988). Additionally, Taq polymerase commonly used in PCR has a nucleotide extension rate of ~100 nucleotides/s (Pavlov et al. 2004). Therefore, considering 1 sec each for denaturation, annealing, and extension, it is possible to amplify a 100 bp amplicon in 90 sec provided the time for temperature cycling can be eliminated. A number of DNA polymerases with much higher enzymatic activity are also known today and are becoming the basis for rapid PCR (Pavlov et al. 2004). Nucleic acid amplification in commercial PCR systems is characterized by high thermal mass, low temperature ramping rates, high amplification time, and high power consumption (Wittwer et al. 1989a). In contrast to commercial PCR machine, static-chamber microPCR has smaller sample volume (nL to μL) and smaller foot print of microchip and heater. Flow-through microPCR does not require temperature cycling, resulting in a much faster amplification than static chamber microPCR system. In flow-through microPCR, the PCR reagent mixture flows through a channel passing through the three temperature zones (95 ^{o}C, 55 ^{o}C, and 72 ^{o}C). During the flow, the PCR reagent mixture comes in thermal equilibrium with the temperature zone instantaneously (in much less than the time spent in that zone). Consequently, the PCR time in flow-through microPCR is limited by the polymerase extension rate. As in a pipe-flow problem, the retention time of PCR reagent mixture in flow-through system is a function of flow rate, channel cross-sectional area, and channel length. Starting with 10^{8} copies, Kopp et al. demonstrated the fastest flow-through microPCR in 90 sec, the theoretical limit of DNA amplification time (Kopp et al. 1998).

Microfluidic chips for PCR and isothermal assays are commonly fabricated by a number of inorganic and organic materials such as silicon, glass, polydimethylsiloxane (PDMS),

polymethylmethacrylate (PMMA), polycarbonate (PC), SU-8, and cyclic olefin polymer (COP) (Fiorini and Chiu 2005; Zhang and Xing 2007b). Due to specific properties of these materials, single material or a hybrid of two or more materials are commonly selected for chip fabrication. For example, silicon provides high temperature ramping rates due to its high thermal conductivity. Glass provides clear window for optical detection. Also glass is suitable for capillary electrophoresis due to the electro-osmotic-flow property in glass chips is suitable for capillary electrophoresis. Commonly reported micro/microfluidic chips are either fabricated either with silicon or glass or a hybrid of both. Microchips made of silicon or glass is generally not disposable due to high cost of fabrication. Polymeric microchips are inexpensive and disposable. Hence they are becoming more common. Polymeric chips exhibit higher fabrication flexibility, optical transparency, lower fabrication cost, and better biocompatibility. One drawback of polymeric chips is the slow thermal response due to their lower thermal conductivity (approximately 3-order of magnitude lower than silicon). Therefore, polymeric chips may be more suitable for isothermal gene amplification, which does not require any thermal cycling. Commonly applied microchip fabrication techniques are photolithography, silicon bulk micromachining, soft lithography, injection molding, hot embossing, CO_2 laser ablation (Zhang and Xing 2007b). Bonding/sealing of microchip is important to contain PCR reagent mixture and eliminate its evaporation during thermal cycling. A number of techniques like anodic bonding (glass and silicon), hydrofluoric acid bonding (silicon and glass), adhesive bonding (silicon, glass, and polymer), O_2 plasma treatment (PDMS), lamination (polymer) have successfully been applied (Zhang and Xing 2007b).

Here, a quantitatively evaluation of a number of parameters (e.g., thermal mass, conductivity, channel cross-sectional area, and flow rate) that affect the nucleic acid

amplification time in static chamber and flow-through microPCR systems is performed. These parameters can be optimized during the designing of microPCR chips to enhance system's performance and reduce PCR time. Some examples of microPCR systems with innovative approaches and surface treatment of microchips are also briefly discussed. Examples of integrated microPCR systems, which include sample processing and detection steps together with the nucleic acid amplification step are discussed. Relatively, newer isothermal nucleic acid amplification methods and the challenges associated with their translation on microchips are discussed. As an example, a novel isothermal gene amplification method, LAMP, is discussed in the context of simple sample processing and instrument-free diagnostic systems. Miniaturized nucleic acid analysis systems are evaluated under the World Health Organization's guidelines for POC diagnostic devices, showing the potential of microLAMP systems towards simpler integration of sample processing steps with other analytical steps in one device for POC diagnostics. Here, the main aim is to critically evaluate the effect of various physical parameters on the performance of microPCR and microLAMP systems for rapid and low-cost gene analysis with the applications towards POC infectious disease diagnostics.

2.2 Static chamber microPCR systems

Static chamber microPCR chips with different materials, reaction throughputs, volumes, starting copy numbers or amount of nucleic acids, heating and cooling rates, cycle numbers, and amplification times has been reported (Table 2.1). The first micro-machined static chamber microPCR system was reported by Northrup and coworkers in 1993 (Northrup et al. 1993a). The system consisted of a silicon chip with a single 50 μL well, a computer controlled peltier unit for thermal cycling, and silicone adhesive for well sealing. DNA amplification was completed in approximately 1 h. A year later, a microPCR chip with 5-fold lower in volume (10 μL) was

demonstrated (Wilding et al. 1994a). The chip was made of silicon with a single reaction chamber covered by glass layer. Thermal cycling was performed by thermoelectric heater and cooler. However, PCR time was increased to 1 h and 45 min. Higher PCR time with the 5-fold reduction in the reaction volume may be due to lower heating rate (not reported). End products in both the systems were detected off-chip by gel electrophoresis. Since then, static chamber microPCR system has been replicated by numerous research groups, with the focus towards reducing the amplification time, reaction volume, and cost, and integration of amplification, detection, and analysis steps. Toward the first step, microchips were integrated with thin film heaters to consolidate the amplification module. Three types of heating assemblies are commonly applied to static chamber microPCR systems. These are: i) external heater i.e. customized or commercial thermal cycler (Liu et al. 2001a), ii) integrated heater by using metallic thin film (Lee et al. 2004), and iii) non-contact heater by using high energy radiation (e.g., infrared rays) (Oda et al. 1998b). Rapid nucleic acid amplification can be achieved on the microchip integrated with thin film heater or microchip with non-contact heater than on the microchip placed on external heater. Additionally, heating source could be the bulkiest component of the microPCR system considering the small dimension of the microchip and low volume of the reaction solution. The reason for the differences in the PCR time for these heating assemblies are quantitatively evaluated and described in the section below.

2.2.1 External heaters

External heaters are metallic blocks (e.g., copper or aluminum) attached to a peltier unit for thermal cycling. Commonly these metallic blocks have cavities for placing PCR tubes. Static chamber microPCR chip is directly placed on the thermal cycler with flat metallic plate (attached with peltier) for temperature ramping. Due to slow thermal cycling rate of commercial thermal

cycler, it takes nearly same time to perform PCR in microchip as it will take in plastic vials. The only advantage of performing PCR in microchip on commercial thermal cycler is the reduction in the reaction volume applied to the microchip. Some of the reasons of using external heaters/thermal cyclers with static chamber microPCR chip are; i) fabrication of thin film heater on microPCR chip requires sophisticated facilities and instruments and is an expensive process, ii) temperature control of thin film heaters is achieved by a combination of proportional-integral-differential (commonly with LabVIEW software from National Instruments), which requires the knowledge of electrical circuitry, and iii) fluorescence microscopes with temperature control stage and customized software are available for real-time detection of PCR on chip. Therefore, a number of researchers have applied commercial or custom-made thermal cyclers to perform PCR in microchips.

Table 2.1 Selected parameters of static chamber microPCR systems

Chip Material	Reaction	Volume (nL)	Copy/amount	Heating source (thermal cycler)	Heating/cooling rate (^{o}C/s)	Cycle	PCR time (min)	Reference
Polycarbonate	-	20,000	0.2 ng	Commercial	-	25	223	(Liu et al. 2001b)
Glass	4	12,000	0.12 ng	Commercial	-	25	223	(Waters et al. 1998b)
Glass-PDMS	8	10,000	-	Commercial	-	45	82.5	(Zhang et al. 2010)
Silicon	1248	40	0.4-8 DNA copies	Commercial		40	62	(Matsubara et al. 2004b)
PDMS-glass	400	3	-	Commercial	3/3		60	(Liu et al. 2003b)
PDMS	1	2000	60 ng	Custom-made	2/1.2	30	43	(Shin et al. 2003a)
Glass-PDMS	1	2240	5 RNA copies	Custom-made	6/4	25	84	(Kaigala et al. 2006)
Silicon	1248	40	0.4 - 8 DNA copies	Custom-made	-	40	56	(Matsubara et al. 2005b)
Glass-PDMS	3	900	0.017 ng	Custom-made	-	35	57	(Xiang et al. 2005a)
Silicon	1	50,000	-	Custom-made	-	-	60	(Northrup et al. 1993b)
Glass-PDMS	4	3000	0.01 ng	Custom-made	-	35	87.5	(House et al. 2010)
Glass-PDMS	100	120	-	Custom-made	-	40	65	(Liu et al. 2009)
Polycarbonate	1	10,000	20 DNA copies	Custom-made	4/6	45	101	(Qiu et al. 2010)
Silicon	1	10,000	0.2 ng	Custom-made	-	35	105	(Wilding et al. 1994b)
Glass-PDMS	1	1750	11 ng	Custom-made	4.5	35	117	(Prakash et al. 2006a)
Glass-PDMS	9	5000	0.5 ng	Custom-made	-	40	122	(Ramalingam et al. 2010)

Table 2.1
(cont'd)

Glass	1	0.08	15 DNA copies	Custom-made	2/3-4	10	20	(Khandurina et al. 2000a)
Glass-PDMS	72	0.45	34 RNA copies	-	-	30	45	(Marcus et al. 2006a)
PDMS	1	5000	0.1 ng	Custom-made	3.1/3.1	40	45	(Cady et al. 2005a)
Glass-PDMS	1	100	10 cells	Custom-made	5/3	35	50	(Beyor et al. 2009a)
COC	1	50,000	1.25×10^6 cells	Custom-made	10/5	40	50	(Sauer-Budge et al. 2009)
Polypropylene	1024	200	5 DNA copies	Custom-made	-	45	55	(Dahl et al. 2006a)
Glass	4	3800	0.16 ng	Thin film	2/1	30	35	(Pan et al. 2010)
Glass-PDMS	1	600	24 RNA copies	Thin film	10	35	44	(Kaigala et al. 2008)
Silicon-glass	10	100	100,000	Thin film	175/125	40	5.7	(Neuzil et al. 2006a)
Silicon-PMMA	1	200	0.06 ng	Thin film	80/60	30	7	(Lee et al. 2004)
Glass	8	200	5 ng	Thin film	20/20	20	10	(Lagally et al. 2001)
Silicon	1	3000	~60 ng	Thin film	11/11	30	13	(Rodriguez et al. 2003)
Silicon	1	5000	-	Thin film	12.7/12.7	35	25	(Wu et al. 2011a)
Silicon-glass	1	1000	100,000 RNA copies	Thin film	-	50	28	(Neuzil et al. 2010)
Glass	1	500	12 cDNA copies	Thin film	11.5/5.6	50	19	(Pipper et al. 2007a)
Glass-PDMS	1	10,000	-	Thin film	20.5/7	20	15	(Hsieh et al. 2005b)
Glass-plastic	1	25,000	5 ng	Thin film	8/8	30	28	(Shen et al. 2005a)

Table 2.1
(cont'd)

Glass-PDMS-PMMA	1	10,000	1000 ng	Thin film	20/10	20	18	(Huang et al. 2006)
Glass-PDMS	1	10,000	0.06 ng	Thin film	20/10	25	22	(Liao et al. 2005a)
Glass-PDMS	4	390	10 RNA copies	Thin film	15/10	30	27	(Liu et al. 2006a)
Silicon-glass	1	240	0.24 ng	Thin film	20/20	35	22	(Pal et al. 2005)
Silicon-glass	4	3000	1.2 ng	Thin film	6/3.5	30	30	(Zou et al. 2005b)
SU-8	1	25,000	28600 DNA copies	Thin film	20/11	40	30	(Wang et al. 2006)
Silicon-glass	1	1000	278 DNA copies	Thin film	20	40	20	(Cho et al. 2006b)
Glass	5	100,000	1000 ng	Hot air	-	30	15	(Wittwer et al. 1989b)
Silica	1	62,500	0.25 ng	Hot air	-	25	8	(Swerdlow et al. 1997a)
Glass	1	28,000	5 ng	Infrared rays	10/20	17	14	(Oda et al. 1998a)
Silica	1	160	593	Infrared rays	65/20	10	11.5	(Huhmer and Landers 2000a)
Glass-PDMS	1	550	15-45 ng	Infrared rays	-	30	11	(Easley et al. 2006b)
Polyimide	1	1700	69,000 DNA copies	Infrared rays	10/10	15	4	(Giordano et al. 2001b)

.

For example, Liu et al. reported a polycarbonate microPCR chip with a volume of 20 µL integrated with capillary electrophoresis for integrated gene analysis (Liu et al. 2001a). DNA amplification was performed in 223 min for 25 cycles by thermally cycling the microchip on a commercial thermal cycler. Waters et al. designed a glass microchip with 4 reaction wells each with a volume of a 12 µL (Waters et al. 1998a). Similarly, temperature cycling was performed on a commercial thermal cycler providing amplification in 223 min for 25 cycles. Kaigala et al. designed a 2 µL glass-PDMS microPCR chip for the detection of BK virus (Kaigala et al. 2006). Thermal cycling was performed on a custom made thermoelectric system with a heating and cooling rate of 5 ^{o}C /s and 3 ^{o}C /s respectively, leading to an amplification time of 84 min in 25 cycles. Later, the same group integrated microPCR chip with capillary electrophoresis to achieve a $1000 portable system for gene amplification and detection (Kaigala et al. 2008). Increase in heating rate to 10 ^{o}C /s and a 4-fold reduction in the reaction volume, provided a faster amplification in 44 min for 40 cycles. PDMS is an inexpensive and commonly applied elastomeric polymer for microchip fabrication. However, the water diffusion and vapor loss property of PDMS at elevated temperature is an issue for low-volume applications. To address this problem, a protocol of implanting polyethylene barrier in PDMS was developed, which eliminated the evaporation problem (Prakash et al. 2006b). Inter-diffusion of the dissolved polyethylene into PDMS structure resulted into irreversible co-adhesion. Approximately, 3-fold reduction in solution evaporation was achieved in the polyethylene implanted microchip. Another solution of covering PDMS surface with parlene film drastically reduced the solution evaporation (Shin et al. 2003b).

For high throughput DNA amplification, Matsubara et al. developed a nanoliter array based microPCR chip (Matsubara et al. 2004a). A total of 1248 reactions wells each with 40 nL

volume were fabricated on a 1×3 inch^2 silicon chip. A commercial thermal cycler was employed for temperature cycling. In a following report, a miniaturized thermal cycler was developed for PCR in the same 1248 reaction well microchip (Matsubara et al. 2005a). TaqMan assay was applied for the amplification of 3 different serotypes and 5 genes of *E. coli*. Amplification was achieved in 62 min for the system with commercial thermal cycler and 56 min for the system with miniaturized thermal cycler. Heating/cooling rates of these thermal cyclers were not reported. Despite the higher thermal conductivity of silicon than polymers, higher amplification time might be due to the higher heating and cooling rates of the cycler. Dahl et al. developed a 1024 open well-based polypropylene chip with a volume of 200 nL per reaction for the amplification of RNase P gene from human genomic DNA and high throughput gene expression studies (Dahl et al. 2006b). Thermal cycling was performed on a custom-made cycling system with a DNA amplification time of 55 min for 45 cycles. Liu et al. developed a PDMS-glass microPCR chip for 400 independent reactions each with a volume of 3 nL per reaction (Liu et al. 2003a). Microchip was placed on a commercial thermal cycler with heating and cooling rates of 3 ^{o}C /s. A 294-bp segment of the human β-actin cDNA fragment was amplified in 60 min. Marcus et al. demonstrated 72 real-time PCR reactions each with 450 pL volume in a glass-PDMS microchip (Marcus et al. 2006b). Thermal cycling of the chip was performed on flat plate thermal cycler leading to PCR time of 45 min. Analysis of the above examples show that only reduction in PCR reagent mixture volume does not reduce PCR time. High PCR time in the reported static chamber microPCR systems was due to the low heating and cooling rates of the applied thermal cyclers and low conductivity of glass or polymeric microchips.

2.2.2 Integrated heaters

Integrated heaters are thin metallic layers ranging from fraction of micrometers to several millimeters in thickness directly fabricated on the back-side of microPCR chip. In some examples, thin films are fabricated on a substrate (e.g., glass or silicon), which is directly placed in the contact of microPCR chip. Platinum, gold, aluminum, tungsten, indium tin oxide is commonly used as materials for heaters. Thin film heaters are fabricated by physical vapor deposition, sputtering, and laser deposition techniques. Integration of microchip with thin filter heater provides efficient heat transfer to the PCR reagent mixture. Improper heating leads to irreproducible thermal profiles with low PCR specificity and non-reproducible DNA amplifications. Several researchers have applied finite element models (e.g., Coventor Ware, ANSYS, FLUENT) to analyze the thermal response of thin film heaters (Lin et al. 2000; Zou et al. 2005a; Dinca et al. 2009). These studies were helpful in optimizing the size, shape, position of thin film heaters, resulting in uniform temperature distribution on the microchip. A number of studies have demonstrated that thin film heaters provide higher heating/cooling rates than commercial thermal cyclers, leading to rapid gene amplification (Zhang and Xing 2007a).

For example, Neuzil and coworkers demonstrated nucleic acid amplification only in 5.7 min, which is the fastest till date (Neuzil et al. 2006a). A silicon chip was fabricated in the form of a cantilever with a disc at the end. A microscope glass cover slip was placed on the top of the disc integrated with a thin film heater and a temperature sensor. A new concept of virtual reaction chamber, where the mineral oil covers the PCR reagent mixture was applied to perform PCR. A 100 nL PCR reagent mixture encapsulated with mineral oil was placed on a disposable glass chip for thermal cycling. This type of arrangement provided an extraordinary heating and cooling rates of 175 ^{o}C /s and 125 ^{o}C /s respectively. Rapid amplification was due to the low

thermal mass of the system, especially the thin film heaters as suggested by the authors. High throughput was achieved by running 10 PCR reactions simultaneously. Real-time nucleic acid amplification was monitored by placing the chip on a microscope attached to a photomultiplier tube. Amplicons were analyzed by capillary electrophoresis to confirm the performance of PCR at this high thermal cycling rate. It was shown that microPCR was highly specific. Lee et al. fabricated a sub-microliter volume static chamber microPCR chip with very high thermal response or low thermal mass (Lee et al. 2004). Microchip was composed of silicon membrane base covered by PMMA top, etched with fluidic networks. Silicon membrane was fabricated by the bulk-micromachining of silicon. Platinum heaters and sensors were placed on the silicon membrane. Heating rate of 80 ^{o}C /s and a cooling rate of 60 ^{o}C /s was achieved. DNA amplification in a 200 nL chamber was demonstrated in only 7 min with 30 cycles. Combination of low thermal mass of heating membrane, efficient heat transfer in silicon, and low PCR reaction volume resulted into faster heating and cooling and rapid DNA amplification. Lagally et al. developed a glass-based microPCR chip with 8 parallel 200 nL PCR chambers integrated with platinum thin film heater, and capillary electrophoresis channels (Lagally et al. 2001). Temperature control was accomplished through a proportional/ integral/derivative (PID) module with the LabVIEW program. Heating and cooling rates of 20 ^{0}C /s were achieved. Multiplex microPCR was carried out to amplify a specific region of X and Y chromosomes from human genomic DNA in 10 min. After amplification, the sample was detected in the integrated capillary electrophoresis channels. Similarly, Rodriguez et al. reported a silicon microPCR chip integrated with glass-based capillary electrophoresis channels (Rodriguez et al. 2003). Heating and cooling rates of 11 ^{o}C /s were achieved. Moreover, 30 cycles of micro-PCR were completed in 13 min.

Hsieh et al. developed a battery-operated portable microPCR system integrated with glass-PDMS chip and platinum thin film heater (Hsieh et al. 2005a). Temperature was measured by an integrated sensor and controlled by a microcontroller. Heating and cooling rate of 20.5 ^{o}C /s and 7 ^{o}C /s was achieved. A high reaction volume of 10 µL was used. A 276 bp *lytA* gene for *Salmonella pneumoniae* was amplified in 15 min. Detection of PCR product was carried out separately by gel electrophoresis. Due to low power consumption (1.2 W/s) of controller, this system could operate for 10 h with one time charging. Generally, microPCR chips are disposed after DNA amplification to avoid any contamination by the amplification product. Disposing microPCR chips attached with thin film heaters is not a very cost-effective option. Shen and coworkers addressed this problem by designing a 25 µL microPCR reaction chamber sandwiched between a glass slip and a plastic cover (Shen et al. 2005b). Glass chip and plastic cover was separated by using a double sided adhesive tape between the glass and plastic cover. Thin film heater was fabricated on the backside of glass slide. A reasonable heating and cooling rate of 8 ^{o}C /s was achieved. A 244 bp gene fragment of hepatitis C virus was amplified in 28 min. The above examples show that DNA amplification can be achieved faster in static chamber microPCR chips integrated with thin film heaters as compared to commercial or customized thermal cyclers. Applying thin film heaters to static chamber microPCR chips reduces PCR time by enhancing the heat transfer and increasing the heating/cooling rates (Khandurina et al. 2000b; Liao et al. 2005b; Huang et al. 2006; Liu et al. 2006b). Moreover, lower reagent volumes, application of heat conductive chip materials, and precise temperature control are other critical factors for rapid gene amplification.

2.2.3 Non-contact heaters

A disadvantage associated with contact heaters (e.g. peltier and thin film) is that a certain amount of thermal mass is added to the system, which slows down the thermal cycling. Only an effective contact between the heating source and PCR reaction vessel leads to efficient heat transfer resulting into reproducible PCR with high yield. Heat transfer problems associated with heating blocks can be eliminated by applying non-contact heating approach. Non-contact heating options are applied to achieve faster heating/cooling and rapid DNA amplification. Some examples of non-contact heating include heating PCR reagent mixture by hot air, infrared (IR) light, laser, induction, microwave (Zhang et al. 2006). Hot-air and IR-based heating has been commonly applied to microPCR systems than other non-contact heating options.

Hot air based thermal cycling of PCR reagent mixture was initiated by Wittwer and coworkers (Wittwer et al. 1989a). PCR reagent mixture contained in glass capillary was heated/ cooled by rapidly switching the air streams at desired temperatures. A 536-bp beta-globin fragment of human genomic DNA was amplified in 15 min. Swerdlow et al. demonstrated a hot-air assisted PCR in the injection valve of high performance liquid chromatography (Swerdlow et al. 1997b). All the necessary steps, including loading of PCR reaction mixture, amplification, and detection by capillary electrophoresis was performed in 20 min with a PCR time of 8 min. Hot air heats the PCR reagent mixture and the reaction vessel non-selectively, which is not an efficient utilization of heat/power.

IR source is another effective non-contact heating option. Water absorbs IR light in the wavelength range of 900-4000 nm, where the excitation of vibrational bands of water molecules results in bulk heating of solution. Due to this property, IR source heats only the PCR reagent mixture and does not heat the microchip and other parts depending on the selected material.

Moreover, IR light can be manipulated by applying lens and filters for focusing and eliminating wavelengths (ultraviolet) that could be absorbed by other materials and could also interfere with PCR. IR-based non-contact heating of microchamber was initiated by Landers and coworkers (Oda et al. 1998b). Glass microchamber with a total volume of 28 µL was fabricated by borosilicate glass. A tungsten lamp was applied as an IR radiation source for heating and solenoid-gated compressed air source for cooling. This combination provided 10 ^{o}C/s and 20^{o}C/s of heating and cooling rates respectively. The total PCR time including pre-cycle denaturation, cycling time and post-cycle extension time was 14 min. In another report, IR-mediated thermal cycling of 160 nL of PCR reagent mixture in fused-silica capillary was demonstrated (Huhmer and Landers 2000b). Nano-liter volume of PCR reaction mixture required only 10 PCR cycles to produce detectable amount of amplified products by capillary electrophoresis. High heating (65^{o}C /s) and cooling rates (20 ^{o}C /s) were achieved. Based on IR-mediated heating, Giordano et al. demonstrated the fastest PCR only in 240 s.(Giordano et al. 2001c) PCR reaction was performed in a polyimide microchip with a reaction volume of 1.7 µL. Polyimide is a useful material for IR heating due to its high optical transmission in IR range and high glass transition temperature (350 ^{o}C). For accurate temperature control, a thermocouple was placed inside the reaction chamber. Taq polymerase inactivation was observed due to the direct contact of metal with the PCR reagent mixture. Addition of 0.75% polyethylene glycol in the PCR reagent mixture eliminated the problem of polymerase inactivation. These non-contact heating assemblies do not contribute any thermal mass to the microPCR systems resulting into faster thermal cycling and DNA amplification. IR-sources (e.g., tungsten lamp) applied in the above examples were bulky and could not be a part of a portable/handheld microPCR system.

Miniaturized IR lasers are commercially available, which should satisfy the requirements of efficiency and compactness and can be used in integrated microPCR systems.

2.2.4 Analysis of static chamber microPCR systems

The main objective of this analysis is to understand the key factors responsible for rapid DNA amplification in static chamber microPCR systems. Static chamber microPCR systems discussed above applied microchips fabricated with different materials, reaction volumes, starting DNA copies or cells, external and non-contact heaters, integrated heaters with different materials. As a result these microPCR systems have different heating/cooling rates and nucleic acid amplification times. A general comparison of the above examples shows that PCR time is related to heating/cooling rates. Additionally, heating/cooling rates are dependent on the volume of PCR reaction mixture, conductivity of microchip material, and type of heater. For example, Neuzil et al. applied the reaction volume of 100 nL, conductive silicon chip integrated with thin film heater, and achieved the highest heating/cooling rates, leading to the fastest PCR in 5.7 min (Neuzil et al. 2006b). On the other case, Liu et al. used a 20 µL PC chip on a commercial thermal cycler and achieved the slowest PCR in 223 min (Liu et al. 2001a). Although the heating/cooling rates of the commercial thermal cycler was not reported but it might be in the range of 1-2 ^{o}C/s. Therefore, the type of heaters applied to microchip has major effect on PCR time. Static chamber microPCR chips heated with external heaters and thin film heaters from selected publications (x-axis) are plotted with respect to their reported PCR time (y-axis) (Figure 1.1). PCR time for microchips heated with thin film heaters is in the range of 5 - 30 min, and 1 - 3 h for microchips heated with external heaters (commercial or custom-made) respectively. This qualitative comparison shows that microchips heated with thin film heaters have shorter PCR time than

microchips heated with external heaters. Also microchips with thin film heaters have higher heating/cooling rates than the microchips with external heaters. Heating rates and PCR times are plotted for the selected examples of static chamber micro-PCR chips heated with external heaters and thin film heaters (Figure 2.1).

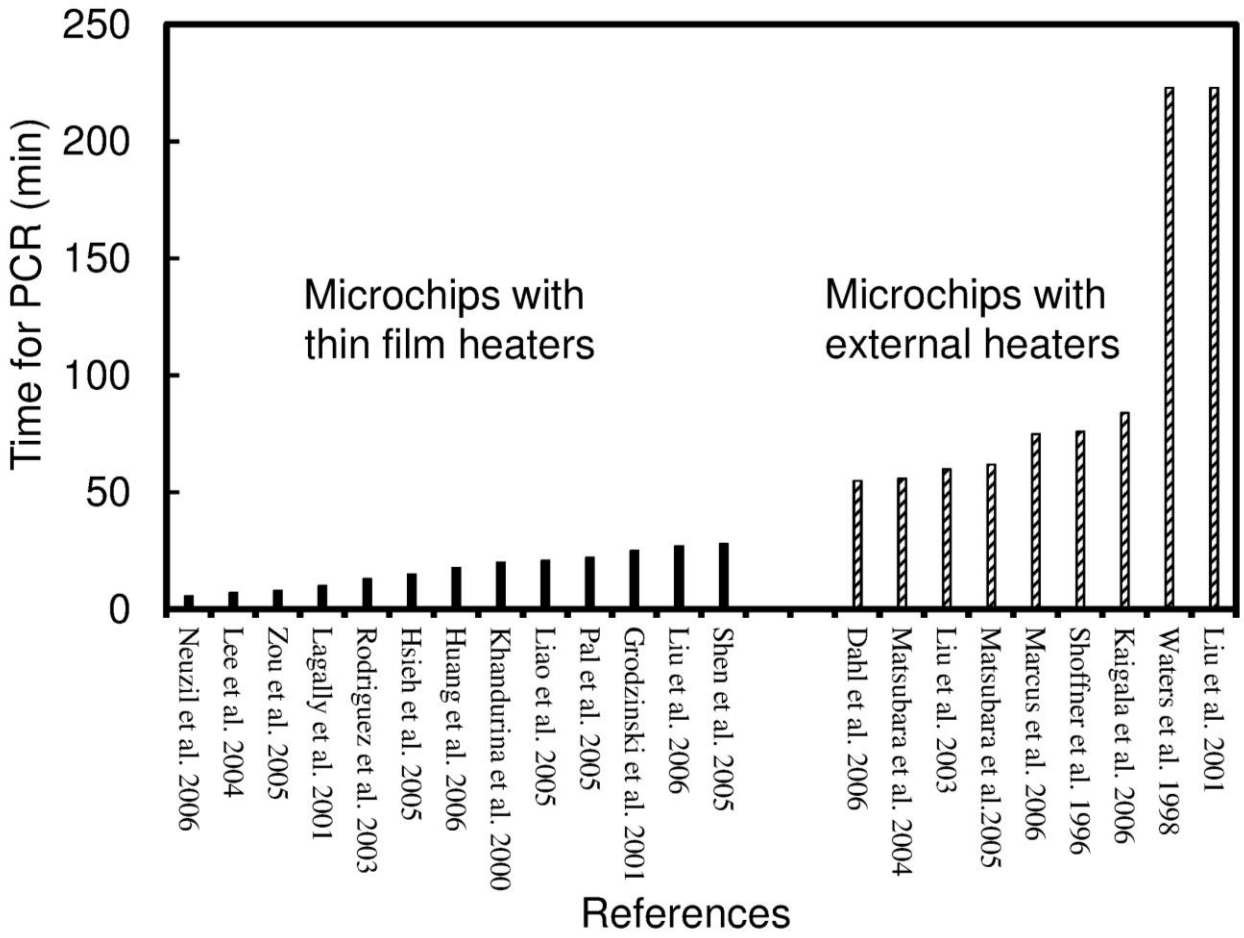

Figure 2.1 Comparison of PCR time for static chamber microPCR chips with thin films (black bars) and external heaters (shaded bars)

Higher heating rates were achieved for microchips integrated with thin film heaters. Lower heating rates were obtained for microchips placed on external heaters due to the slow thermal cycling of commercial thermal cyclers. Also rapid amplification was achieved on the microchips integrated with thin film heaters due to faster thermal cycling. Generally, external

heaters/thermal cyclers have heating rates of 1 - 2 ^{o}C/s (Wittwer et al. 1989a), whereas thin film heaters can be easily heated from 10 ^{o}C/s to 175 ^{o}C/s (Shen et al. 2005b; Neuzil et al. 2006b). PCR time is inversely related to heating/cooling rates. However, it cannot be directly predicted based on the heating/cooling rate. PCR time is directly dependent on the time needed for each cycle. Cycling times can vary between seconds to few minutes per temperature cycle. During the thermal cycling, time is required for bringing the temperature of the microchip to the cycle equilibrium temperature and efficiently transferring heat to the PCR reagent mixture. Temperature cycling rate is dependent on the thermal mass and conductivity of static chamber microPCR chip. Therefore, rapid PCR can be achieved by a microPCR system using a temperature conductive microchip with low thermal mass. In an study, it was observed that replacing the plastic vials by glass capillaries and heating blocks by thin aluminum compartments reduced the PCR time to 15 min (Wittwer et al. 1989a). It was proposed that rapid amplification was achieved by reducing the thermal mass of the PCR system. Thermal mass, which is a measure of the ability of the material to store thermal energy, can be described by the multiplication factor of $\rho . C_p . V$, where ρ is the density of material, C_p is the specific heat, and V is the volume of system. MicroPCR chips with low thermal mass would easily release the heat during the cooling step, providing high thermal cycling rate. For heat conductive microchips (e.g., silicon), heat transfer between the heater and the PCR reagent mixture would be rapid. This would save the time which would otherwise be added in the thermal cycling time, if low heat conductive microchips (e.g., polymer or glass) are applied.

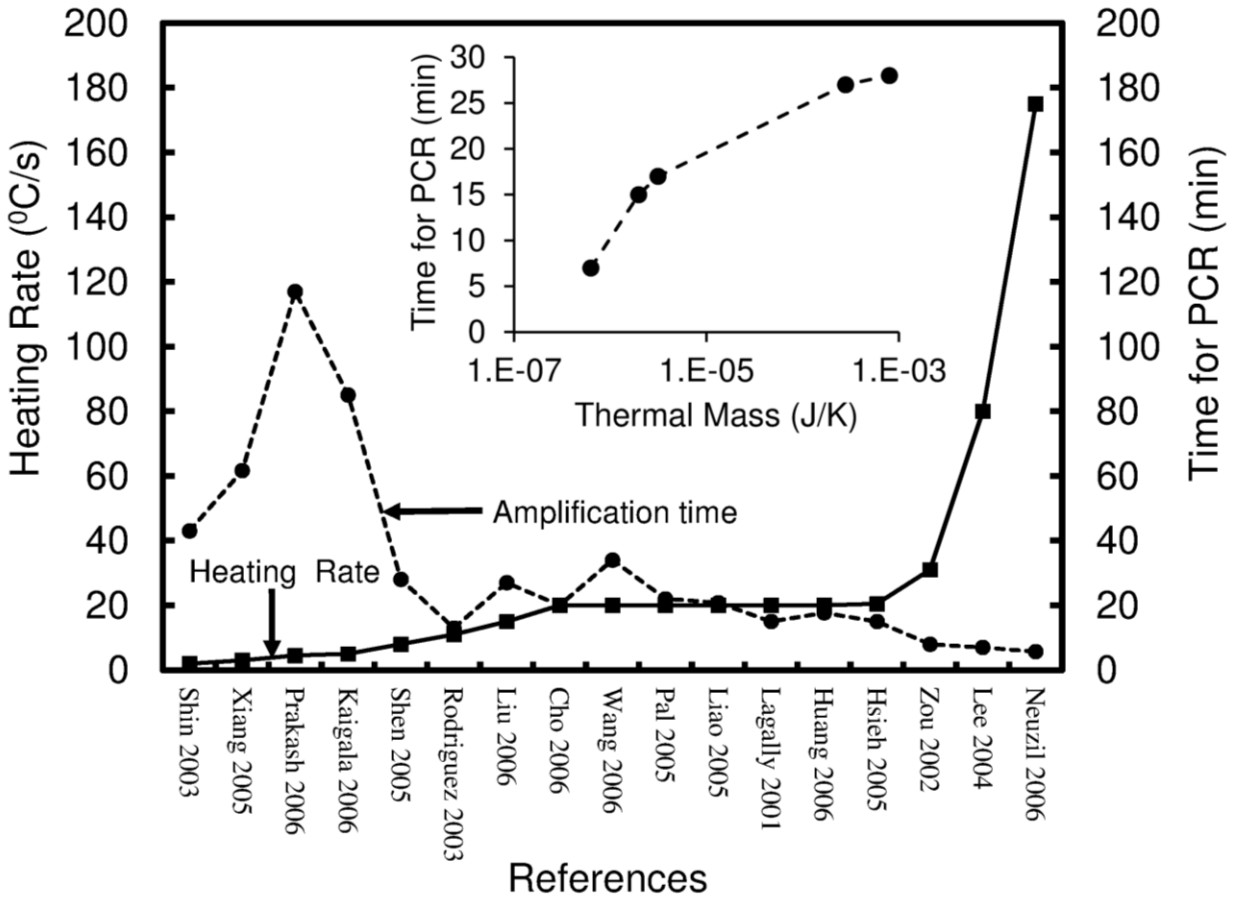

Figure 2.2 Effect of heating rates (■) on PCR times (●) for static chamber microPCR systems. Inset shows the relation between thermal mass of thin film heaters and PCR time

In earlier discussions, thermal mass was qualitatively correlated with the PCR time. Here, the numerical values of the thermal mass of heaters are calculated and correlated with the PCR time (Figure 2.2, Table 2.2). Inset of Figure 2.2, shows the relation between PCR time and the calculated thermal mass of selected examples. In a commercial PCR machine, thermal cycling is achieved by an aluminum/copper block attached to a peltier unit. However, in static chamber micro-PCR systems, metallic films of platinum, gold, and copper are commonly applied as heaters. For comparison, dimension of an aluminum block was assumed to be 5 cm × 5 cm × 5 cm. The specific heat and density of aluminum is 385 J /g. K and 8.96 g /cm^3 respectively.

Therefore, the calculated thermal mass of a 1120 g aluminum block would be 431.2 kJ /K. Thermal mass of thin film heaters were calculated (Table 2.2) by their given dimensions. Thermal mass of copper block was much higher than the calculated thermal mass of thin film heaters. Due to their high thermal conductivity, thin film heaters could be heated very fast to the temperature needed for PCR. Also due to their low thermal mass, they would release the heat easily during the cooling step. Therefore very high heating/cooling rates could be achieved by thin film heaters. However, PCR time would not only depend on the heating/cooling rate of heater. It would depend on how efficiently the heat is transferred from the heater to the PCR reagent mixture through the microPCR chip and gets released during the cooling step. Therefore, it is important that the comparison of the thermal mass of the whole microPCR system (microchip, PCR reagent, and heater) should be done with the PCR time.

Table 2.2 Calculated thermal mass of thin film heaters for static chamber microPCR systems

Reference	PCR time (min)	Heater material	Heater dimension (μm^3)	Thermal mass (J /K)
(Lee et al. 2004)	7	platinum	$1500 \times 500 \times 0.3$	6.27×10^{-7}
(Hsieh et al. 2005b)	15	platinum	$\pi \times (1500)^2 \times 0.1$	1.97×10^{-6}
(Liu et al. 2003b)	27	platinum	$(5\times10^4) \times (1\times10^4) \times 0.2$	2.79×10^{-4}
(Shen et al. 2005a)	28	copper	$120000 \times 55 \times 35$	7.95×10^{-4}

Physical dimensions of microchips and properties of the applied materials (e.g., adhesive tape) of were reported for few examples of Table 2.2. For example, Lee et al. (Lee et al. 2004) and Shen et al. (Shen et al. 2005b) have reported all the parameters about microchip, PCR reagent, and heater. Lee et al. applied a 200 nL silicon chip (covered with PMMA film) with a dimension of 1.5 mm × 0.5 mm × 0.25 mm (Lee et al. 2004). Shen et al. applied a 25 µL glass

chip with a dimension of 22 mm × 22 mm × 0.15 mm.(Shen et al. 2005b) Glass chip was covered by an adhesive tape and plastic cover. However, the physical properties of adhesive tape and plastic cover were not given. Therefore, for both the examples we have calculated the thermal mass of PCR chips and reagents for comparison. Specific heat and density of silicon is 0.70 J/g. K and 2.3 g /cm^3 respectively. Specific heat and density of borosilicate glass is 0.88 J/g. K and 2.2 g /cm^3 respectively. For Lee et al. (Lee et al. 2004), thermal mass of PCR reagent mixture and microchip was 0.84 × 10^{-3} J/K and 0.30 × 10^{-3} J/K respectively. For Shen et al. (Shen et al. 2005b), thermal mass of PCR reagent mixture and microchip was 0.11 J/K and 0.14 J/K respectively. The total thermal mass of microchip with reagent mixture for Lee et al. (Lee et al. 2004) and Shen et al. (Shen et al. 2005b) was 0.001 J/K and 0.25 J/K respectively. Thermal mass of the thin films were not included in the calculations due to their very low values. It shows that the combined thermal mass of the microchip and PCR reagent volume was approximately three orders higher than the thermal mass of heater. Therefore, for the microchip and thin film heater combination, PCR time should be affected more by the thermal mass of microPCR chip and reagent mixture than the thermal mass of thin film heater. However, for the microchip and external heater combination, PCR time should be more effected by the thermal mass of heating blocks rather than microchip or PCR reagent.

2.3 Flow-through microPCR systems

Flow-through microPCR chips are commonly fabricated in silicon, glass, or a hybrid of both (Zhang and Xing 2007b). Few studies have also reported polymeric (PDMS, PMMA) flow-through microPCR chips (Zhang and Xing 2007b). Flow-through microPCR chips have serpentine channels, which pass through three constant temperature zones or heaters necessary

for PCR. Instead of being stationary in the chamber, PCR reagent mixture is pumped unidirectionally from the channel inlet passing repetitively through these thermal regions and the amplified product is collected at the outlet. Generally, syringe or peristaltic pumps are used to precisely control the flow of PCR reagent mixture in the microchannels. As described earlier, heat inertia of a flow-through microPCR system is only the thermal mass of PCR reagent mixture. The temperature transition time depends on the solution flow-rate and the time to achieve thermal equilibrium. Consequently, the PCR time is limited by the extension rate of DNA polymerase and could be much faster than static chamber micro-PCR. For rapid DNA amplification, flow-through microPCR systems requires the optimization of channel cross-sectional area, solution flow rate, and channel length, which are compared in Table 2.3.

The concept of flow-through PCR was introduced by Nakano et al., based on gene amplification in a loop of Teflon capillary passing through three oil baths maintained at three different temperatures (Nakano et al. 1994) The length of the capillary in each temperature bath and flow rate of reagent mixture was fixed to achieve the optimized time for denaturation, annealing, and extension. DNA amplification was achieved in 12 min. Similarly, Curcio and Roeraade developed a PCR system by coiling a 15 m long Teflon tube on copper heating blocks maintained at three different temperatures (Curcio and Roeraade 2003) A new concept of high throughput was demonstrated by introducing PCR reagent mixture plugs with water immiscible organic plugs. A compact cylindrical thermal-cycling device for flow-through PCR was reported by Park et al. with gene amplification in a 3.5 m long fused silica capillary coil passing through three heating blocks (Park et al. 2003a). DNA amplification was achieved in 5.5 min with a reagent mixture flow-rate of 5 µL /min. Although the footprints of these setups were not in

microscale but the concepts were helpful for the development of flow-through microPCR systems.

Kopp et al. were the first to demonstrate the fastest flow-through microPCR system in 90 s (Kopp et al. 1998). Serpentine channels (40 μm × 90 μm × 2.2 m) for 20 cycles were fabricated on biocompatible glass substrate. The glass chip was placed on three copper blocks maintained at 3 different temperatures. A syringe pump was used to inject PCR reagent mixture (10 μL) with varying flow rates of 5.8 nL/s to 72.9 nL /s corresponding to PCR time of 18.8 min to 90 s respectively. However, the DNA concentration (1×10^8 copies) in the PCR reagent mixture was very high. Detection sensitivity of microPCR system is as important as speed because very low dose (e.g. 10 to 100 cells for *E. coli* O157:H7) can be a serious health risk.(Nataro and Kaper 1998) The initial demonstration was rapid but not very sensitive and required relatively high reagent volume. Later, Obeid et al. demonstrated an improved version (in terms of sensitivity and reagent volume) of flow-through microPCR chip with lower volume.(Obeid et al. 2003a) Also, the chip had the flexibility of selecting the cycle numbers. Therefore, a range of starting DNA copies (2.5×10^6 - 1.6×10^8) was successfully amplified. Incorporating air plugs between the PCR reagent mixtures increased the throughput (3 parallel reactions) of the system. In addition, fabrication of an extra cycle for provided the conversion of RNA to complementary DNA before the PCR cycle leading to the amplification of DNA and RNA. Improved sensitivity (2.5×10^6 copies), lower reaction volume (2-7.6 μL), and 5 min of PCR time was achieved. In order to avoid bulky copper heaters, Hashimoto et al. evaluated the thermal effects by varying the PCR reagent mixture flow rates on a 20 cycle spiral channel polycarbonate chip (Hashimoto et al. 2004a). Effect of flow rates (1-20 mm/s) on the temperature distribution along the

microchannel was simulated. Effect on the temperature transition and resident times of PCR reagent mixture with different flow-rates were estimated for the optimization of experimental condition. Amplification of 2×10^7 copies of a 500 bp DNA template was completed in 1.7 min. Additionally, detection of single base pair mutations on a polycarbonate flow-through microchip was reported by the same group (Hashimoto et al. 2006b). Three different assays (flow-through PCR, ligation detection reaction, and hybridization) were performed on single microchip. DNA amplification on this 30-cycle serpentine channel microchip was achieved in 18.7 min. This example shows the possibility of integrating the pre/post-PCR genetic analysis steps on flow-through microPCR system. Schneegaß and coworkers used a flow-through chip made of silicon to improve the temperature transition (Schneegaß et al. 2001). To achieve a smaller footprint, platinum heaters were fabricated on the backside of the chip. Regions made of silicon ensured the efficient heat transfer from the heaters to the PCR reagent mixture. However, silicon creates the problem of temperature overlap between the channels due to its high thermal conductivity. Incorporating air pockets between the channels reduced the heat transfer effect between channels. Generally high surface area of channels leads to the adsorption of bio-molecules, which affects the PCR efficiency (Shoffner et al. 1996a). The static and dynamic surface treatment before and during the PCR step was applied for the optimization of PCR conditions. Also the effect of flow rate on the amplification efficiency was studied. An optimum flow rate of 33 nL/s was demonstrated for a 25 cycle, 17.5 min flow-through microPCR. Xiaoyu et al. reported a spiral channel microPCR chip integrated with platinum thin film heater (Xiaoyu et al. 2005). The chip was a hybrid of PDMS and glass with a reagent volume of 42 µL. Amplification of a 450 bp segment of *E. coli* HB101 was achieved in 30 min.

Table 2.3 Parameters for systems with flow-through design including flow-through microPCR systems

Factors/Reference	(Kopp et al. 1998)	(Obeid et al. 2003b)	(Park et al. 2003b)	(Hashimoto et al. 2004b)	(Schneegaß et al. 2001)	(Hashimoto et al. 2006a)	(Sadler et al. 2003b)	(Chou et al. 2002b)
Time for PCR (min)	1.5	5	5.5	1.7	17.5	18.7	27	40
Number of cycle	20	20	33	20	25	30	40	30
Flow rate (nL/s)	72.9	21	83.33	22.5	33	6.67	325	250
Cross-sectional area (μm^2)	3600	5181	7850	7500	19625	5000	250,000	250,000
Channel length (m)	2.2	3.43	3.5	-----	1.512	1.57	.....	-----
Volume of PCR solution (µL)	10	7.6	50	-----	33	0.168	24	19
Target copy	1×10^8	2.5×10^6 -1.6×10^8	-----	2×10^7 -1×10^8	------	------	------	-----
Substrate	Glass	Borosilicate glass	Fused silica capillary coils	Polycarbonate	Glass	Polycarbonate	LTCC	LTCC
Design	serpentine	serpentine	helical	spiral loops	serpentine	serpentine	serpentine	serpentine
Thermal source	Copper blocks	Copper blocks	Copper blocks	Resistive heaters	Platinum thin film heaters	Film resistance heaters	Ag-Pd thin films	Screen printed Ag-Pd films
Surface treatment, type	Dichlorodimethylsilane, dynamic	Dichlorodimethylsilane, static	Trimethylchlorosilane/DMF/imidazole, static	Bovine serum albumin (BSA), static	Hexamethyldisilane/ BSA, static and dynamic	No treatment	-----	-----

LTCC: Low temperature co-fired ceramics, PI: Proportional Integral PID: Proportional Integral Derivative, CFD: Computational Fluid Dynamics, Ag-Pd: Silver-Palladium

Chou et al. demonstrated the application of a new substrate material, low temperature co-fired ceramics for flow-through microPCR chip (Chou et al. 2002a). Screen printed silver-palladium paste was used as heaters. Computational fluid dynamics simulation was done to optimize heater input power, solution flow rate, sensor placement, and air gap size for thermal isolation. With a solution flow rate of 250 nL/s, a 20 cycle chip amplified a 209 bp DNA template in 40 min. PCR products of flow-through microPCR chips are commonly analyzed off the chip by gel electrophoresis. Development of optically transparent flow-through microPCR chips could be useful for real-time detection of PCR products. Although, flow-through PCR chips made of glass is transparent but the overall system is not optically clear due to the associated heaters. Thin film of indium tin oxide is conductive and transparent and can be easily coated on any substrate by electron beam evaporation, physical vapor deposition, and sputtering technique. Sun et al. had used quartz glass chip coated with thin film of indium tin oxide heaters, which made their system completely transparent (Sun et al. 2002). For this study, temperature in the microchannels was initially calibrated by measuring the fluorescent spectra of temperature indicator dye under the flow conditions. It was confirmed that indium tin oxide heaters provided a local homogeneous temperature distribution on the chip. A 450 bp *E.coli* gene was amplified in 22.5 min. Recently a group have demonstrated a real-time flow-through micro-reverse transcriptase PCR system for the detection of viral phage (Pjescic et al. 2010b). Reverse transcriptase microPCR was performed in serpentine channels fabricated by xurography and sandwiched between two glass substrates. LC green, a DNA intercalating dye was applied for the florescence imaging of chip by a CCD camera. Approximately 1×10^8 copies of viral phage were amplified in 15 min with 23 cycles. A single fluorescence image of the chip during the amplification was sufficient to extract real-time amplification curves. Increasing the exposure

time of CCD camera from 125 ms to 1000 ms increased the signal-to-noise ratio (SNR) by 10-fold.

Fabrication of microfluidic channels in glass or silicon requires sophisticated tools and overall is an expensive process. A cost-effective version of flow-through microPCR chip was developed by Kim at al. (Kim et al. 2006). Microfluidic channels were fabricated on a PDMS chip by soft lithographic techniques. PDMS chip was laminated with glass and heated by aluminum blocks. PDMS is hydrophobic in nature and generally adsorbs the enzymes used in PCR reagent mixture. The effect of extension time and the treatment of microchannels by polyvinylpyrrolidone on the PCR efficiency were studied. MicroPCR chip required only 8 min to amplify a 430 bp DNA template. Another low cost flow-through microchip made of PMMA substrate was reported by Sun et al. (Sun et al. 2008). PMMA is a transparent plastic with high mechanical stability and moderate thermal transition temperature (105 ^{o}C). It is suitable for cost-effective fabrication of microfluidic channels by CO_2 laser ablation or hot embossing. Sealing of polymeric chips is a common problem (Grodzinski et al. 2001). For comparison of heat tolerance at 95 ^{o}C, PMMA chip was bonded with a PC cover (glass transition temperature 150 ^{o}C) and PMMA cover. It was found that PMMA-PC sealing had better performance than PMMA-PMMA sealing. Due to lower glass transition of PMMA than PC, at 95 ^{o}C, PMMA-PMMA bonding was deteriorated leading to air bubbles and leakages. A number of solution flow rates (125 nL/s to 500 nL/s) for PMMA-PC flow through microchip were tested. For the amplification of a 500 bp DNA template, 26 cycles were completed between 8.5 - 34 min.

The above examples show that rapid gene amplification between 90 s to 10 min is possible in flow-through microPCR systems. Due to the applications of polymeric microchips,

flow-through microPCR systems can also be cost-effective. One major drawback of flow-through microPCR systems is the low detection sensitivity in the range of 10^6 to 10^8 copies. On the other hand, static chamber microPCR could be sensitive to approximately 10^2 copies (Cho et al. 2006a). Also, surface modification of microchip is needed due to adsorption of PCR reagent mixture in the channels of high surface area to volume ratio. Additionally, integration of parallel and real-time amplification steps is difficult to incorporate in these systems. It might due to all these reasons, including the bulky pumps to drive PCR reagent mixture, no commercial flow-through microPCR system is yet available, even though its rapid nature was proven a decade ago.

2.3.1 Analysis of flow-through microPCR systems

In the flow-through microPCR chip, nucleic acid amplification is achieved by driving the PCR reagent mixture through three thermally isolated reaction zones. As the PCR reagent mixture attains the temperature equilibrium with the heating zones instantaneously and thermal cycling is not required, PCR time is greatly reduced (Hashimoto et al. 2004a). However, there are other parameters e.g., PCR reagent mixture flow-rate, channel cross-sectional area, and channel length that directly influences the PCR time in flow-through microPCR system. The relation between PCR time and the ratio of cross-sectional area of the channel to the flow-rate of PCR reagents is plotted in Figure 2.3. PCR times and the flow-rates were used as reported in the publications. Cross-sectional areas of the channels were calculated by the reported channel dimensions.

Comparison of the selected flow-through microPCR systems (Table 2.3 and Figure 2.3) indicates that the PCR time is linearly dependent on the inverse of the flux of the PCR reagent

mixture. Therefore, rapid amplification in a flow-through microPCR system can be achieved either by increasing the flow-rate and/or decreasing the channel cross-sectional area. For example, the system presented by Kopp et al.(Kopp et al. 1998) had the flow-rate of 72.9 nL /s with the minimum cross-sectional area of 3600 μm^2. Due to the minimum value of the ratio of cross-sectional area and flow-rate (49 μm^2-s/nL), PCR was achieved in 90 s. Other factors for rapid PCR were relatively smaller volume of PCR reagent mixture and lower cycle number. Chou et al. (Chou et al. 2002a) and Sadler et al. (Sadler et al. 2003a) applied flow rates of 325 nL /s and 250 nL /s, which lead to PCR in 27 min and 40 min respectively. In their cases, the applied flow-rates and channel cross-sectional areas were highest among all the examples. Therefore, their ratio of cross-sectional area and flow-rate were higher than Kopp et al. (Kopp et al. 1998), leading to high PCR time. Ratio of cross-sectional area and flow-rate for other examples were in between to Kopp et al.(Kopp et al. 1998), Cho et al.(Chou et al. 2002b) and Sandler et al. (Sadler et al. 2003b).

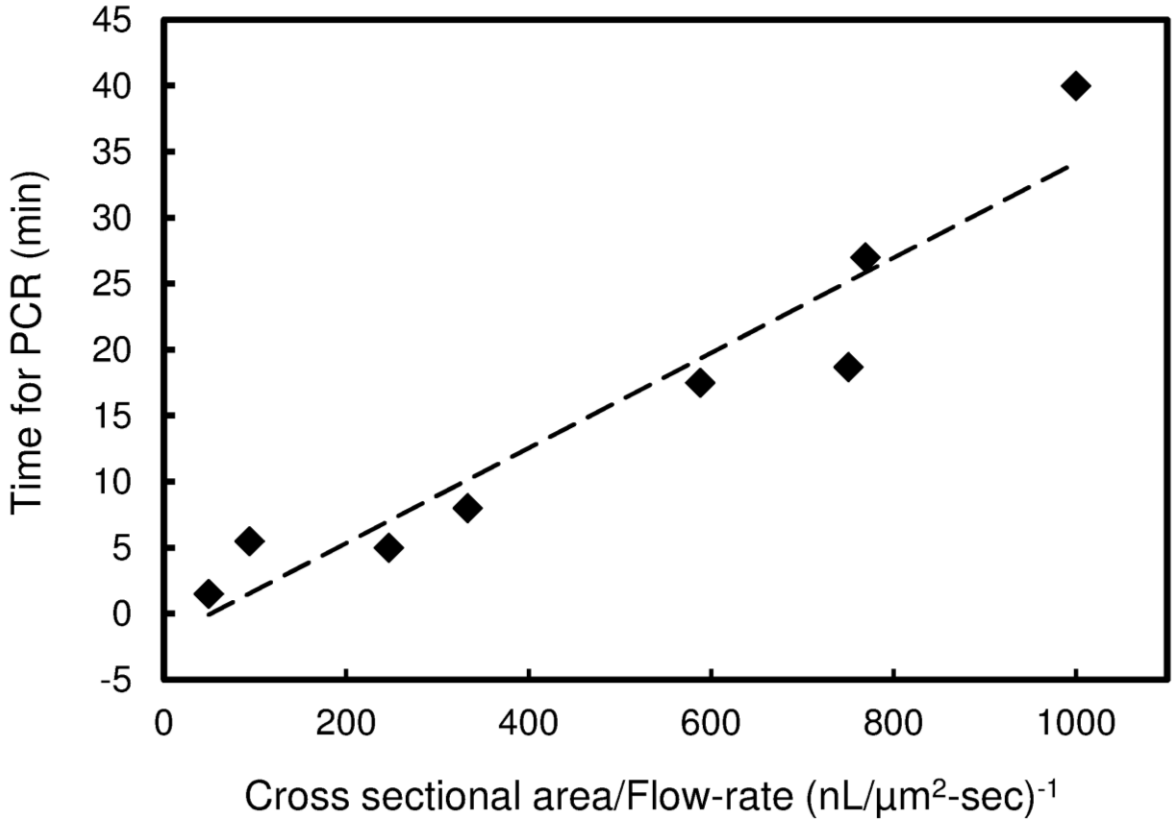

Figure 2.3 Relationship between PCR time and the ratio of cross-sectional area and flow-rate. Symbols and solid line corresponds, respectively to the data from studies reported on flow-through microPCR systems and best fit line

2.4 MicroPCR systems with innovative concepts

Miniaturized PCR systems based on simpler concepts such as convective, thermal gradient, and oscillatory microPCR have the potential for low-cost disease diagnostics. The concept of Rayleigh-Benard convective PCR was first reported by Krishnan and coworkers in 2002 (Krishnan et al. 2002). Rayleigh-Benard convective PCR applies the principle of natural convection to amplify DNA in a very simple format. Rayleigh-Benard cell has a cylindrical cavity filled with PCR reagent mixture and covered by two plates at 61 ^{o}C and 97 ^{o}C covering the top and bottom. Due to the temperature difference across the cavity, a static temperature gradient is generated, which repeatedly circulates PCR reagent mixture through temperature

zones necessary for amplification. Increasing the convective flow velocity in the cavity reduces the PCR time due to the faster solution cycling. It was observed that flow velocity increases with increasing temperature difference and cylinder dimensions. A 295 bp segment of the human β-actin gene was amplified by this system. Sample volume was 35 μL and PCR time was ~90 min. In a different publication the same authors performed flow visualization (tracking the motion of microspheres) and computational studies for convective PCR (Krishnan et al. 2004a). Multi-well arrays (15 μL each) were fabricated from a Plexiglas block for multiplex convective PCR. A 191 bp fragment associated with membrane proteins of influenza-A virus and a 295 bp segment of the human β-actin gene were amplified in 15 min. Recently, Agrawal et al., presented a pocket-sized convective PCR thermal cycler (Agrawal et al. 2007). A triangular loop of fluoropolymer tubing was heated by thermoelectric heaters from two inclined sides. The benefit of using fluoropolymer tubing is that it is stable at high temperature (205 ^{o}C) and compatible to PCR. The versatility of this device was demonstrated by amplifying a multiplex mixture of targets from five different respiratory viruses in 50 min. The hardware (single heater, heat control circuit, 2 AA batteries) costs approximately $10 with few cents per reaction for the disposable tubing. This is the demonstration of the cheapest prototype for nucleic acid amplification. This technology has recently been adopted by Gahaga Biosciences and launched with a commercial name of LavaAmp. Cost of this thermal cycler has not yet fixed but expected to be approximately $ 300 (personal communication). Some general advantages of convective PCR are simple hardware (no moving parts) and possibility of multiplexing and integration. Currently the amplified products are measured separately by gel or capillary-electrophoresis.

Continuous-flow thermal gradient PCR was initially reported by Crews et al. (Crews et al. 2008) Thermal cycling was achieved by cycling PCR reagent mixture within a spatial

temperature gradient. Temperature gradient was created by heating the glass microchip (with embedded serpentine channels) along one edge and cooling along the opposite edge. By using an IR camera, a 3D temperature distribution was recorded and the temperature was optimized for the experimental conditions. By this innovative concept of continuous-flow thermal gradient, a 40 cycle PCR was achieved in less than 9 min. Recently, an example of thermal gradient-based real-time flow-through microPCR system has been reported (Pjescic et al. 2010a). A 23 cycle serpentine-shaped adhesive tape was sandwiched between two glass slides. The sandwiched chip was placed between two aluminum heaters at 60 ^{o}C and 90 ^{o}C to generate a thermal gradient profile for PCR. PCR reagent mixed with DNA intercalating due was pumped with a flow rate of 2 μL/min in the channel and imaged by a CCD camera under the illumination of light emitting diode. A 110 bp of viral phase DNA template with 10^{8} copies /μL was amplified in 15 min. The major advantage of the single heating/cooling region is the small footprint of the microchip, no thermal crosstalk between channels, simple hardware, and short PCR time.

Oscillatory-flow PCR was proposed and experimentally validated by Wang et al. (Wang et al. 2005). Oscillating-flow PCR chip was fabricated by the silicon microfabrication technique. The chip had straight channel with three independent temperature zones necessary for PCR. A droplet of 1 μL PCR reagent mixture was pumped back and forth 35 times in an oscillatory-flow mode through the straight channel. Amplification of human papillomavirus DNA amplification was achieved in 15 min. Numerical simulation had shown that less than 1 s is required for the droplet to maintain thermal equilibrium with the set temperature. In this study, PCR reagent mixture was maintained at each temperature for 4 s with an additional 4 min of extension. Münchow et al. demonstrated that a 40 cycle oscillatory-flow PCR could amplify a 372 bp template in 5 min (Munchow et al. 2005). Functionally, an oscillatory-flow PCR is like a hybrid

of static chamber and flow-through PCR. It combines the flexibility of incorporating multiple channels for high throughput applications, smaller chip size, and fast temperature transitions for rapid PCR.

2.5 Surface treatment of microPCR systems

Surface chemistry plays an important role for the success of PCR in microPCR systems. Due to small dimensions of microPCR systems, surface-to-volume ratio gets extremely high. For example, the surface-to-volume ratio of a microsystem (characteristic length of 1 μm) is 10^6 times higher than a system with a characteristic length of 1 m. PCR reaction solution generally consists of DNA polymerase, target DNA, primers, and salts (Saiki et al. 1988). For an optimized reaction, the concentration of PCR components should be maintained during the course of the reaction. Miniaturization leads to non-specific adsorption of biomolecules on the surfaces which change the concentration of the PCR components in the reaction mixture. This phenomenon reduces the efficiency and efficacy of microPCR systems. MicroPCR chips are mostly manufactured by silicon. The effect of native silicon induced PCP inhibition is widely reported in literature. Coating of surfaces by PCR compatible materials or passivating agents such as silicon oxide, BSA, polymers (poly vinyl pyridine and polyethylene glycol), silanes and surfactants have shown considerable improvements in microPCR efficiency (Table 2.4). Based on the application mechanism, surface treatment can be classified into two types; static and dynamic passivation.

In static passivation, surface is coated with a PCR compatible substance before performing PCR on the chip. Passivating agents strongly adhere to the surface by covalent bonding. It is performed by filling and incubating the reaction chamber/channel (s) by a

passivation agent for a certain time followed by washing and curing the chip. Although it follows a complex protocol but provide better performance. However, it is a time consuming (~24 h) process. Covalent linked static coatings for silicon substrate are oxide deposition, polymer film deposition, and silanization. Dynamic passivation occurs during the operation of microPCR chip. Passivation agent is mixed with the PCR reaction mixture. During the PCR reaction, the passivation agent preferentially binds on the inner surface of the microchip and prevents the adsorption of PCR reaction components. The most frequently applied passivating agents for dynamic coating are BSA, polyvinyl pyridine, polyethylene glycol, and non-ionic surfactant (Tween).

Shoffner et al. studied the effect of native silicon on PCR inhibition (Shoffner et al. 1996b). Deposition of a thin layer of oxide or protein on silicon microchip slightly improved PCR product yield. Felbel et al. suggested that a combination of silanization and BSA treatment of silicon surface would be more effective than only one type of treatment (Felbel et al. 2004b). Matsubara et al. also found that native silicon inhibits PCR (Matsubara et al. 2004c; Matsubara et al. 2005c). Moreover, surface adsorption was predominant due to the high surface area to volume ratio of nanometer-sized wells. Depositing an oxide layer followed by BSA treatment improved the PCR yield as observed by the increment in the fluorescent signals. Krishnan et al. studied the problem of non-uniformity of PCR reactions within the oxide coated silicon microchannels (Krishnan et al. 2004b). The problem was due to the adsorption of positively charged magnesium ions on the negatively charged silicon-oxide surface. Coating with Teflon and proving higher concentration of magnesium ions in PCR solution showed improvements in PCR efficiency.

Table 2.4 Examples of commonly used surface treatment strategies and their effect on microPCR efficiency

Substrate	Type of treatment	Effect	References
Silicon	No treatment	PCR inhibition	(Shoffner et al. 1996c)
Silicon	Silicon nitride	PCR inhibition	(Shoffner et al. 1996c)
Silicon	Silicon oxide	Slightly improved PCR product yield, PCR inhibition	(Shoffner et al. 1996c)
Silicon	Silanization + BSA	Increased specificity and yield of PCR product	(Felbel et al. 2004a)
Silicon	Silanization + polyadenylic acid (protein)	Increased yield of PCR product	(Shoffner et al. 1996c)
Silicon	Silicon oxide + BSA	Increased fluorescence signal and reduced PCR inhibition	(Matsubara et al. 2005b), (Cho et al. 2006b)
Glass	BSA	Reduced adsorption of polymerase and DNA	(Khandurina et al. 2000a)
Glass	Polymers	Increased PCR efficiency	(Giordano et al. 2001a)
Glass	Silanization + Tween 20 + polyvinyl pyridine	Reduced adsorption of enzyme and DNA	(Kopp et al. 1998)
PDMS	Parylene	Eliminated bubble formation, sample evaporation, and polymerase adsorption	(Shin et al. 2003a)
SU-8	Silanization	Decreased the amount of polymerase needed and increased PCR compatibility	(El-Ali et al. 2004a)
SU-8	BSA	Eliminated PCR inhibition	(Wang et al. 2006)
Polycarbonate	BSA	Reduced adsorption of polymerase and DNA, enhanced PCR compatibility	(Liu et al. 2001b), (Hashimoto et al. 2004b)
Pico TiterPlate (Fiber)	BSA + Tween	Eliminated PCR inhibition	(Leamon et al. 2003a)
Polyimide	Polyethylene glycol	Reduced Taq polymerase inactivation	(Giordano et al. 2001b)

Giordano et al. compared the silanization process with different types of coatings such as polyethylene glycol, polyvinylpyrrolidone, hydroxyethylcellulose, and polydimethylacrylamide on the PCR yield of a glass microPCR chip (Giordano et al. 2001a).Untreated glass inhibited the PCR process. Surface treatment with polymeric agents showed comparable results as silanization together with being simple and less time consuming. Shin et al. applied a coating of inert material called parylene on PDMS microchip (Shin et al. 2003c). This coating solved several critical problems of bubble formation, sample evaporation, and protein adsorption for porous PDMS substrate. El-Ali et al. observed that silanization of SU-8 chip (a negative photo resist) increased the PCR product yield (El-Ali et al. 2004b). Liu et al. observed a reduced adsorption of enzyme and DNA by coating the polycarbonate chip with BSA (Liu et al. 2001b). Leamon et al. demonstrated that inclusion of 0.5% BSA and 0.05% Tween 80 in the PCR reaction solution improved PCR efficiency (Leamon et al. 2003b). Channels of flow-through microPCR chips are commonly treated with silanes, BSA, and nonionic surfactants (Table 2.3). In addition to surface passivation, increasing the concentration of PCR components in reaction solution has also been recommended.

2.6 Integrated microPCR systems

The aim of integrated microPCR system is to analyze real biological samples with a sample-in-answer-out capability. So far the efforts to develop simple and rapid nucleic acid-based devices have focused predominantly on amplification and detection steps, with sample processing remaining the bottleneck in the development of completely integrated systems. Applications of miniaturized devices in clinical or environmental analysis require processing of complex biological samples as whole blood, saliva, nasal aspirate, and environmental fluid on the same device. The presence of inhibitory substances in biological samples like humic acids,

cell debris, particulates, metals etc. hamper microfluidic operations and biochemical reactions. Generally, low initial target copies are present in biological samples, which requires target enrichment step before amplification. Therefore, nucleic acid samples for microPCR are commonly prepared off chip by applying established bench-scale procedures. Common steps for sample processing includes, cell capture, cell concentration, cell lysis, nucleic acid extraction and purification. The ability to integrate laboratory operations and automatic handling of biological samples into a microPCR system is a key to the success of micro-total-analysis systems. The examples discussed below can be divided into two major types, i) microPCR systems integrated with amplification and detection modules, and ii) microPCR systems integrated with sample processing, amplification, and detection modules.

Researchers at Lawrence Livermore National Lab developed a portable and a hand-held device for the nucleic acid analysis. Both the devices were based on the concept of static chamber microPCR. Example of the portable device is advanced nucleic acid analyzer (Belgrader et al. 1998). The platform was made of silicon (container for plastic reaction tubes) substrate heated by resistive heaters. It took 16 min to complete 10 PCR reactions simultaneously. Real-time PCR analysis was performed on a separate laptop, as this device was not capable to automatic data processing. Further developments lead to a hand-held device named as handheld advanced nucleic acid analyzer.(Higgins et al. 2003) It was based on silicon chamber and platinum heaters for the rapid heating and cooling of 4 plastic reaction tubes. Amplification was achieved in 30 min. Moreover, results were analyzed within the device and displayed on its screen. Currently, handheld advanced nucleic acid analyzer is marketed as Bio-Seeq through Smiths Detection for $ 31,000. The heating and cooling rates and reaction volume for these devices were 1.5 ^{o}C /s and 25 µL respectively, very similar to conventional PCR

machines. As the single PCR cycle was 23 s long, compared to approximately 240 s for conventional PCR, rapid amplification was achieved. These systems can be further improved by applying efficient thermal cycler, replacing plastic vials by highly conductive reaction containers, and lowering the reaction volume. Pal et al. developed an integrated static chamber microPCR system for genetic analysis of influenza virus (Pal et al. 2005). Microfluidic chip with addressable valves and thermal components (heaters and sensors) were integrated on a one system. RNA samples from the A/LA/1/87 influenza virus were amplified by reverse-transcriptase PCR and detected by electrophoretic separation. MicroPCR was completed in 22 min. These examples used pre-processed nucleic acids for DNA/RNA amplification.

Integration of sample processing, amplification, and detection steps were also reported on one system. For example Cady et al. integrated solid phase DNA extraction with real-time PCR on a microfluidic silicon chip (Cady et al. 2005b). Silica-coated micro-pillars were used to extract DNA from *Listeria monocytogens* cells. Temperature of the microchip was cycled by a thermoelectric heater/cooler achieving a heating and cooling rates of 3.1 ^{o}C /s. Approximately 10^{4} cells of *L. monocytogens* were detected in 45 min. Legendre et al. reported a hybrid silica bead/sol-gel based solid phase extraction and amplification of DNA from 600 nL whole blood (Legendre et al. 2006). DNA amplification was achieved in 15 min by applying IR-based thermal cycling. PCR products were detected by capillary electrophoresis. Easley et al. integrated a static chamber microPCR with solid phase DNA extraction and detection by capillary electrophoresis on the same device (Easley et al. 2006a). They demonstrated the performance of the device by detecting *Bacillus anthracis* in blood sample and *Bordetella pertussis* in nasal aspirate. Starting with sub-microliter sample volume, complete analysis required less than 30 min. DNA amplification was achieved in 11 min by employing IR-based thermal cycling. Pipper et al.

reported a fully integrated system, which included sample processing, amplification, and detection of avian influenza virus (H5N1) (Pipper et al. 2007b). Viral RNA was isolated directly from throat swab sample, purified, and pre-concentrated using a droplet containing superparamagnetic particles. The purified RNA was then released in a droplet, containing reverse transcriptase PCR mixture. The droplet moved over the different temperature zones for thermal cycling. The droplet acted as solid phase nucleic-acid extractor, pump, valve, mixer, and real-time thermal cycler. Heating and cooling rates were 11.5 ^{o}C/s and 5.6 ^{o}C/s respectively. Complete genetic analysis required only 28 min. An integrated microPCR system for the detection of bacteria including lysis, DNA purification, PCR, and fluorescence readout has been published recently (Sauer-Budge et al. 2009). Thermal cycling was achieved by a ceramic heater (10 ^{o}C/s) and air cooling (5 ^{o}C/s). Detection of 1.25×10^{6} cells of *B. subtilis* was performed in approximately 40 min. Chen et al. developed a self-contained polycarbonate cassette for the detection of *B. cereus* and HIV virus in saliva samples (Chen et al. 2010). All the necessary liquid buffers and reagents were pre-stored in small pouches on the chip. All the steps including, ell lysis, nucleic acid isolation, PCR, amplicon labeling, and detection by a lateral flow assay were performed on the cassette. Amplification time was 28 min with a heating and cooling rate of 5.2 ^{o}C/s and 6 ^{o}C/s respectively. The detection limit of this device was 10^{3}-10^{4} CFU/mL. Beyor et al. demonstrated a glass-PDMS chip for cell concentration, purification, PCR, and detection by capillary electrophoresis (Beyor et al. 2009b). The chip was used to detect *E. coli* K2 and *E. coli* O157:H7 with a detection limit of 0.2 CFU/µL. Commercial nucleic acid analysis systems have also been developed by microfluidic companies in a variety of formats and functionalities, including ACLARA BioSciences, Fluidigm Corporation, Affymetrix, Agilent

Technologies, Alderon Biosciences, Roche Molecular Diagnostics, and Motorola Inc (Lee and Hsing 2006). These miniaturized diagnostic tools would provide faster and accurate diagnosis, significantly reducing the health care costs.

2.7 Isothermal nucleic acid amplification methods on microchip platforms

Isothermal amplification methods use the enzymes for *in vivo* synthesis of DNA/RNA at a constant reaction temperature (Gill and Ghaemi 2008). A number of isothermal nucleic acid assays have been developed with different types and numbers of enzymes and primers, incubation temperatures, amplification times, and detection methods (Table 2.5). Isothermal nucleic acid amplification assays such as loop-mediated isothermal amplification (Fang et al. 2010; Ahmad et al. 2011), multiple displacement amplification (Marcy et al. 2007), helicase dependent amplification (Ramalingam et al. 2009; Mahalanabis et al. 2010), recombinase polymerase amplification (Lutz et al. 2010; Shen et al. 2011), and nucleic acid sequence-based amplification (Gulliksen et al. 2004; Tsaloglou et al. 2011) have also been translated on microchip-based platforms. Unlike PCR, polymerase extension rate is the limiting factor in the isothermal nucleic acid amplification assays. Therefore, detection times of these assays in conventional detection formats (e.g., commercial real-time PCR instrument) are considerably high. However, optimization of primer design and reaction, and application of highly fluorescent Syto dyes and sensitive detectors would reduce the detection time to less than 30 min (Ahmad et al. 2011; Kimura et al. 2011). Microchip-based isothermal nucleic acid amplification assays do not require any sample or temperature circulation, which translates into simpler and less expensive instrumentation.

Table 2.5 Selected examples of isothermal nucleic acid amplification methods

Method	Genetic target	Reaction temperature (^{o}C)	Reaction duration (min)	Major Reaction components	Reference
Loop-mediated isothermal amplification	DNA/RNA	60-65	30-90	1 enzyme (*Bst* polymerase),4-6 primers	(Notomi et al. 2000b)
Transcription-mediated amplification	DNA/RNA	60	140	2 enzymes (T7 RNA polymerase, reverse transcriptase), 2 primers	(Hofmann et al. 2005)
Helicase dependent amplification	DNA	65	75-90	3 enzymes (UvrD helicase, DNA polymerase I, DNA-binding protein), 2 primers	(Vincent et al. 2004)
Recombinase polymerase amplification	DNA/RNA	37	20	3 enzymes (*Bsu* polymerase, uvsX recombinase, DNA-binding protein), 2 primers	(Piepenburg et al. 2006)
Nucleic acid sequence-based amplification	RNA	41	105	3 enzymes (reverse transcriptase, T7 RNA polymerase, RNase H), 2 primers	(Compton 1991)

2.7.1 MicroLAMP systems

Due to the simplicity and robustness of LAMP assays, microLAMP systems have potential for POC disease diagnosis. LAMP is a relatively new gene amplification technique initially reported in 2000 (Notomi et al. 2000a). Appealing features of LAMP include high specificity, high sensitivity, speed, and high product yield. LAMP is performed at a moderate

incubation temperature between 60 ^{o}C to 65 ^{o}C. Major reaction components are an enzyme with strand displacement activity (*Bst* polymerase) and four primers. Addition of two more primers called loop primers further enhances the sensitivity and speed of LAMP reactions (Nagamine et al. 2002). Positivity of LAMP reaction in PCR vial is confirmed by observing the turbidity (Mori et al. 2001) or fluorescence (Chen and Ge 2010; Jia et al. 2010), either in endpoint or real-time formats by incubating the vial in a water bath, disposable pocket hand warmers (Hatano et al. 2010), or commercial thermal cycler (Mori and Notomi 2009). High amplicon yield of the LAMP reaction (500 ng /mL) simplifies the fluorescence detection due to increased signal intensity in the presence of highly fluorescent dyes (Seyrig et al. 2010). Amplification times of tube-based LAMP assays typically vary between 30-90 min, depending on the starting DNA template (Seyrig et al. 2010).

Endpoint and real-time LAMP assays employed with turbidity or fluorescence-based detection schemes have also been translated on microchips made of silicon and polymer (Tourlousse 2010; Niemz et al. 2011). Positive endpoint microLAMP is confirmed either visually (Fang 2010; Wu et al. 2011b) or by fluorescence microscopy (Matsubara et al. 2002; Lam et al. 2008). Fluorescence (Abe et al. 2011; Liu et al. 2011) or turbidity (Fang et al. 2010) increment during real-time microLAMP is commonly monitored by photodiodes. MicroLAMP is further quantified by measuring the threshold time (Tt) for a selected cutoff of signal, where the signal is above the background (Fang et al. 2010; Abe et al. 2011). Our group has optimized this technique for real-time fluorogenic LAMP (using Syto-82 dye) on traditional real-time PCR equipment and hand-held field deployable device (Gene-Z), both employing photodiodes (Stedtfeld 2009; Tourlousse 2010). Recently, we have demonstrated that applying a CCD with exposure control effect to real-time fluorescence microLAMP assays drastically increases the

SNR and reduces the Tt value in comparison to commercial real-time PCR instrument (Ahmad et al. 2011).

2.7.2 Instrument-free LAMP systems

At present, microLAMP systems do not completely satisfy WHO criteria of equipment-free/electricity-free operation. However, recent research has shown the possibility of equipment-free microLAMP in future. For example, researchers at PATH (Seattle, WA) demonstrated electricity-free LAMP by using calcium oxide heat source thermally in combination with a phase change material (LaBarre et al. 2010; LaBarre et al. 2011). The phase change material is designed to melt at 65 ^{o}C with the heat generated by the reaction of calcium oxide and water. This phase change material absorbs this heat and releases latent heat at relatively contact temperature. It has been shown that the combination of 20 g of calcium oxide and 6.8 mL of water provides sufficient heat that melts the phase change material and maintains 65 ± 0.75 ^{o}C temperature for 45 min. Fluorescence and turbidity-based endpoint LAMP assays (in 0.2 mL PCR vials) targeting *Plasmodium falciparum* was evaluated on this chemical heater and also compared against a commercial PCR instrument. Detection limit of *Plasmodium falciparum* on both the systems was approximately 50 copies. Among the few limitations of this approach are the slow warm up time (time required for the temperature of heater and reaction tube to reach equilibrium) of 15 min, high incubation time for endpoint LAMP assay, and non-usability of phase change material after single reaction. The warm up time could be reduced by applying the chemical heater to micro chip due to its lower thermal mass. Also applying highly fluorescent dye such as Syto-82 should further reduce the detection time of instrument-free microLAMP assays.

WHO recommends that the POC diagnostic devices developed for low-resource settings should be ASSURED; affordable, sensitive, specific, user-friendly, rapid and robust, equipment free, and deliverable to end users (Mabey et al. 2004; Yager et al. 2008). For example, immunoassay-based strips fit the ASSURED model albeit with limited sensitivity and specificity. On the other hand, nucleic-acid based assays provide excellent sensitivity and specificity but often are non-affordable, slow, and require high power. Miniaturized instrument-free LAMP systems have huge potential for low-cost POC diagnostics.

2.7.3 Simple sample processing in LAMP reactions

Direct gene amplification from bacterial cells would save the time and cost of sample processing. It will also simplify the device instrumentation and power consumption. Studies have shown that LAMP assays could be performed from eukaryotic/prokaryotic cells, without getting affected by cell debris. For example, Iwasaki et al. developed a LAMP assay for genotyping single nucleotide polymorphism in drug-responsive human cytochrome gene directly from whole blood by heating it at 95 ^{o}C for 5 min (Iwasaki et al. 2003). LAMP assay was compared against the gold standard PCR-restriction fragment length polymorphism analysis. Despite the presence of PCR inhibitory substances such as heme and immunogluobulin G in blood, LAMP assays were successful in detecting single nucleotide polymorphisms in the presence of cell debris only in 30 min. On the other hand, PCR-restriction fragment length polymorphism analysis needed the heat treatment and purification of genomic DNA. Poon et al. demonstrated LAMP assay for detecting *Plasmodium falciparum* by directly heating the blood at 99 ^{o}C for 10 min.(Poon et al. 2006) Approximately 100 samples were tested with LAMP and compared against PCR and microscopic count. PCR was not possible without the purification of genomic DNA. Among 13

heat treated blood samples (positive for *Plasmodium falciparum*) which were also positive by LAMP, 7 showed negative results by PCR. Clinical sensitivity and specificity of LAMP assay were 95% and 99% respectively. Also the detection limit of LAMP assay was 6 parasites/ µL, which was 10-fold higher than the microscopic count method. The same group developed a reverse-transcription LAMP assay for detecting avian influenza (H5N1) virus directly from viral culture (Jayawardena et al. 2007). Detection sensitivity of heat treated sample (99 ^{o}C for 10 min) in LAMP assay was found to be 9.6 PFU/ reaction, which was approximately 1000-fold less sensitive than assay which used purified RNA. As DNA-based LAMP assays have not shown any effect of sample heat treatment on the detection sensitivity, this effect might be due to the sensitivity of RNA towards the heat. In another study, LAMP assay was also performed directly from oilseed rape plant by mechanically disrupting the tissue (Lee et al. 2009). In all these examples, LAMP assays required either prior heating of the sample between 95 ^{o}C to 99 ^{o}C (3-10 min) or a mechanical step for cell lysis before mixing the lysate in the reaction solution. Additionally, these cell-based LAMP assays were performed in 25 mL PCR vials and not yet translated on microchips. Due to the requirement of prior heating of sample for cell lysis, microchip-based LAMP would have an extra manual step. We have found that real-time and quantitative microLAMP assays could be performed by directly incubating the Gram-negative and Gram-positive bacterial cells in the reaction mixture at 63 ^{o}C (unpublished). Direct gene amplification from bacterial cell at the incubation temperature would not require any prior heating or upstream sample processing step, which would further simplify microLAMP system instrumentation. Direct cell-based amplification would be highly useful for translating LAMP assays on microchips with sample-in-answer-out capability.

2.8 Conclusions

POC genetic diagnostics critically depends on miniaturization of amplification, detection, and sequencing techniques. Isothermal amplification techniques, which are still emerging, have a better potential for POC diagnostics. Isothermal amplification techniques (e.g., loop-mediated isothermal amplification) are promising for the low-cost and integrated nucleic acid analysis. Here, parameters that effect the nucleic acid amplification time in microPCR systems are quantitatively evaluated and analyzed. Till date, the fastest nucleic acid amplification for static chamber and flow-through micro-PCR system is reported in 5.67 min and 90 s, respectively. For static chamber microPCR systems, application of integrated thin film heater and highly conductive microchip lowers the thermal mass, reduce the thermal transition time, increase heating/cooling rates, and reduce the nucleic acid amplification time. Amplification time for static chamber microPCR systems can be further reduced (e.g., to 4 min) by applying IR-based non-contact heaters. However, it would not be a practical option for cost-effective POC diagnostic devices. Application of high flow-rates and smaller channel cross-sectional areas reduces the amplification time in flow-through micro-PCR systems. However, to achieve specificity and reproducibility in microPCR assays, extensive surface treatment and optimization of flow-rate, channel area, and length are needed. Examples of integrated microPCR systems show the possibility of POC disease diagnostics. However, they are still expensive to apply for resource-limited settings. In fact it has been shown that the commercial POC diagnostic systems based on isothermal assays are considerably cheaper than systems with PCR-based assays. Examples of instrument-free LAMP systems and simpler sample processing in LAMP assays have been demonstrated. However, completely integrated LAMP-based nucleic acid amplification device with on chip sample processing has yet to be achieved. There is possibility

to translate microLAMP assays into rapid, sensitive, specific, multiplex, and low-cost diagnostic platforms. Comparison of microPCR with microLAMP systems shows that the latter is equally sensitive, specific and rapid in addition to being simpler and less expensive due its isothermal character. It is essential that nucleic acid amplification steps should be integrated with sample preparation and detection steps to establish a completely integrated POC infectious disease diagnostic devices. Almost all the analytical steps of sample processing, amplification, and detection have reached to a mature stage. The next step should be the integration and automation of all the functionalities to realize integrated diagnostic systems.

REFERENCES

2.9 References

Abe T, Segawa Y, Watanabe H, Yotoriyama T, Kai S, Yasuda A, Shimizu N, Tojo N (2011) Point-of-care testing system enabling 30 min detection of influenza genes. Lab on a Chip 11:1166-1167

Agrawal N, Hassan YA, Ugaz VM (2007) A pocket-sized convective PCR thermocycler. Angew Chem Int Ed 46:4316-4319

Ahmad F, Seyrig G, Stedtfeld RD, Tourlousse DM, Tiedje JM, Hashsham SA (2011) A CCD-based fluorescence imaging system for real-time loop-mediated isothermal amplification-based rapid and sensitive detection of waterborne pathogens on microchips. Biomedical Microdevices 13:929-937

Belgrader P, Benett W, Hadley D, Long G, Mariella R, Milanovich F, Nasarabadi S, Nelson W, Richards J, Stratton P (1998) Rapid pathogen detection using a microchip PCR array Instrument. Clin Chem 44:2191-2194

Beyor N, Yi LN, Seo TS, Mathies RA (2009a) Integrated capture, concentration, polymerase chain reaction, and capillary electrophoretic analysis of pathogens on a chip. Analytical Chemistry 81:3523-3528

Beyor N, Yi LN, Seo TS, Mathies RA (2009b) Integrated Capture, Concentration, Polymerase Chain Reaction, and Capillary Electrophoretic Analysis of Pathogens on a Chip. Anal Chem 81:3523-3528

Burns MA, Johnson BN, Brahmasandra SN, Handique K, Webster JR, Krishnan M, Sammarco TS, Man PM, Jones D, Heldsinger D, Mastrangelo CH, Burke DT (1998) An integrated nanoliter DNA analysis device. Science 282:484-487

Cady NC, Stelick S, Kunnavakkam MV, Batt CA (2005a) Real-time PCR detection of Listeria monocytogenes using an integrated microfluidics platform. Sensors and Actuators B-Chemical 107:332-341

Cady NC, Stelick S, Kunnavakkam MV, Batt CA (2005b) Real-time PCR detection of Listeria monocytogenes using an integrated microfluidics platform. Sens Actuators B-Chemical 107:332-341

Chen D, Mauk M, Qiu X, Liu C, Kim J, Ramprasad S, Ongagna S, Abrams WR, Malamud D, Corstjens PL, Bau HH (2010) An integrated, self-contained microfluidic cassette for isolation, amplification, and detection of nucleic acids. Biomed Microdevices 12:705-719

Chen S, Ge B (2010) Development of a toxR-based loop-mediated isothermal amplification assay for detecting Vibrio parahaemolyticus. BMC Microbiology 10:1-9

Cho YK, Kim J, Lee Y, Kim YA, Namkoong K, Lim H, Oh KW, Kim S, Han J, Park C, Pak YE, Ki CS, Choi JR, Myeong HK, Ko C (2006a) Clinical evaluation of micro-scale chip-based PCR system for rapid detection of hepatitis B virus. Biosens Bioelectron 21:2161-2169

Cho YK, Kim J, Lee Y, Kim YA, Namkoong K, Lim H, Oh KW, Kim S, Han J, Park C, Pak YE, Ki CS, Choi JR, Myeong HK, Ko C (2006b) Clinical evaluation of micro-scale chip-based PCR system for rapid detection of hepatitis B virus. Biosensors and Bioelectronics 21:2161-2169

Chou CF, Changrani R, Roberts P, Sadler D, Burdon J, Zenhausern F, Lin S, Mulholland A, Swami N, Terbrueggen R (2002a) A miniaturized cyclic PCR device - modeling and experiments. Microelectron Eng 61:921-925

Chou CF, Changrani R, Roberts P, Sadler D, Burdon J, Zenhausern F, Lin S, Mulholland A, Swami N, Terbrueggen R (2002b) A miniaturized cyclic PCR device - modeling and experiments. Microelectronic Engineering 61:921-925

Compton J (1991) Nucleic-Acid Sequence-Based Amplification. Nature 350:91-92

Crews N, Wittwer C, Gale B (2008) Continuous-flow thermal gradient PCR. Biomed Microdevices 10:187-195

Curcio M, Roeraade J (2003) Continuous segmented-flow polymerase chain reaction for high-throughput miniaturized DNA amplification. Anal Chem 75:1-7

Dahl A, Sultan M, Jung A, Schwartz R, Lange M, Steinwand M, Livak KJ, Lehrach H, Nyarsik L (2006a) Quantitative PCR based expression analysis on a nanoliter scale using polymer nano-well chips. Biomedical Microdevices 9:307-314

Dahl A, Sultan M, Jung A, Schwartz R, Lange M, Steinwand M, Livak KJ, Lehrach H, Nyarsik L (2006b) Quantitative PCR based expression analysis on a nanoliter scale using polymer nano-well chips. Biomed Microdevices 9:307-314

Dinca MP, Gheorghe M, Aherne M, Galvin P (2009) Fast and accurate temperature control of a PCR microsystem with a disposable reactor. J Micromech Microeng 19:1-15

Easley CJ, Karlinsey JM, Bienvenue JM, Legendre LA, Roper MG, Feldman SH, Hughes MA, Hewlett EL, Merkel TJ, Ferrance JP, Landers JP (2006a) A fully integrated microfluidic genetic analysis system with sample-in-answer-out capability. Proc Natl Acad Sci USA 103:19272-19277

Easley CJ, Karlinsey JM, Bienvenue JM, Legendre LA, Roper MG, Feldman SH, Hughes MA, Hewlett EL, Merkel TJ, Ferrance JP, Landers JP (2006b) A fully integrated microfluidic genetic analysis system with sample-in-answer-out capability. Proceedings of the National Academy of Sciences of the United States of America 103:19272-19277

El-Ali J, Perch-Nielsen IR, Poulsen CR, Bang DD, Telleman P, Wolff A (2004a) Simulation and experimental validation of a SU-8 based PCR thermocycler chip with integrated heaters and temperature sensor. Sensors and Actuators A 110:3-10

El-Ali J, Perch-Nielsen IR, Poulsen CR, Bang DD, Telleman P, Wolff A (2004b) Simulation and experimental validation of a SU-8 based PCR thermocycler chip with integrated heaters and temperature sensor. Sens Actuators, A 110:3-10

Fang X, Chen, H., Yu, S., Jiang, X., Kong, J., (2010) Predicting Viruses Accurately by a Multiplex Microfluidic Loop-Mediated Isothermal Amplification Chip. Analytical Chemistry 83:690-695

Fang X, Liu Y, Kong J, Jiang X (2010) Loop-Mediated Isothermal Amplification Integrated on Microfluidic Chips for Point-of-Care Quantitative Detection of Pathogens. Analytical Chemistry 82:3002-3006

Felbel J, Bieber I, Pipper J, Kohler JM (2004a) Investigations on the compatibility of chemically oxidized silicon (SiOx)-surfaces for applications towards chip-based polymerase chain reaction. Chemical Engineering Journal 101:333-338

Felbel J, Bieber I, Pipper J, Kohler JM (2004b) Investigations on the compatibility of chemically oxidized silicon (SiOx)-surfaces for applications towards chip-based polymerase chain reaction. Chem Eng J 101:333-338

Fiorini GS, Chiu DT (2005) Disposable microfluidic devices: fabrication, function, and application. Biotechniques 38:429-446

Gill P, Ghaemi A (2008) Nucleic acid isothermal amplification technologies - A review. Nucleosides Nucleotides & Nucleic Acids 27:224-243

Giordano BC, Copeland ER, Landers JP (2001a) Towards dynamic coating of glass microchip chambers for amplifying DNA via the polymerase chain reaction. Electrophoresis 22:334-340

Giordano BC, Ferrance J, Swedberg S, Huhmer AF, Landers JP (2001b) Polymerase chain reaction in polymeric microchips: DNA amplification in less than 240 seconds. Analytical Biochemistry 291:124-132

Giordano BC, Ferrance J, Swedberg S, Huhmer AF, Landers JP (2001c) Polymerase chain reaction in polymeric microchips: DNA amplification in less than 240 seconds. Anal Biochem 291:124-132

Gracias KS, McKillip JL (2007) Nucleic acid sequence-based amplification (NASBA) in molecular bacteriology: A procedural guide. Journal of Rapid Methods and Automation in Microbiology 15:295-309

Grodzinski PL, R.H.Chen, B.Blackwell, J., Liu Y, Rhine D, Smekal T, Ganser D, Romero C, Yu H, Chan T, Kroutchinina N (2001) Development of Plastic Microfluidic Devices for Sample Preparation. Biomed Microdevices 3:275-283

Gulliksen A, Solli L, Karlsen F, Rogne H, Hovig E, Nordstrom T, Sirevag R (2004) Real-time nucleic acid sequence-based amplification in nanoliter volumes. Analytical Chemistry 76:9-14

Hashimoto M, Barany F, Soper SA (2006a) Polymerase chain reaction/ligase detection reaction/hybridization assays using flow-through microfluidic devices for the detection of low-abundant DNA point mutations. Biosensors and Bioelectronics 21:1915-1923

Hashimoto M, Barany F, Soper SA (2006b) Polymerase chain reaction/ligase detection reaction/hybridization assays using flow-through microfluidic devices for the detection of low-abundant DNA point mutations. Biosens Bioelectron 21:1915-1923

Hashimoto M, Chen PC, Mitchell MW, Nikitopoulos DE, Soper SA, Murphy MC (2004a) Rapid PCR in a continuous flow device. Lab Chip 4:638-645

Hashimoto M, Chen PC, Mitchell MW, Nikitopoulos DE, Soper SA, Murphy MC (2004b) Rapid PCR in a continuous flow device. Lab on a Chip 4:638-645

Hatano B, Maki T, Obara T, Fukumoto H, Hagisawa K, Matsushita Y, Okutani A, Bazartseren B, Inoue S, Sata T, Katano H (2010) LAMP using a disposable pocket warmer for anthrax detection, a highly mobile and reliable method for anti-bioterrorism. Japanese Journal of Infectious Diseases 63:36-40

Higgins JA, Nasarabadi S, Karns JS, Shelton DR, Cooper M, Gbakima A, Koopman RP (2003) A handheld real time thermal cycler for bacterial pathogen detection. Biosens Bioelectron 18:1115-1123

Hofmann WP, Dries V, Herrmann E, Gartner B, Zeuzem S, Sarrazin C (2005) Comparison of transcription mediated amplification (TMA) and reverse transcription polymerase chain reaction (RT-PCR) for detection of hepatitis C virus RNA in liver tissue. Journal of Clinical Virology 32:289-293

House DL, Chon CH, Creech CB, Skaar EP, Li DQ (2010) Miniature on-chip detection of unpurified methicillin-resistant Staphylococcus aureus (MRSA) DNA using real-time PCR. Journal of Biotechnology 146:93-99

Hsieh TM, Luo CH, Lee GB, Liao CS, Huang FC (2005a) A Micromachined Low-power-consumption Portable PCR System. J Med Biol Eng 26:43-49

Hsieh TM, Luo CH, Lee GB, Liao CS, Huang FC (2005b) A Micromachined Low-power-consumption Portable PCR System. Journal of Medical and Biological Engineering 26:43-49

Huang FC, Liao CS, Lee GB (2006) An integrated microfluidic chip for DNA/RNA amplification, electrophoresis separation and on-line optical detection. Electrophoresis 27:3297-3305

Huhmer AF, Landers JP (2000a) Noncontact infrared-mediated thermocycling for effective polymerase chain reaction amplification of DNA in nanoliter volumes. Analytical Chemistry 72:5507-5512

Huhmer AF, Landers JP (2000b) Noncontact infrared-mediated thermocycling for effective polymerase chain reaction amplification of DNA in nanoliter volumes. Anal Chem 72:5507-5512

Iwasaki M, Yonekawa T, Otsuka K, Suzuki W, Nagamine K, Hase T, Tatsumi K, Horigome T, Notomi T, Kanada H (2003) Validation of the loop-mediated isothermal amplification method for single nucleotide polymorphism genotyping with whole blood. Genome Letters 2:119-126

Jayawardena S, Cheung CY, Barr I, Chan KH, Chen HL, Guan Y, Peiris JSM, Poon LLM (2007) Loop-mediated isothermal amplification for influenza A (H5N1) virus. Emerging Infectious Diseases 13:899-901

Jia HX, Li ZP, Liu CH, Cheng YQ (2010) Ultrasensitive detection of microRNAs by exponential isothermal amplification. Angewandte Chemie-International Edition 49:5498-5501

Kaigala GV, Hoang VN, Stickel A, Lauzon J, Manage D, Pilarski LM, Backhouse CJ (2008) An inexpensive and portable microchip-based platform for integrated RT-PCR and capillary electrophoresis. Analyst 133:331-338

Kaigala GV, Huskins RJ, Preiksaitis J, Pang XL, Pilarski LM, Backhouse CJ (2006) Automated screening using microfluidic chip-based PCR and product detection to assess risk of BK virus-associated nephropathy in renal transplant recipients. Electrophoresis 27:3753-3763

Khandurina J, McKnight TE, Jacobson SC, Waters LC, Foote RS, Ramsey JM (2000a) Integrated system for rapid PCR-based DNA analysis in microfluidic devices. Analytical Chemistry 72:2995-3000

Khandurina J, McKnight TE, Jacobson SC, Waters LC, Foote RS, Ramsey JM (2000b) Integrated system for rapid PCR-based DNA analysis in microfluidic devices. Anal Chem 72:2995-3000

Kim JA, Lee JY, Seong S, Cha SH, Lee SH, Kim JJ, Park TH (2006) Fabrication and characterization of a PDMS-glass hybrid continuous-flow PCR chip. Biochem Eng J 29:91-97

Kimura Y, Hoon MJLd, Aoki S, Ishizu Y, Kawai Y, Kogo Y, Daub CO, Lezhava A, Arner E, Hayashizaki Y (2011) Optimization of turn-back primers in isothermal amplification. Nucleic Acids Research 39:e59

Kopp MU, de Mello AJ, Manz A (1998) Chemical amplification: Continuous-flow PCR on a chip. Science 280:1046-1048

Krishnan M, Agrawal N, Burns MA, Ugaz VM (2004a) Reactions and fluidics in miniaturized natural convection systems. Anal Chem 76:6254-6265

Krishnan M, Burke DT, Burns MA (2004b) Polymerase chain reaction in high surface-to-volume ratio SiO2 microstructures. Anal Chem 76:6588-6593

Krishnan M, Ugaz VM, Burns MA (2002) PCR in a Rayleigh-Benard convection cell. Science 298:793

LaBarre P, Gerlach J, Wilmoth J, Beddoe A, Singleton J, Weigl B. (2010). Non-instrumented nucleic acid amplification (NINA): instrument-free molecular malaria diagnostics for low-resource settings, *32nd Annual International Conference of the IEEE EMBS* Buenos Aires, Argentina: IEEE.

LaBarre P, Hawkins KR, Gerlach J, Wilmoth J, Beddoe A, Singleton J, Boyle D, Weigl B (2011) A simple, inexpensive device for nucleic acid amplification without electricity-toward instrument-free molecular diagnostics in low-resource settings. Plos One 6:e19738

Lagally ET, Emrich CA, Mathies RA (2001) Fully integrated PCR-capillary electrophoresis microsystem for DNA analysis. Lab on a Chip 1:102-107

Lam L, Sakakihara S, Ishizuka K, Takeuchi S, Arata HF, Fujita H, Noji H (2008) Loop-mediated isothermal amplification of a single DNA molecule in polyacrylamide gel-based microchamber. Biomedical Microdevices 10:539-546

Leamon JH, Lee WL, Tartaro KR, Lanza JR, Sarkis GJ, deWinter AD, Berka J, Lohman KL (2003a) A massively parallel PicoTiterPlate (TM) based platform for discrete picoliter-scale polymerase chain reactions. Electrophoresis 24:3769-3777

Leamon JH, Lee WL, Tartaro KR, Lanza JR, Sarkis GJ, deWinter AD, Berka J, Weiner M, Rothberg JM, Lohman KL (2003b) A massively parallel PicoTiterPlate based platform for discrete picoliter-scale polymerase chain reactions. Electrophoresis 24:3769-3777

Lee D, La Mura M, Allnutt T, Powell W, Greenland A (2009) Isothermal amplification of genetically modified DNA sequences directly from plant tissues lowers the barriers to

high-throughput and field-based genotyping. Journal of Agricultural and Food Chemistry 57:9400-9402

Lee DS, Park SH, Yang HS, Chung KH, Yoon TH, Kim SJ, Kim K, Kim YT (2004) Bulk-micromachined submicroliter-volume PCR chip with very rapid thermal response and low power consumption. Lab on a Chip 4:401-407

Lee TMH, Hsing IM (2006) DNA-based bioanalytical microsystems for handheld device applications. Anal Chim Acta 556:26-37

Legendre LA, Bienvenue JM, Roper MG, Ferrance JP, Landers JP (2006) A simple, valveless microfluidic sample preparation device for extraction and amplification of DNA from nanoliter-volume samples. Anal Chem 78:1444-1451

Liao CS, Lee GB, Liu HS, Hsieh TM, Luo CH (2005a) Miniature RT-PCR system for diagnosis of RNA-based viruses. Nucleic Acids Research 33:e156

Liao CS, Lee GB, Liu HS, Hsieh TM, Luo CH (2005b) Miniature RT-PCR system for diagnosis of RNA-based viruses. Nucl Acids Res 33:e156

Lin YC, Yang CC, Huang MY (2000) Simulation and experimental validation of micro polymerase chain reaction chips. Sens Actuators, B 71:127-133

Liu C, Mauk MG, Bau HH (2011) A disposable, integrated loop-mediated isothermal ampification cassette with thermally actuated valves. Microfluidics and Nanofluidics:10.1007/s10404-10011-10788-10403

Liu CN, Toriello NM, Mathies RA (2006a) Multichannel PCR-CE microdevice for genetic analysis. Analytical Chemistry 78:5474-5479

Liu CN, Toriello NM, Mathies RA (2006b) Multichannel PCR-CE microdevice for genetic analysis. Anal Chem 78:5474-5479

Liu HB, Ramalingam N, Jiang Y, Dai CC, Hui KM, Gong HQ (2009) Rapid distribution of a liquid column into a matrix of nanoliter wells for parallel real-time quantitative PCR. Sensors and Actuators B-Chemical 135:671-677

Liu J, Hansen C, Quake SR (2003a) Solving the "world-to-chip" interface problem with a microfluidic matrix. Anal Chem 75:4718-4723

Liu J, Hansen C, Quake SR (2003b) Solving the "world-to-chip" interface problem with a microfluidic matrix. Analytical Chemistry 75:4718-4723

Liu YJ, Ganser D, Schneider A, Liu R, Grodzinski P, Kroutchinina N (2001a) Microfabricated polycarbonate CE devices for DNA analysis. Anal Chem 73:4196-4201

Liu YJ, Ganser D, Schneider A, Liu R, Grodzinski P, Kroutchinina N (2001b) Microfabricated polycarbonate CE devices for DNA analysis. Analytical Chemistry 73:4196-4201

Lutz S, Weber P, Focke M, Faltin B, Hoffmann J, Muller C, Mark D, Roth G, Munday P, Armes N, Piepenburg O, Zengerle R, von Stetten F (2010) Microfluidic lab-on-a-foil for nucleic acid analysis based on isothermal recombinase polymerase amplification (RPA). Lab on a Chip 10:887-893

Mabey D, Peeling RW, Ustianowski A, Perkinds MD (2004) Tropical infectious diseases: diagnostics for the developing world. Nature Reviews Microbiology 2:231-240

Mahalanabis M, Do J, ALMuayad H, Zhang JY, Klapperich CM (2010) An integrated disposable device for DNA extraction and helicase dependent amplification. Biomedical Microdevices 12:353-359

Marcus JS, Anderson WF, Quake SR (2006a) Parallel picoliter RT-PCR assays using microfluidics. Analytical Chemistry 78:956-958

Marcus JS, Anderson WF, Quake SR (2006b) Parallel picoliter RT-PCR assays using microfluidics. Anal Chem 78:956-958

Marcy Y, Ishoey T, Lasken RS, Stockwell TB, Walenz BP, Halpern AL, Beeson KY, Goldberg SMD, Quake SR (2007) Nanoliter reactors improve multiple displacement amplification of genomes from single cells. Plos Genetics 3:1702-1708

Mark D, Haeberle S, Roth G, von Stetten F, Zengerle R (2010) Microfluidic lab-on-a-chip platforms: requirements, characteristics and applications. Chem Soc Rev 39:1153-1182

Matsubara Y, Kerman K, Kobayashi M, Yamamura S, Morita Y, Takamura Y, Tamiya E (2004a) On-chip nanoliter-volume multiplex TaqMan polymerase chain reaction from a single copy based on counting fluorescence released microchambers. Anal Chem 76:6434-6439

Matsubara Y, Kerman K, Kobayashi M, Yamamura S, Morita Y, Takamura Y, Tamiya E (2004b) On-chip nanoliter-volume multiplex TaqMan polymerase chain reaction from a single copy based on counting fluorescence released microchambers. Analytical Chemistry 76:6434-6439

Matsubara Y, Kerman K, Kobayashi M, Yamamura S, Morita Y, Takamura Y, Tamiya E (2004c) On-chip nanoliter-volume multiplex TaqMan polymerase chain reaction from a single copy based on counting fluorescence released microchambers. Anal Chem 76:6434-6439

Matsubara Y, Kerman K, Kobayashi M, Yamamura S, Morita Y, Tamiya E (2005a) Microchamber array based DNA quantification and specific sequence detection from a single copy via PCR in nanoliter volumes. Biosens Bioelectron 20:1482-1490

Matsubara Y, Kerman K, Kobayashi M, Yamamura S, Morita Y, Tamiya E (2005b) Microchamber array based DNA quantification and specific sequence detection from a single copy via PCR in nanoliter volumes. Biosensors and Bioelectronics 20:1482-1490

Matsubara Y, Kerman K, Kobayashi M, Yamamura S, Morita Y, Tamiya E (2005c) Microchamber array based DNA quantification and specific sequence detection from a single copy via PCR in nanoliter volumes. Biosens Bioelectron 20:1482-1490

Matsubara Y, Kobayashi M, Morita Y, Tamiya E (2002) Application of a microchamber array for DNA amplification using a novel dispensing method. Archives of Histology and Cytology 65:481-488

Mori Y, Nagamine K, Tomita N, Notomi T (2001) Detection of loop-mediated isothermal amplification reaction by turbidity derived from magnesium pyrophosphate formation. Biochemical and Biophysical Research Communications 289:150-154

Mori Y, Notomi T (2009) Loop-mediated isothermal amplification (LAMP): A rapid, accurate, and cost-effective diagnostic method for infectious diseases. Journal of Infection and Chemotherapy 15:62-69

Munchow G, Dadic D, Doffing F, Hardt S, Drese KS (2005) Automated chip-based device for simple and fast nucleic acid amplification. Expert Rev Mol Diagn 5:613-620

Nagamine K, Hase T, Notomi T (2002) Accelerated reaction by loop-mediated isothermal amplification using loop primers. Molecular and Cellular Probes 16:223-229

Nakano H, Matsuda K, Yohda M, Nagamune T, Endo I, Yamane T (1994) High speed polymerase chain reaction in constant flow. Biosci Biotechnol Biochem 58:349-352

Nam JM, Stoeva SI, Mirkin CA (2004) Bio-bar-code-based DNA detection with PCR-like sensitivity. Journal of Americal Chemical Society 126:5932–5933

Nataro JP, Kaper JB (1998) Diarrheagenic Escherichia coli. Clin Microbiol Rev 11:142-201

Neuzil P, Novak L, Pipper J, Lee S, Ng LFP, Zhang CY (2010) Rapid detection of viral RNA by a pocket-size real-time PCR system. Lab on a Chip 10:2632-2634

Neuzil P, Zhang CY, Pipper J, Oh S, Zhuo L (2006a) Ultra fast miniaturized real-time PCR: 40 cycles in less than six minutes. Nucleic Acids Research 34:e77

Neuzil P, Zhang CY, Pipper J, Oh S, Zhuo L (2006b) Ultra fast miniaturized real-time PCR: 40 cycles in less than six minutes. Nucl Acids Res e34

Niemz A, Ferguson TM, Boyle DS (2011) Point-of-care nucleic acid testing for infectious diseases. Trends in Biotechnology 29:240-250

Northrup MA, Ching MT, White RM, Watson RT (1993a) DNA amplification with a microfabricated reaction chamber. Proc Transducers 93:924-926

Northrup MA, Ching MT, White RM, Watson RT (1993b) DNA amplification with a microfabricated reaction chamber. Proceedings of Transducers 93:924-926

Notomi T, Okayama H, Masubuchi H, Yonekawa T, Watanabe K, Amino N, Hase T (2000a) Loop-mediated isothermal amplification of DNA. Nucleic Acids Research 28

Notomi T, Okayama H, Masubuchi H, Yonekawa T, Watanabe K, Amino N, Hase T (2000b) Loop-mediated isothermal amplification of DNA. Nucleic Acids Research 28:e63

Obeid PJ, Christopoulos TK, Crabtree HJ, Backhouse CJ (2003a) Microfabricated device for DNA and RNA amplification by continuous-flow polymerase chain reaction and reverse transcription-polymerase chain reaction with cycle number selection. Anal Chem 75:288-295

Obeid PJ, Christopoulos TK, Crabtree HJ, Backhouse CJ (2003b) Microfabricated device for DNA and RNA amplification by continuous-flow polymerase chain reaction and reverse transcription-polymerase chain reaction with cycle number selection. Analytical Chemistry 75:288-295

Oda RP, Strausbauch MA, Huhmer AF, Borson N, Jurrens SR, Craighead J, Wettstein PJ, Eckloff B, Kline B, Landers JP (1998a) Infrared-mediated thermocycling for ultrafast polymerase chain reaction amplification of DNA. Analytical Chemistry 70:4361-4368

Oda RP, Strausbauch MA, Huhmer AF, Borson N, Jurrens SR, Craighead J, Wettstein PJ, Eckloff B, Kline B, Landers JP (1998b) Infrared-mediated thermocycling for ultrafast polymerase chain reaction amplification of DNA. Anal Chem 70:4361-4368

Pal R, Yang M, Lin R, Johnson BN, Srivastava N, Razzacki SZ, Chomistek KJ, Heldsinger DC, Haque RM, Ugaz VM, Thwar PK, Chen Z, Alfano K, Yim MB, Krishnan M, Fuller AO, Larson RG, Burke DT, Burns MA (2005) An integrated microfluidic device for influenza and other genetic analyses. Lab on a Chip 5:1024-1032

Pan XY, Jiang L, Liu KY, Lin BC, Qin JH (2010) A microfluidic device integrated with multichamber polymerase chain reaction and multichannel separation for genetic analysis. Analytica Chimica Acta 674:110-115

Park N, Kim S, Hahn JH (2003a) Cylindrical compact thermal-cycling device for continuous-flow polymerase chain reaction. Anal Chem 75:6029-6033

Park N, Kim S, Hahn JH (2003b) Cylindrical compact thermal-cycling device for continuous-flow polymerase chain reaction. Analytical Chemistry 75:6029-6033

Park S, Zhang Y, Lin S, Wang T-H, Yang S (2011) Advances in microfluidic PCR for point-of-care infectious disease diagnostics. Biotechnology Advances 29:830-839

Pavlov AR, Pavlova NV, Kozyavkin SA, Slesarev AI (2004) Recent developments in the optimization of thermostable DNA polymerases for efficient applications. Trends in Biotechnol 22:253-260

Piepenburg O, Williams CH, Stemple DL, Armes NA (2006) DNA detection using recombination proteins. Plos Biology 4:1115-1121

Pipper J, Inoue M, Ng LF, Neuzil P, Zhang Y, Novak L (2007a) Catching bird flu in a droplet. Nature Medicine 13:1259-1263

Pipper J, Inoue M, Ng LF, Neuzil P, Zhang Y, Novak L (2007b) Catching bird flu in a droplet. Nat Med 13:1259-1263

Pjescic I, Tranter C, Hindmarsh PL, Crews ND (2010a) Glass-composite prototying for flow PCR with in situ DNA analysis. Biomed Microdevices 12:333-343

Pjescic I, Tranter C, Hindmarsh PL, Crews ND (2010b) Glass-composite prototyping for flow PCR with in situ DNA analysis. Biomedical Microdevices 12:333-343

Poon LLM, Wong BWY, Ma EHT, Chan KH, Chow LMC, Abeyewickreme W, Tangpukdee N, Yuen KY, Guan Y, Looareesuwan S, Peiris JSM (2006) Sensitive and inexpensive molecular test for falciparum malaria: Detecting Plasmodium falciparum DNA directly from heat-treated blood by loop-mediated isothermal amplification. Clinical Chemistry 52:303-306

Prakash AR, Adamia S, Sieben V, Pilarski P, Pilarski LM, Backhouse CJ (2006a) Small volume PCR in PDMS biochips with integrated fluid control and vapour barrier. Sensors and Actuators B 113:398-409

Prakash AR, Adamia S, Sieben V, Pilarski P, Pilarski LM, Backhouse CJ (2006b) Small volume PCR in PDMS biochips with integrated fluid control and vapour barrier. Sens Actuators, B 113:398-409

Qiu XB, Mauk MG, Chen DF, Liu CC, Bau HH (2010) A large volume, portable, real-time PCR reactor. Lab on a Chip 10:3170-3177

Ramalingam N, Rui Z, Liu HB, Dai CC, Kaushik R, Ratnaharika B, Gong HQ (2010) Real-time PCR-based microfluidic array chip for simultaneous detection of multiple waterborne pathogens. Sensors and Actuators B-Chemical 145:543-552

Ramalingam N, San TC, Kai TJ, Mak MYM, Gong HQ (2009) Microfluidic devices harboring unsealed reactors for real-time isothermal helicase-dependent amplification. Microfluidics and Nanofluidics 7:325-336

Rodriguez I, Lesaicherre M, Tie Y, Zou Q, Yu C, Singh J, Meng LT, Uppili S, Li SF, Gopalakrishnakone P, Selvanayagam ZE (2003) Practical integration of polymerase chain reaction amplification and electrophoretic analysis in microfluidic devices for genetic analysis. Electrophoresis 24:172-178

Sadler DJ, Changrani R, Roberts P, Chou CF, Zenhausern F (2003a) Thermal management of BioMEMS: Temperature control for ceramic-based PCR and DNA detection devices. IEEE Trans Compon Packag Technol 26:309-316

Sadler DJ, Changrani R, Roberts P, Chou CF, Zenhausern F (2003b) Thermal management of BioMEMS: Temperature control for ceramic-based PCR and DNA detection devices. IEEE Transactions on Components and Packaging Technologies 26:309-316

Saiki RK, Gelfand DH, Stoffel S, Scharf SJ, Higuchi R, Horn GT, Mullis KB, Erlich HA (1988) Primer-Directed Enzymatic Amplification of DNA with a Thermostable DNA-Polymerase. Science 239:487-491

Sauer-Budge AF, Mirer P, Chatterjee A, Klapperich CM, Chargin D, Sharon A (2009) Low cost and manufacturable complete microTAS for detecting bacteria. Lab on a Chip 9:2803-2810

Schneegaß I, Brautigam R, Kohler JM (2001) Miniaturized flow-through PCR with different template types in a silicon chip thermocycler. Lab on a Chip 1:42-49

Seyrig G, Ahmad F, Stedtfeld RD, Tourlousse DM, Hashsham SA (2010). Simple, Powerful, and Smart: Using LAMP for Low Cost Screening of Multiple Waterborne Pathogens In K. Sen & N. J. Ashbolt (Eds.), Environmental Microbiology: Current Technology and Water Applications: Caister Academic Press 103-125

Shen F, Davydova EK, Du WB, Kreutz JE, Piepenburg O, Ismagilov RF (2011) Digital Isothermal Quantification of Nucleic Acids via Simultaneous Chemical Initiation of Recombinase Polymerase Amplification Reactions on SlipChip. Analytical Chemistry 83:3533-3540

Shen K, Chen X, Guo M, Cheng J (2005a) A microchip-based PCR device using flexible printed circuit technology. Sensors and Actuators B 105:251-258

Shen K, Chen X, Guo M, Cheng J (2005b) A microchip-based PCR device using flexible printed circuit technology. Sens Actuators, B 105:251-258

Shin YS, Cho K, Lim SH, Chung S, Park SJ, Chung C, Han DC, Chang JK (2003a) PDMS-based micro PCR chip with parylene coating. Journal of Micromechanics and Microengineering 13:768-774

Shin YS, Cho K, Lim SH, Chung S, Park SJ, Chung C, Han DC, Chang JK (2003b) PDMS-based micro PCR chip with parylene coating. J Micromech Microeng 13:768-774

Shin YS, Cho K, Lim SH, Chung S, Park SJ, Chung C, Han DC, Chang JK (2003c) PDMS-based micro PCR chip with parylene coating. J Micromech Microeng 13:768-774

Shoffner MA, Cheng J, Hvichia GE, Kricka LJ, Wilding P (1996a) Chip PCR. I. Surface passivation of microfabricated silicon-glass chips for PCR. Nucl Acids Res 24:375-379

Shoffner MA, Cheng J, Hvichia GE, Kricka LJ, Wilding P (1996b) Chip PCR. I. Surface passivation of microfabricated silicon-glass chips for PCR. Nucleic Acids Res 24:375-379

Shoffner MA, Cheng J, Hvichia GE, Kricka LJ, Wilding P (1996c) Chip PCR. I. Surface passivation of microfabricated silicon-glass chips for PCR. Nucleic Acids Research 24:375-379

Stedtfeld RD. (2009). *Development and validation of a multiplex hand-held gene analyzer.* Unpublished PhD Dissertation, Michigan State University, East Lansing.

Sun K, Yamaguchi A, Ishida Y, Matsuo S, Misawa H (2002) A heater-integrated transparent microchannel chip for continuous-flow PCR. Sens Actuators, B 84:283-289

Sun Y, Satyanarayan MVD, Nguyen NT, Kwok YC (2008) Continuous flow polymerase chain reaction using a hybrid PMMA-PC microchip with improved heat tolerance. Sens Actuators, B 130:836-841

Swerdlow H, Jones BJ, Wittwer CT (1997a) Fully automated DNA reaction and analysis in a fluidic capillary instrument. Analytical Chemistry 69:848-855

Swerdlow H, Jones BJ, Wittwer CT (1997b) Fully automated DNA reaction and analysis in a fluidic capillary instrument. Anal Chem 69:848-855

Tourlousse DM. (2010). *Development of low-cost and easy-to-use tools for multiplex pathogen detection.* Unpublished PhD dissertation, Michigan State University, East Lansing.

Tsaloglou MN, Bahi MM, Waugh EM, Morgan H, Mowlem M (2011) On-chip real-time nucleic acid sequence-based amplification for RNA detection and amplification. Analytical Methods 3:2127-2133

Vincent M, Xu Y, Kong HM (2004) Helicase-dependent isothermal DNA amplification. Embo Reports 5:795-800

Wang W, Li ZX, Luo R, Lu SH, Xu AD, Yang YJ (2005) Droplet-based micro oscillating-flow PCR chip. J Micromech Microeng 15:1369-1377

Wang Z, Sekulovic A, Kutter JP, Bang DD, Wolff A (2006) Towards a portable microchip system with integrated thermal control and polymer waveguides for real-time PCR. Electrophoresis 27:5051-5058

Waters LC, Jacobson SC, Kroutchinina N, Khandurina J, Foote RS, Ramsey JM (1998a) Multiple sample PCR amplification and electrophoretic analysis on a microchip. Anal Chem 70:5172-5176

Waters LC, Jacobson SC, Kroutchinina N, Khandurina J, Foote RS, Ramsey JM (1998b) Multiple sample PCR amplification and electrophoretic analysis on a microchip. Analytical Chemistry 70:5172-5176

Wilding P, Shoffner MA, Kricka LJ (1994a) PCR in a silicon microstructure. Clin Chem 40:1815-1818

Wilding P, Shoffner MA, Kricka LJ (1994b) PCR in a silicon microstructure. Clinical Chemistry 40:1815-1818

Wittwer CT, Fillmore GC, Hillyard DR (1989a) Automated Polymerase Chain-Reaction in Capillary Tubes with Hot Air. Nucl Acids Res 17:4353-4357

Wittwer CT, Fillmore GC, Hillyard DR (1989b) Automated Polymerase Chain-Reaction in Capillary Tubes with Hot Air. Nucleic Acids Research 17:4353-4357

Wu J, Kodzius R, Xiao K, Qin J, Wen W (2011a) Fast detection of genetic information by an optimized PCR in an interchangeable chip. Biomedical Microdevices:DOI 10.1007/s10544-10011-19595-10546

Wu QQ, Jin W, Zhou C, Han SH, Yang WX, Zhu QY, Jin QH, Mu Y (2011b) Integrated glass microdevice for nucleic acid purification, loop-mediated isothermal amplification, and online detection. Analytical Chemistry 83:3336-3342

Xiang Q, Xu B, Fu R, Li D (2005a) Real time PCR on disposable PDMS chip with a miniaturized thermal cycler. Biomedical Microdevices 7:273-279

Xiang Q, Xu B, Fu R, Li D (2005b) Real time PCR on disposable PDMS chip with a miniaturized thermal cycler. Biomed Microdevices 7:273-279

Xiaoyu J, Zhiqiang N, Wenyuan C, Weiping Z (2005) Polydimethylsiloxane (PDMS)-based spiral channel PCR chip. Electron Lett 41:890-891

Yager P, Domingo GJ, Gerdes J (2008) Point-of-care diagnostics for global health. Annual Review of Biomedical Engineering 10:107-144

Zhang CS, Xing D (2007a) Miniaturized PCR chips for nucleic acid amplification and analysis: latest advances and future trends. Nucleic Acids Research 35:4223-4237

Zhang CS, Xing D (2007b) Miniaturized PCR chips for nucleic acid amplification and analysis: latest advances and future trends. Nucl Acids Res 35:4223-4237

Zhang CS, Xu JL, Ma WL, Zheng WL (2006) PCR microfluidic devices for DNA amplification. Biotechnology Advances 24:243-284

Zhang Y, Ozdemir P (2009) Microfluidic DNA amplification--a review. Analytica Chimica Acta 638:115-125

Zhang Y, Park S, Yang S, Wang TH (2010) An all-in-one microfluidic device for parallel DNA extraction and gene analysis. Biomedical Microdevices 12:1043-1049

Zou QB, Miao YB, Chen Y, Sridhar U, Chong CS, Chai TC, Tie Y, Teh CHL, Lim TM, Heng C (2002) Micro-assembled multi-chamber thermal cycler for low-cost reaction chip thermal multiplexing. Sens Actuators, A 102:114-121

Zou ZQ, Chen X, Jin QH, Yang MS, Zhao JL (2005a) A novel miniaturized PCR multi-reactor array fabricated using flip-chip bonding techniques. J Micromech Microeng 15:1476-1481

Zou ZQ, Chen X, Jin QH, Yang MS, Zhao JL (2005b) A novel miniaturized PCR multi-reactor array fabricated using flip-chip bonding techniques. Journal of Micromechanics and Microengineering 15:1476-1481

CHAPTER III

3. A CCD-BASED FLUORESCENCE IMAGING SYSTEM FOR REAL-TIME LOOP-MEDIATED ISOTHERMAL AMPLIFICATION-BASED RAPID AND SENSITIVE DETECTION OF WATERBORNE PATHOGENS ON MICROCHIPS

3.1 Introduction

Waterborne bacteria and protozoa that have been commonly associated with disease outbreaks are *Campylobacter jejuni*, *Escherichia coli* O157:H7, *Legionella pneumophila*, *Shigella flexneri*, *Salmonella enterica*, *Vibrio cholerae*, *Cryptosporidium parvum*, and *Giardia intestinalis* (Lee 2002; Hoffman et al. 2009). Some of these pathogens such as *C. jejuni*, *E. coli* O157: H7, and *S. enterica* have also been implicated in outbreaks of food-related illnesses (Boore et al. 2010). In the United States, 833 documented waterborne disease outbreaks have occurred between 1971 and 2006 resulting in 577,991 cases of illness and 106 deaths (Craun et al. 2010). In many cases, these deaths are due to the lack of appropriate diagnosis rather than availability of effective and economical prevention and treatment options (Yager et al. 2008).

In recent times, isothermal nucleic acid amplification techniques including, helicase-dependent amplification (Vincent et al. 2004), recombinase polymerase reaction (Piepenburg et al. 2006), and loop-mediated isothermal amplification (LAMP) (Notomi et al. 2000) have been developed for sensitive and specific detection of pathogenic microorganisms. LAMP has attracted most attention due to its simplicity, ruggedness, and low-cost (Poon et al. 2006). Aside from its isothermal character, important features of LAMP include, moderate reaction temperature of 63 ^{o}C, excellent specificity due to the use of 4 to 6 specific primers, need for a single enzyme, and superior tolerance to substances that typically inhibit PCR (Kaneko et al.

2007). Another advantage of LAMP is the generation of high amounts of white magnesium pyrophosphate precipitate and DNA amplicon (~400 ng /µL) (Mori et al. 2001), allowing a simpler and inexpensive means for detection. A positive LAMP reaction in 0.2 mL PCR vials is confirmed by observing the turbidity (Mori et al. 2001) or fluorescence (Chen and Ge 2010), either in endpoint or real-time formats by using water bath or commercial real-time PCR instrument (Mori and Notomi 2009). Amplification times of tube-based LAMP assays typically vary between 30-90 min, depending on the starting DNA template (Seyrig et al. 2011).

Endpoint and real-time LAMP assays employed with turbidity or fluorescence-based detection schemes have also been translated on microchips for point-of-care diagnostics (Niemz et al. 2011). Positive endpoint microLAMP is confirmed either visually (Fang 2010) or by fluorescence microscopy (Matsubara et al. 2002; Lam et al. 2008). Fluorescence (Abe et al. 2011; Liu et al. 2011) or turbidity (Fang et al. 2010) increment during real-time microLAMP is monitored by photodiodes. MicroLAMP is quantified by measuring the threshold time (Tt) for a selected cutoff of signal, where the signal is above the background (Fang et al. 2010; Abe et al. 2011). Due to low responsivity (ratio of generated photocurrent to incident photons) and lack of any exposure control or internal gain features in simple photodiodes (Kostov 2009), reaction time for real-time microLAMP is generally fixed and depends on the characteristics of LAMP primers and target DNA, amount of target DNA, and reaction conditions (Kimura et al. 2011). A same set of LAMP primers under the similar reaction conditions has been evaluated for endpoint LAMP by gel electrophoresis (En et al. 2008) and real-time turbidity-based microLAMP by photodiode (Fang et al. 2010). Detection time of approximately 1 h and a sensitivity of 10 fg / µl were achieved on both formats. Photodetectors such as avalanche photodiodes and silicon

photomultipliers can internally amplify the current up to 10^7-fold, drastically enhancing the responsivity, but they have not yet applied to microLAMP assays (Grigoriev et al. 2007).

On the other hand, increasing the CCD exposure time improves signal-to-background (Yang et al. 2008) or signal-to-noise ratio (SNR) (Pjescic et al. 2010), enhancing the detection limit of biochemical assays. Additionally, application of a DNA intercalating dye like Syto-82 to real-time PCR showed comparatively higher fluorescence signal than the background (Gudnason et al. 2007). Therefore, increasing the CCD exposure time might increase the SNR and reduce Tt of Syto-82-based microRT$_f$-LAMP, due to the direct relation between the exposure time and SNR and inverse relation between SNR and Tt. However, the effect of CCD exposure time on the SNR or Tt of microRT$_f$-LAMP has not yet been reported. To our knowledge, this is the first report applying a simple CCD camera for monitoring microRT$_f$-LAMP assays of waterborne pathogens. Also CCD has wider field-of-view than photodiodes, providing high throughput gene amplification detection (Dahl et al. 2007).

In this study, a $300 CCD camera, commonly used for astronomical imaging, was optimized for monitoring RT$_f$-LAMP assays of 6 waterborne pathogens on polymeric microchips. Also the effect of CCD exposure time on the SNR and Tt of microRT$_f$-LAMP assays was evaluated. RT$_f$-LAMP assay on microchip required only 2 μL of sample volume and can be completed within 20 min with sensitivity of a single DNA copy. This low-cost CCD-based fluorescence imaging system can be applied to high throughput microfluidic chips for rapid and parallel detection of pathogens in low resource settings.

3.2 Materials and methods

3.2.1 DNA targets

Genomic DNA of *S. enterica* (700702D), *C. parvum* (PRA67D), *C. jejuni* (700819D), *L. pneumophila* (33152D), *E. coli* O157:H7 (BAA460D), and *V. cholerae* (39315) was obtained from the American Type Culture Collection (ATCC, Manassas, VA). Before use, dried genomic DNA was resuspended in nuclease-free sterile water (Fischer Scientific, Pittsburgh, PA). Double stranded DNA standard (1 kb, 1 µg/µL) was obtained from Invitrogen (Invitrogen Corporation, Carlsbad, CA).

3.2.2 LAMP primer design

LAMP primers were designed for 11 virulence genes specific to 6 waterborne pathogens (Table 3.1). For *C. jejuni* 0414 gene, primers from the literature were used (Yamazaki et al. 2008). Sequences of all primers are provided in the appendix. Prior to primer design, consensus sequences were generated by aligning multiple gene sequences with Bioedit Sequence Alignment Editor (Ibis Biosciences, Carlsbad, CA). A set of six specific LAMP primers (F3, B3, FIP, BIP, LF and LB) were designed for each target by using Primer Explorer V4 (Eiken Chemicals Co., Tokyo, Japan). Primers were synthesized by Integrated DNA Technologies (IDT, Coralville, IA).

Table 3.1 Genes selected for detection of pathogenic microorganisms

Microorganism	Gene target(s)	Description
Cryptosporidium parvum	gp60	60 kDa glycoprotein
	hsp70	70 kDa heat shock protein
Legionella pneumophila	dotA	cytoplasmic protein
	lepB	effector protein
Vibrio cholerae	ctxA	cholera toxin
	toxR	two-component regulator
Campylobacter jejuni	0414	oxidoreductase subunit
	cdtA	cytolethal distending toxin
Escherichia coli O157:H7	eae	intimin
	stx2	shiga-toxin 2
Salmonella enterica	invA	invasion protein
	phoB	response regulator

3.2.3 Microchip fabrication

Microchips with two different designs were fabricated for dsDNA standard dilution series imaging and monitoring RT_f-LAMP assays. Microchips used for dsDNA standard dilution series imaging consisted of 16 circular wells with 1 mm diameter and 2 µL volume per well. Microchips for RT_f-LAMP had seven V-shaped reaction wells with a volume of 2 µL per well (Figure 3.1). V-shaped reaction wells provided easy solution dispensing and effective sealing of microchip. Both types of microchips were fabricated with 100 µm thick ZeonorFilm® (ZF14-100; Zeon Chemicals, Louisville, KY) by hot embossing using a sacrificial thermoplastic counter tool (acrylonitrile butadiene styrene, ABS from K-mac Plastics). Embossing molds were fabricated via stereolithography (FineLine Prototyping; Raleigh, NC) with the circular and V-shaped features. A sheet of ZeonorFilm® was sandwiched between the ABS plastic and embossing mold, and preheated to 150 °C in a press (Carver press model 4386; Carver, Wabash, IN). An embossing pressure of 1000 lbs was applied for 3 min. The system was subsequently

cooled to 105 °C while maintaining the embossing pressure. Sample dispensing ports with 750 µm diameter were patterned into the PCR tape (MicroAmp® Optical Adhesive Film; Applied Biosystems; Foster City, CA) using a commercial-grade knife plotter (CraftROBO model CC33OL-20; Graphtec). The patterned PCR tape was manually aligned onto the chip, and pressed at 2000 lbs. with a piece of silicon rubber (70 A, McMaster-Carr, Los Angeles, CA) to seal the chip. Microchips used for dsDNA standard dilution series imaging were not sealed from the top.

3.2.4 Experimental setup

Gene amplification and detection system was built by integrating light source, optical filters, thin film heater, and a CCD camera (Figure 3.1). A 530 nm green LED (05027-PM12, LED Supply) was used as the excitation light source. The LED was attached to a black anodized aluminum heatsink (HS13137, LED Supply), optic holder (L2-OH-S35, LED Supply), collimating lens (L2-OP-025, LED Supply), and an engineered glass diffuser (ED1-C50, Thorlabs, Newton, NJ) to achieve widely distributed homogenous light. The LED was driven at 700 mA with a power supply (HY5003, Power Supply Depot, Lake Park, FL). The excitation light was filtered through a 534 ± 20 nm bandpass filter (FF01-534/20-25, Semrock, Rochester, NY). The emission light was filtered through a 572 ± 20 nm bandpass filter (FF01-572/28-25, Semrock) connected to the CCD camera. Imaging of microchips for dsDNA standard dilution series and RT_f-LAMP assays was done by a 16 bit, 0.25 megapixel monochrome CCD camera (MEADE DSI Pro, Irvine, CA) equipped with a 16 mm relay lens (15774, Deal Extreme). DSI Pro CCD is an interline-scan monochromatic camera commonly applied for astronomical

imaging (Gottscheber and Dech 2010). It is equipped with AutoStar Envisage imaging software with manual control over the gain (0-100), offset (0-100), and exposure time (0.1 ms-1 h). Offset and gain of the CCD camera were optimized as shown in the Figure 3.2. A gain of 100 and an offset of 60 were selected for imaging, as this combination provided the most optimum contrast in the images.

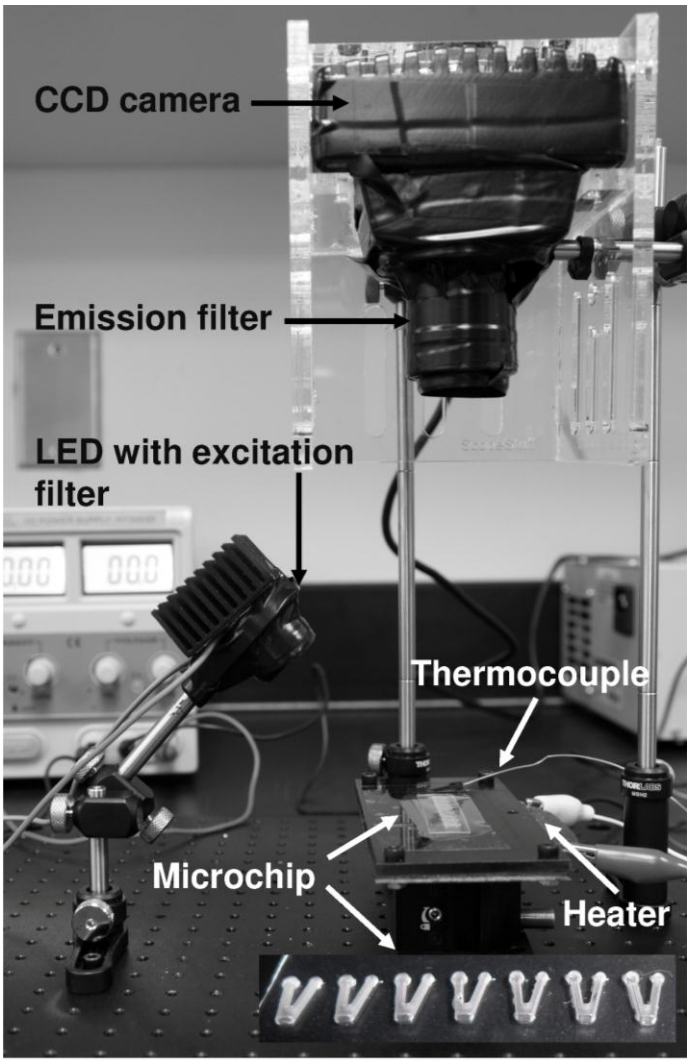

Figure 3.1 Photograph of the experimental setup consisting of an LED attached with excitation filter (534 ± 20 nm) for illumination, a thin film heater and thermocouple for temperature control, and a monochromatic CCD camera with emission filter (572 ± 20 nm) for imaging. The inset shows the microchip with seven V-shaped reaction wells used for RT_f-LAMP reactions. This system was placed in the dark during imaging to avoid any ambient light

The temperature control system consisted of a thermocouple (5SRTC-TT-T-40-36, Omega), a pulse width modulator IC (DRV102T, Texas Instruments), a USB DAQs (USB-DAQ 6009, National Instruments), a thin film heater (Electro-Flex Heat Inc.), and a LabVIEW VI developed in-house. To control the temperature of the microchip at 63 °C, a feedback mechanism involving (PID) and pulse width modulation (PWM) was implemented. Signals from the thermocouple were amplified and conditioned using a LabView thermocouple input module. The analog output generated from the PID controller was used to adjust the duty cycle of the PWM driver. The component cost of this experimental setup was approximately $1000.

3.2.5 DNA dilution series and real-time LAMP

Serial dilutions (10-fold) of dsDNA standards ranging from 5 ng / µL to 0.005 ng / µL were prepared in sterile water. dsDNA standard dilutions were mixed with 2 µM Syto-82. Negative control had only water and 2 µM of Syto-82 (Invitrogen Corporation, Carlsbad, CA). Approximately, 2 µL of dsDNA standard dilution series with 10 ng, 1 ng, 0.1 ng, 0.01 ng, and water were placed on the microchip with circular wells. All experiments were performed in triplicate.

Reaction mixtures for LAMP contained 1.6 µM each of FIP and BIP primer, 0.200 µM each of F3 and B3 primer, 0.8 µM each of LF and LB primer, 0.8 M betaine (Sigma, St Louis, MO), 1.4 mM of each dNTP (Invitrogen Corporation, Carlsbad, CA), 20 mM Tris-HCl (pH 8.8), 10 mM $(NH_4)_2SO_4$, 10 mM KCl, 8 mM $MgSO_4$, 8 mM Triton X-100, 0.64 units/µL of large fragment of *Bst* DNA polymerase (New England Biolabs Inc., Ipswich, MA), 2 µM of Syto-82, and 10^5 genomic copies of target DNA. To evaluate the dynamics of RT_f-LAMP and establish

standard curves for quantitative analysis, 10-fold serially diluted genomic DNA of *C. jejuni* ranging from 10^5 to 1 copy was prepared. LAMP reaction mixtures without any DNA template were also prepared to serve as negative controls. Positive and negative LAMP controls with the volume of 25 µL were loaded in 0.2 mL PCR tubes (VWR International, West Chester, PA) and incubated at 63 °C for 45 min on a commercial real-time PCR instrument (Chromo4™, Bio-Rad Laboratories, Hercules, CA). Fluorescence signals of the RT_f-LAMP assays were measured every minute in channel 2 (excitation wavelength range from 500-535 nm and emission wavelength range from 560-580 nm). For RT_f-LAMP on microchip, 2 µL of LAMP solutions was dispensed in each of the 6 wells using a pipettor, manually sealed with a PCR tape, and placed on the experimental setup for incubation at 63 °C. All experiments were performed in triplicate.

3.2.6 Fluorescence measurement, extraction, and analysis

Opticon™ software (Bio-Rad Laboratories, Hercules, CA) was used to measure and extract raw fluorescence signals of RT_f-LAMP assays on the real-time PCR instrument. For the florescence imagining system, CCD camera imaged the microchips and saved the images in flexible image transport system format. For dsDNA standard dilution series, images of the microchip (with circular wells) were recorded for increasing exposure times from 1 ms to 60 s. For microRT_f-LAMP assay, time-lapse images of microchip (with V-shaped wells) were recorded every 30 s at fixed exposure time. Imaging was stopped when the signals from the positive wells reached to saturation value of 65,535 a. u. CCD images were opened in Image J

(National Institutes of Health, Bethesda, MD) and a microarray profile plugin (http://www.optinav.com/imagej.html) was applied to extract fluorescence signals from all the wells. For dsDNA standard dilution series, average fluorescence signals from the triplicates were plotted with respected to exposure time. To calculate SNR values of RT_f-LAMP assays on real-time PCR instrument and microchip, raw signal intensities were baseline corrected by subtracting the average fluorescence signals obtained in the first 3 min and dividing by their standard deviation. Tt was then defined as the time at which the SNR reached an arbitrary cut-off of 10 or higher. SNR and the corresponding Tt values were calculated for individual LAMP reaction of triplicates and an average value of Tt is reported here. Fluorescence signals were normalized by dividing the all the signals with the maximum signal value. Average of the normalized fluorescence signals from the triplicates was plotted with respect to amplification time. Data analysis and plotting was done with Microsoft Excel (Microsoft, Redmond, WA).

3.3 Results and discussion

3.3.1 CCD optimization

To observe the effect of offset and gain on the fluorescence signal collected by CCD, COP microchip containing 10 ng dsDNA standard stained with 2 µM Syto-82 was imaged by the CCD camera with increasing offset and gain at a fixed exposure time of 1 s. An increase in the fluorescence signals was observed with increasing gain and offset values (Figure 3.2). Initially the gain and exposure time was fixed to 100 and 1 s respectively and the offset was varied from 0 to 100 then the offset and exposure time was fixed to 60 and 1 s respectively and the gain was varied from 0 to 100. For the first condition, fluorescence signal was saturated to 65,535 a. u. at a gain of 100 and an offset of 80. For the second condition, maximum fluorescence signal of

58,283 a. u. was observed at a gain of 100 and an offset of 60. However, for the same gain and offset of 100 and 60, the fluorescence signal was 62,208 a. u. in the first condition. As the circular well microchip used for DNA imaging was not sealed, solution evaporation might have increased the solution concentration, resulting in higher fluorescence signal in the first condition. A gain of 100 and an offset of 60 were selected for further CCD imaging, as this combination provided the most optimum contrast in the images.

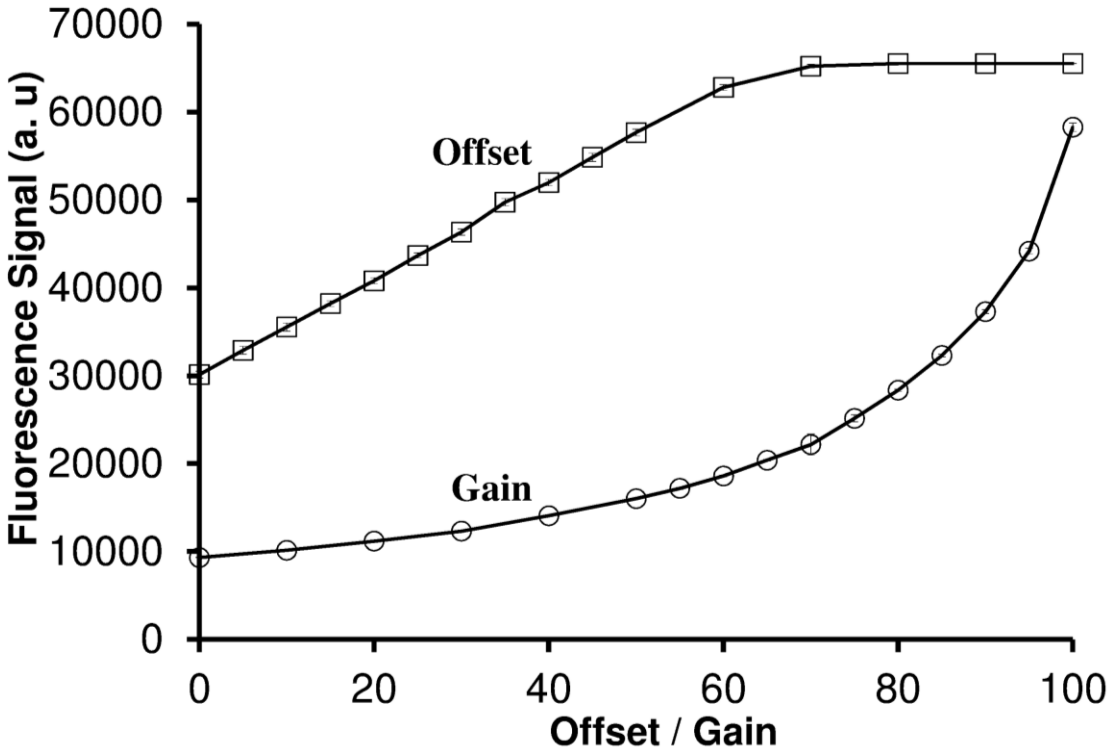

Figure 3.2 Optimization of offset and gain for the CCD camera. Plot of average fluorescence signal from 10 ng dsDNA standard stained with 2 µM Syto-82 with respect to increasing offset and gain at a fixed exposure time of 1 s.

3.3.2 Effect of CCD exposure time on the fluorescence signals of dsDNA standard dilution series

The effect of CCD exposure time on the fluorescence signals from 10 ng, 1 ng, 0.1 ng, 0.01 ng, and 0 ng dsDNA standard stained with 2 µM Syto-82 were evaluated by imaging the

microchip with increasing exposure times from 1 ms to 60 s. Images of dsDNA standard dilution series on microchip with increasing exposure times are shown in Figure 3.3.

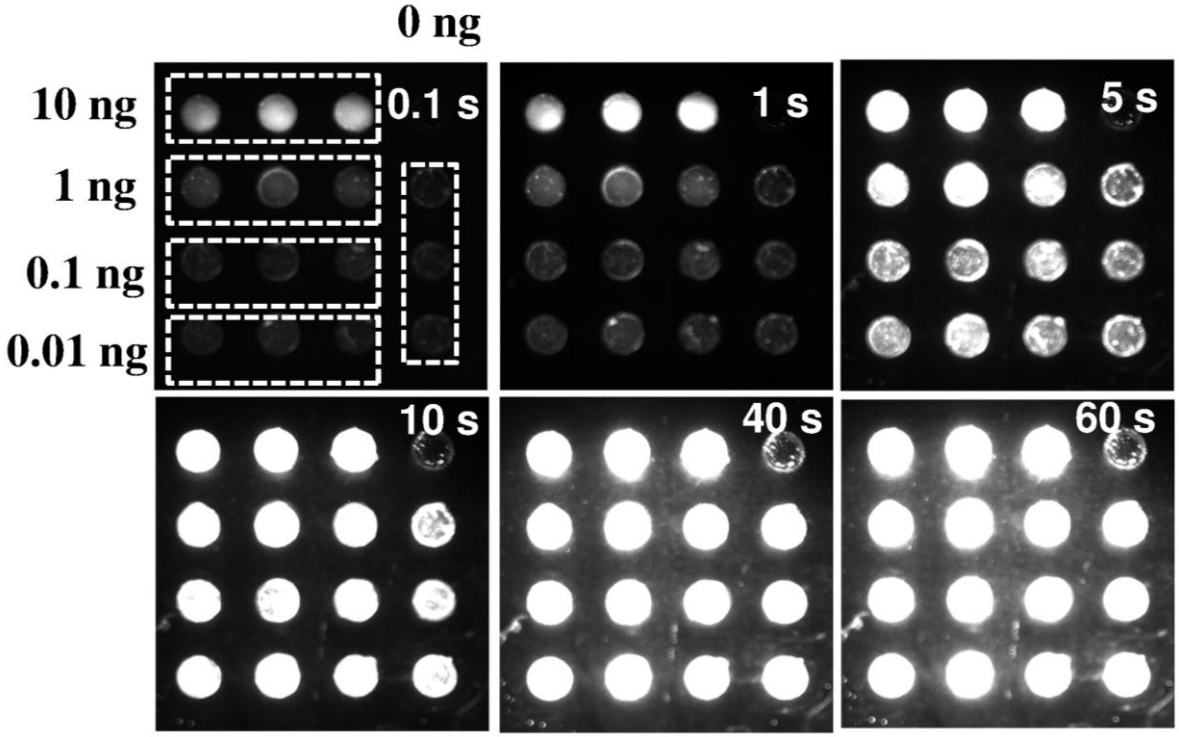

Figure 3.3 CCD images of 16 well microchip with dsDNA standard dilution series (10 ng, 1 ng, 0.1 ng, 0.01 ng, and negative control) stained with 2 µM Syto-82 and with increasing exposure times

The fluorescence signals from all the DNA concentrations and the negative controls increased with increasing exposure times and finally reached to saturation (Figure 3.4). From an exposure time between 1 ms to 0.1 s, fluorescence signals varied between 4,029 a. u. to 4,395 a. u. (background) and showed an exponential rise from exposure time between 0.1 s to 10 s. After 10 s of exposure time, the fluorescence signals reached the saturation value of 65,535 a. u. However, the fluorescence signals from 10 ng and 1 ng DNA showed an increase from 0.01 s exposure time. Also the fluorescence signals from 10 ng and 1 ng DNA were relatively higher than the signals from the negative control for the exposure time between 0.5 s to 5 s. For

example, fluorescence signals from 10 ng and 1 ng DNA were approximately 8-fold and 3-fold higher than negative control at 0.5 s of CCD exposure time and 6.5-fold and 5-fold higher than the negative control at 5 s of CCD exposure time, respectively. The lower fluorescence signals from the negative control in comparison to 10 ng and 1 ng DNA standard were due to the low autofluorescence of Syto-82 dye. Syto-82 has a substituted unsymmetrical cyanine structure, providing very low autofluorescence in unbound state due to flexibility of its structure in aqueous environment. This cyanine structure becomes rigid in the presence of nucleic acids, providing high fluorescence signals (Tarnok 2008; Deligeorgiev et al. 2009). (Gudnason et al. 2007) demonstrated a 50-fold lower detection limit with 2 µM Syto-82 in real-time PCR assay, when compared with 14 other DNA intercalating dyes. Fluorescence signals from 0.1 ng and 0.01 ng DNA were nearly similar to the fluorescence signals from the negative control for the applied CCD exposure times. This effect might be due to the lower amount of dsDNA standard available to bind with Syto-82 dye, producing the fluorescence signals similar to the negative control. We hypothesized that applying the exposure time effect to microRT$_f$-LAMP might lead to faster increment in SNR due to the collection of relatively higher fluorescence signals from the positive controls than the background, reducing the Tt of assay.

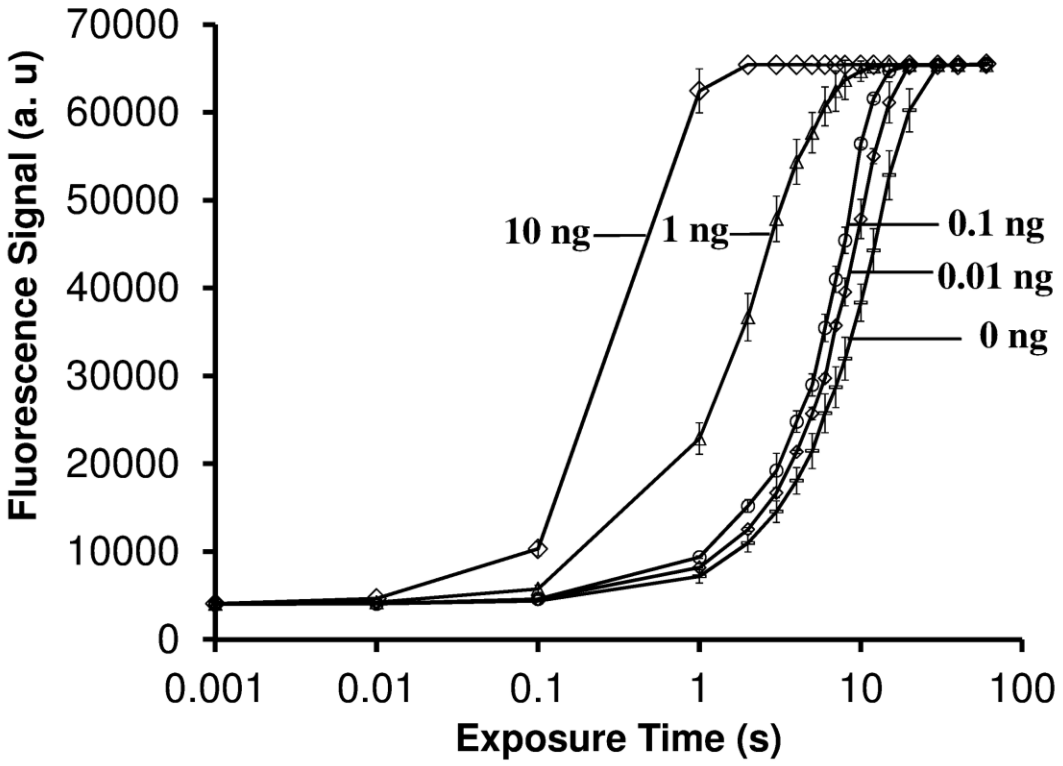

Figure 3.4 Plot of average fluorescence signal with respect to increasing exposure times for the dilution series of dsDNA standard (10 ng, 1 ng, 0.1 ng, 0.01 ng, and 0 ng) stained with 2 µM Syto-82

3.3.3 Effect of CCD exposure time on SNR and Tt values of microRT$_f$-LAMP assays

The effect of CCD exposure time on the SNR and Tt were evaluated for two different LAMP assays for *V. cholerae* toxR gene and *C. parvum* gp60 gene (10^5 gene copies) for the exposure time of 1 s, 3 s, and 5 s. CCD exposure time was limited to 5 s, as applying an exposure time higher than 5 s either saturated the signal in the positive wells or provided a high background. The SNR and Tt values of microRT$_f$-LAMP assays at these exposure times were also compared with a real-time PCR instrument. A systematic increment in the SNR and reduction in the Tt values of microRT$_f$-LAMP assays were obtained with increasing exposure

time as compared to the real-time PCR instrument (Table 3.2 and Figures 3.5 and 3.6). Negative controls did not show any increase in the fluorescence signal.

Table 3.2 Comparison of average SNR and Tt values of RT_f-LAMP for 10^5 DNA copies of *V. cholera* toxR gene and *C. parvum* gp60 gene on microchips (1 s, 3 s, and 5 s CCD exposure time) and the real-time PCR instrument. Standard deviations are the mean of Tt values from triplicates

Microorganism/gene	**SNR, Tt (min)** CCD system 1 s exposure	**SNR, Tt (min)** CCD system 3 s exposure	**SNR, Tt (min)** CCD system 5 s exposure	**SNR, Tt (min)** Chromo4™ -
V. cholera toxR	21.8, 5.8 ± 0.4	14.8, 5 ± 0.0	70.8, 5 ± 0.0	28.3, 7.7 ± 0.6
C. parvum gp60	12.1, 18.7 ± 0.3	12.6, 15 ± 0.0	206, 14.5 ± 0.0	16.3, 24.3± 1.2

For microRT_f-LAMP assay of *V. cholerae* toxR gene, SNR and Tt values for 1 s, 3 s, and 5 s CCD exposure times were 21.8 and 5.8 min, 14.8 and 5 min, and 70.8 and 5 min respectively. Tt at 3 s and 5 s of CCD exposure time was same as 5 min. However, SNR at 5 s of exposure time was approximately 5-fold higher than SNR at 3 s of exposure time. SNR and Tt for the same assay on the real-time PCR instrument were 28.3 and 7.7, respectively. Moreover, Tt values for the microRT_f-LAMP assay with all the applied CCD exposure times were lower than the Tt obtained on the real-time PCR instrument (Figure 3.5). Time lapse images of microchips during the amplification of *V. cholerae* toxR gene at 1s, 3s, and 5 s of exposure time showed that higher fluorescence signals were achieved faster at higher exposure time (Figure 3.7).

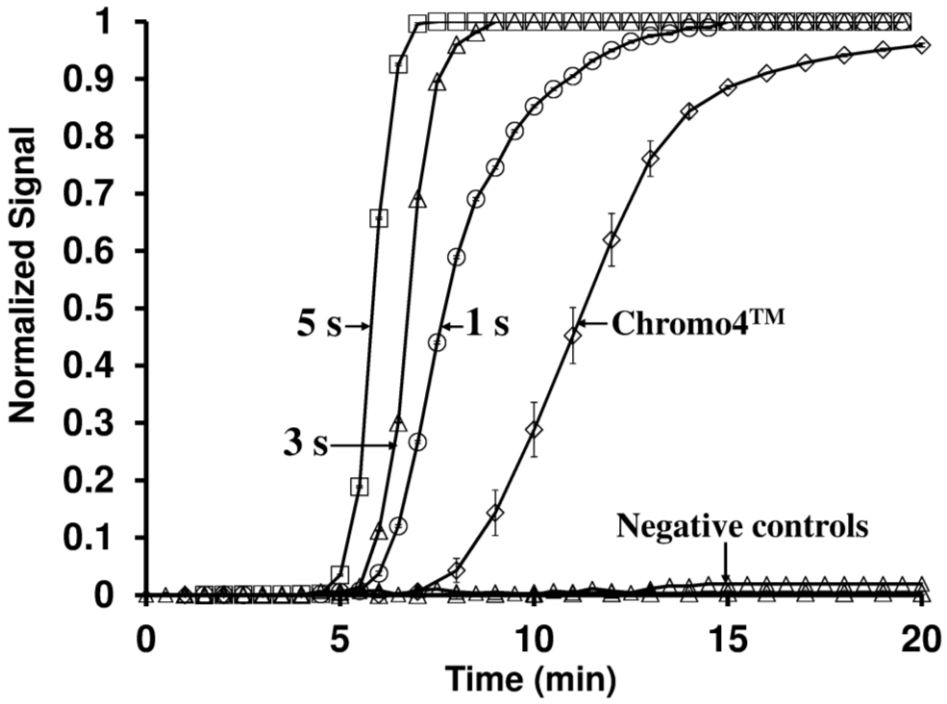

Figure 3.5 RT_f-LAMP curves for 10^5 DNA copies of *V. cholera* toxR gene on the microchips (1 s, 3 s, and 5 s CCD exposure time) and real-time PCR instrument

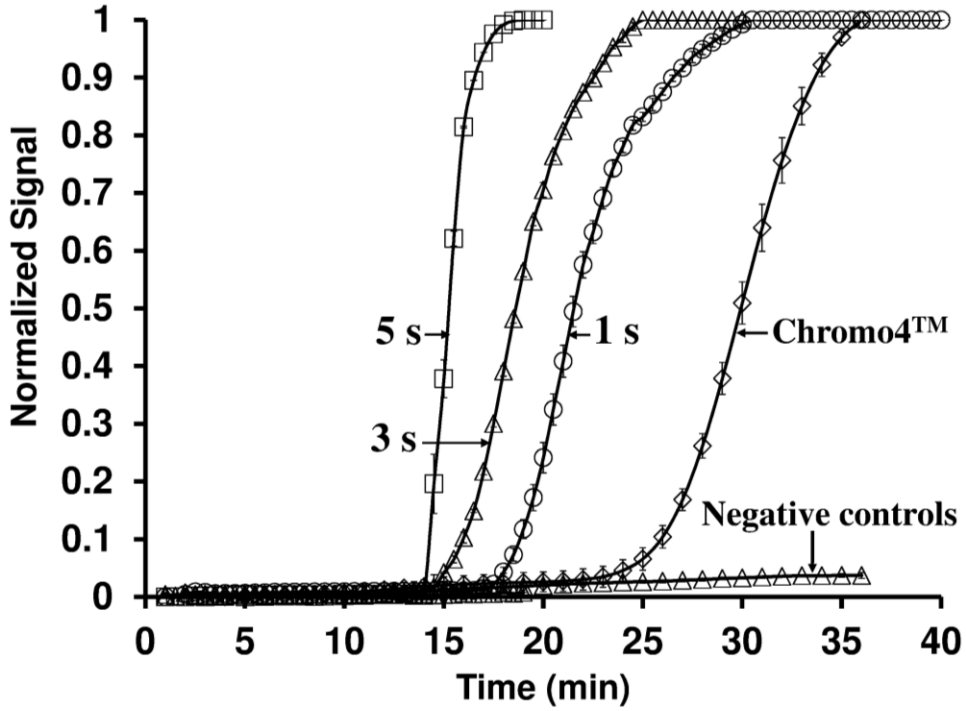

Figure 3.6 RT_f-LAMP curves for 10^5 DNA copies of *C. parvum* gp60 gene on the microchips (1 s, 3 s, and 5 s CCD exposure time) and real-time PCR instrument

For microRT$_f$-LAMP assay of *C. parvum* gp60 gene, SNR and Tt values for 1 s, 3 s, and 5 s CCD exposure time were 12.1 and 18.7 min, 12.6 and 15 min, 206 and 14.5 min, respectively. A difference in Tt value of 0.5 min was observed for microRT$_f$-LAMP assay with 3 s and 5 s of CCD exposure time. However, SNR at 5 s of CCD exposure time was 16-fold higher than the SNR at 3 s of CCD exposure time. SNR and Tt values for the same assay on the real-time PCR instrument were 16.3 and 24.3 min, respectively. A 9.8 min difference in Tt value of microRT$_f$-LAMP with 5 s of CCD exposure time and real-time PCR instrument was observed (Figure 3.6). It was recently demonstrated that the reaction time is highly dependent on the physical properties of LAMP primers such as GC content, melting temperature, and free energy of hybridization (Kimura et al. 2011). As the same LAMP reaction conditions had been applied, the difference in Tt values of these two LAMP assays (*V. cholerae* toxR gene and *C. parvum* gp60 gene) was due to the difference in the characteristics of LAMP primers and target DNA.

Time lapse images of microchips during the amplification of *V. cholerae toxR* gene at 1s, 3s, and 5 s of exposure time showed that higher fluorescence signals were achieved faster at higher exposure time (Figure 3.7).

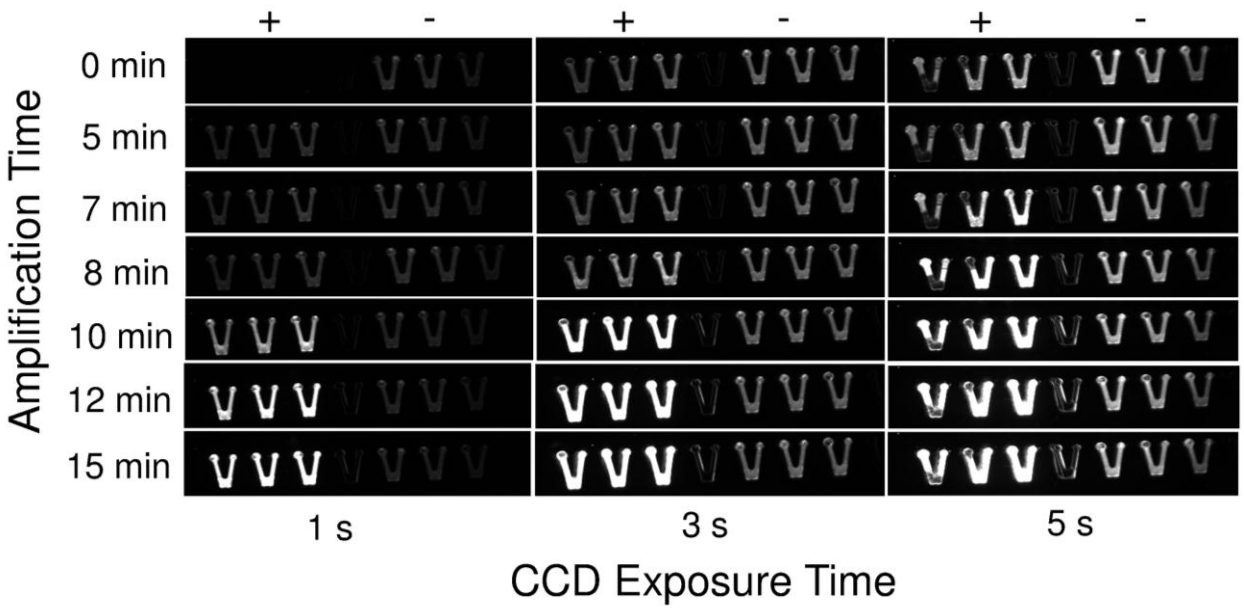

Figure 3.7 Time lapse CCD images of microRT$_f$-LAMP assay for *V. cholera* toxR gene with CCD exposure times of 1 s, 3 s, and 5 s. Fluorescence signals increase with the increasing exposure times

Amplicon yield of a 0 min turbidity-based LAMP with 6000 starting DNA copies was shown to be approximately 400 ng/µl (Mori et al. 2001). Our microRT$_f$-LAMP assays had 10^5 starting DNA copies, reaction volume of 2 µl, and total amplification time of 20 min for 5 s CCD exposure time. If we assume similar reaction kinetics, our microRT$_f$-LAMP assays should generate more than 267 ng amplicons in 2 µl reaction volume in 20 min. That would produce approximately 70 ng amplicons in 5 min (minimum Tt value of microRT$_f$-LAMP), which should provide higher fluorescence from positive microRT$_f$-LAMP relative to the background at higher exposure times. This effect was similar to the increase in the fluorescence signals from 10 ng and 1 ng dsDNA standard in comparison to the negative control by increasing the CCD exposure times (Figure 3.4). Other studies have observed the increment in signal-to-background ratio from chemiluminescence immunoassay with increasing CCD exposure times (Yang et al. 2008).

Similarly, SNR values of positive microRT$_f$-LAMP assays showed consistent increment (relative to the background) with increasing exposure times, reducing the Tt values of these assays. However, this effect could not be expected from the fluorescence LAMP on real-time PCR instrument, which employs photodiode detector.

3.3.4 MicroRT$_f$-LAMP assays of waterborne pathogens

CCD-based imaging system was validated for 12 virulent genes of 6 waterborne pathogens using Syto-82 dye and real time fluorescence LAMP on V-shaped microchips. Major waterborne pathogenic bacteria including, *S. enterica* (invA and phoB gene), *C. jejuni* (0414 and cdtA gene), *L. pneumophila* (dotA and lepB gene), *E. coli* O157:H7 (stx2 and eae gene), and *V. cholerae* (toxR and ctxA gene), and a protozoan, *C. parvum* (hsp70 and gp60 gene) were selected from the list of Centers for Disease Control and Prevention (Lee 2002). MicroRT$_f$-LAMP assays for 12 virulent genes of waterborne pathogens (10^5 gene copies) were performed at 5 s of CCD exposure time and compared with the real-time fluorescence LAMP on a real-time PCR instrument (data not shown). A reduction in Tt values ranging from 2.7 min to 9.8 min was achieved for microRT$_f$-LAMP assays in comparison to real-time PCR instrument (Table 3.3). LAMP primer sets, which were slower (higher Tt) on real-time PCR instrument showed higher reduction in the Tt values on microchip than the LAMP primers which were relatively faster (lower Tt) on the real-time PCR instrument For example, LAMP primer set for *C. parvum* gp60 gene showed the slowest amplification on the real-time PCR instrument with Tt of 24.3 min, which was reduced by 9.8 min on the microchip assay. LAMP primer set for *V. cholerae* toxR gene was the fastest on the real-time PCR instrument with an amplification time of 7.7 min,

which was reduced by 2.7 min on microchip assay. Moreover, standard deviations in the Tt values of microRT_f-LAMP assays were either same or lower than the real-time PCR instrument.

Table 3.3 Comparison of average Tt values of RT_f-LAMP for 10^5 DNA copies of 6 waterborne pathogens (2 genes for each) on the microchips with 5 s CCD exposure and the real-time PCR instrument. Standard deviations are the mean of Tt values from triplicates

Microorganism	**Gene**	**Tt (Chromo4^{TM}) (min)**	**Tt (CCD System) (min)**	**Δ t (min)**
S. enterica	invA	11 ± 0.0	6.5 ± 0.0	4.5
S. enterica	phoB	14.7 ± 0.6	10 ± 0.0	4.7
C. parvum	hsp70	15.3 ± 0.6	11 ± 0.0	4.3
C. parvum	gp60	24.3 ± 1.2	14.5 ± 0.0	9.8
C. jejuni	0414	16.7 ± 0.6	7.8 ± 0.6	8.9
C. jejuni	cdtA	16 ± 0.0	9.3 ± 0.3	6.7
L. pneumophila	dotA	10 ± 0.0	5.5 ± 0.5	4.5
L. pneumophila	lebB	11.6 ± 0.6	6.5 ± 0.0	5.5
E. coli O157:H7	stx2	11 ± 0.0	4.8 ± 0.3	6.2
E. coli O157:H7	eae	18.3 ± 0.6	13.3 ± 0.3	5.0
V. cholerae	toxR	7.7 ± 0.6	5 ± 0.0	2.7
V. cholerae	ctxA	17.3 ± 0.6	10 ± 0.0	7.3

LAMP primer set for *C. jejuni* 0414 gene was evaluated for the dilution series of 14, 1.4, and 0.14 DNA copies, by a real-time turbidimeter (Yamazaki et al. 2008). Average Tt values for real-time fluorescence LAMP assays in our study were similar to their reported average values of Tt for real-time turbidity (Yamazaki et al. 2008). However, there was a high deviation in their Tt values between the replicates (not discussed). Similarly, (Chen and Ge 2010) observed the variations in the Tt values of the replicates of real-time turbidity-based LAMP, when compared with real-time fluorescence-based LAMP for the same target of *V. parahaemolyticus* toxR gene. Other studies have also reported the real-time fluorescence LAMP assays to be faster, sensitive,

and more reproducible than real-time turbidity-based LAMP (Aoi et al. 2006; Chen and Ge 2010). We also observed very low standard deviations in the Tt values of real-time fluorescence LAMP assays on microchips and real-time PCR instrument. Lee et al. (2008) reported an optical system equipped with a photodiode for monitoring real-time turbidity-based microLAMP assay. A slight variation in the intensity of excitation light or its alignment to the detector was able to affect the turbidity value due to the additional scattering of photons (Lee et al. 2008). However, fluorescence signals from CCD-based microchip assays such as microPCR (Dahl et al. 2007) or microRT$_f$-LAMP (in this study) are not affected by the slight sample misalignment.

3.3.5 MicroRT$_f$-LAMP assay for quantitative analysis of *C. jejuni*

To establish standard curves for quantitative analysis, real-time fluorescence LAMP assays targeting 0414 gene were performed on microchips with 5 s CCD exposure time and on a real-time PCR instrument with 10-fold serial dilutions of *C. jejuni* DNA ranging from 10^5 to 1 copy. The standard curves were established by plotting the Tt values versus log of the number of genomic DNA copy used in RT$_f$-LAMP assays (Figure 3.8). Both the microRT$_f$-LAMP and RT$_f$-LAMP assay on commercial real-time PCR instrument were sensitive to a single DNA copy.

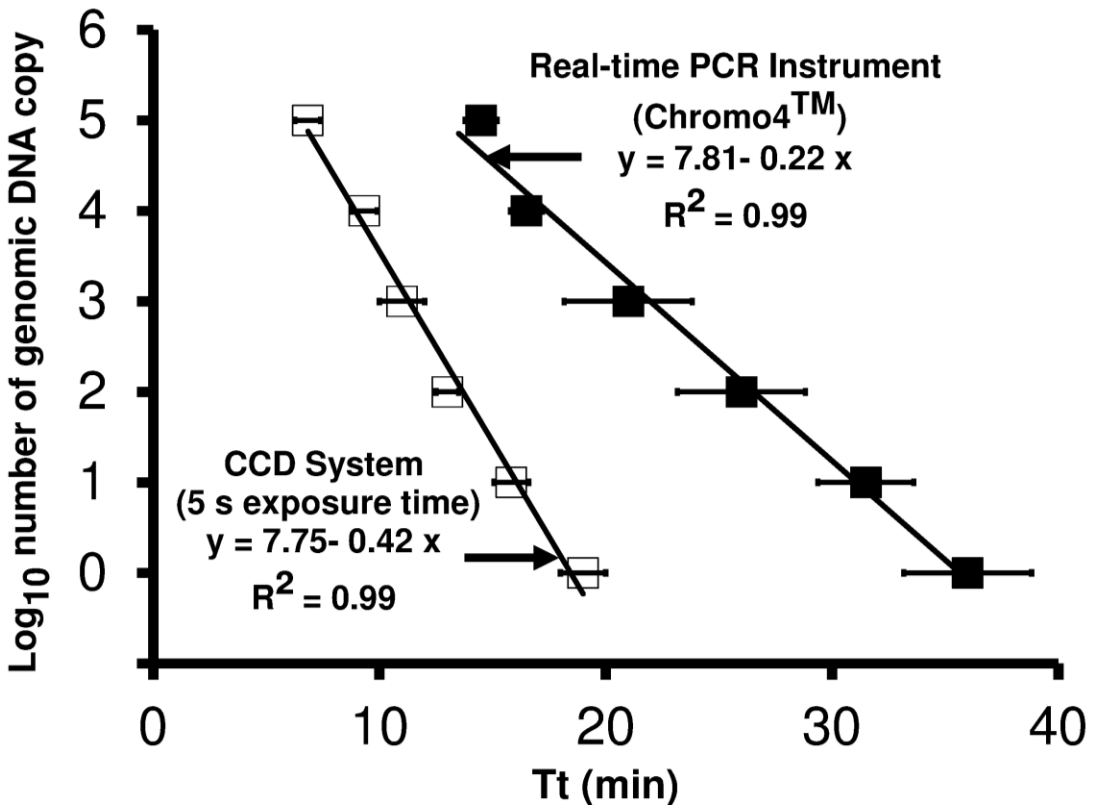

Figure 3.8 Standard curves for the *C. jejuni* 0414 gene amplification on the microchips at 5 s of CCD exposure time and real-time PCR instrument

Yamazaki et al. (2008) had also reported a single copy level sensitivity for this primer set. The correlation coefficients of the log linear regression plots between Tt values and DNA copy numbers for microRT$_f$-LAMP and real-time PCR instrument were the same, 0.99. However, microRT$_f$-LAMP assay was approximately twice faster than the RT$_f$-LAMP assay on the real-time PCR instrument. The result indicates that microRT$_f$-LAMP enables the reproducible and rapid quantification of DNA.

3.4 Conclusions

In this study, we demonstrated that rapid RT_f-LAMP assays can be performed on COP microchips in comparison to a commercial real-time PCR instrument. Increasing the CCD exposure time up to 5 s, increased the SNR by 8-fold and reduced the Tt values from 2.7 min to 9.8 min for 10^5 starting DNA copies of microRT_f-LAMP assays. Additionally, microRT_f-LAMP assay allowed the analysis of low sample volume of 2 μL in less than 20 min with a detection limit of single DNA copy. Due to requirements of single temperature incubation, microRT_f-LAMP assays have the potential to be translated into rapid and low cost battery operated molecular diagnostic devices, suited to applications in resource-limited settings.

REFERENCES

3.5 References

Abe T, Segawa Y, Watanabe H, Yotoriyama T, Kai S, Yasuda A, Shimizu N, Tojo N (2011) Point-of-care testing system enabling 30 min detection of influenza genes. Lab on a Chip 11:1166-1167

Aoi Y, Hosogai M, Tsuneda S (2006) Real-time quantitative LAMP (loop-mediated isothermal amplification of DNA) as a simple method for monitoring ammonia-oxidizing bacteria. Journal of Biotechnology 125:484-491

Boore A, Herman KM, Perez AS, Chen CC, Cole DJ, Mahon BE, Griffin PM, Williams IT, Hall AJ (2010) Surveillance for foodborne disease outbreaks-United States 2007. Morbidity and Mortality Weekly Report 59:973-1007

Chen S, Ge B (2010) Development of a toxR-based loop-mediated isothermal amplification assay for detecting Vibrio parahaemolyticus. BMC Microbiology 10:1-9

Craun GF, Brunkard JM, Yoder JS, Roberts VA, Carpenter J, Wade T, Calderon RL, Roberts JM, Beach MJ, Roy SL (2010) Causes of outbreaks associated with drinking water in the United States from 1971 to 2006. Clinical Microbiology Reviews 23:507-528

Dahl A, Sultan M, Jung A, Schwartz R, Lange M, Steinwand M, Livak KJ, Lehrach H, Nyarsik L (2007) A massively parallel PicoTiterPlate™ based platform for discrete picoliter-scale polymerase chain reactions. Biomedical Microdevices 9:307-314

Deligeorgiev TG, Kaloyanova S, Vaquera JJ (2009) Intercalating cyanine dyes for nucleic acid detection. Recent Patents on Materials Science 2:1-26

En FX, Wei X, Jian L, Qin C (2008) Loop-mediated isothermal amplification establishment for detection of pseudorabies virus. Journal of Virological Methods 151:35-39

Fang X, Chen, H., Yu, S., Jiang, X., Kong, J., (2010) Predicting Viruses Accurately by a Multiplex Microfluidic Loop-Mediated Isothermal Amplification Chip. Analytical Chemistry 83:690-695

Fang X, Liu Y, Kong J, Jiang X (2010) Loop-mediated isothermal amplification integrated on microfluidic chips for point-of-care quantitative detection of pathogens. Analytical Chemistry 82:3002-3006

Gottscheber A, Dech S (2010) Automatic detection of space debris with a MEADE telescope. 61st International Astronautical Congress:1-5

Grigoriev E, Akindinov A, Breitenmoser M, Buono S, Charbon E, Niclass C, Desforges I, Rocca R (2007) Silicon photomultipliers and their bio-medical applications. Nuclear Instruments and Methods in Physics Research Section A 571:130-133

Gudnason H, Dufva M, Bang DD, Wolff A (2007) Comparison of multiple DNA dyes for real-time PCR: effects of dye concentration and sequence composition on DNA amplification and melting temperature. Nucleic Acids Research 35:e127

Hoffman R, Marshall MM, Gibson MC, Rochelle PA (2009) Prioritizing pathogens for potential future regulation in drinking water. Environmental Science and Technology 43:5165-5170

Kaneko H, Kawana T, Fukushima E, Suzutani T (2007) Tolerance of loop-mediated isothermal amplification to a culture medium and biological substances. Journal of Biochemical and Biophysical Methods 70:499-501

Kimura Y, Hoon MJLd, Aoki S, Ishizu Y, Kawai Y, Kogo Y, Daub CO, Lezhava A, Arner E, Hayashizaki Y (2011) Optimization of turn-back primers in isothermal amplification. Nucleic Acids Research 39:e59

Kostov Y (2009). Photodiode-based detection system for biosensors. In Methods in Molecular Biology: Biosensors and Biodetection (Vol. 503): Humana Press 307-323

Lam L, Sakakihara S, Ishizuka K, Takeuchi S, Arata HF, Fujita H, Noji H (2008) Loop-mediated isothermal amplification of a single DNA molecule in polyacrylamide gel-based microchamber. Biomedical Microdevices 10:539-546

Lee SH, Levy, D. A., Craun, G. F., Beach, M. J., Calderon, R. L., (2002) Surveillance for waterborne-disease outbreaks-united States, 1999-2000. Morbidity and Mortality Weekly Report 51:1-28

Lee SY, Huang JG, Chuang TL, Sheu JC, Chuang YK, Holl M, Meldrum DR, Lee CN, Lin CW (2008) Compact optical diagnostic device for isothermal nucleic acids amplification. Sensors and Actuators B 133:493-501

Liu C, Mauk MG, Bau HH (2011) A disposable, integrated loop-mediated isothermal ampification cassette with thermally actuated valves. Microfluidics and Nanofluidics 11:1-12

Matsubara Y, Kobayashi M, Morita Y, Tamiya E (2002) Application of a microchamber array for DNA amplification using a novel dispensing method. Archives of Histology and Cytology 65:481-488

Mori Y, Nagamine K, Tomita N, Notomi T (2001) Detection of loop-mediated isothermal amplification reaction by turbidity derived from magnesium pyrophosphate formation. Biochemical and Biophysical Research Communications 289:150-154

Mori Y, Notomi T (2009) Loop-mediated isothermal amplification (LAMP): a rapid, accurate, and cost-effective diagnostic method for infectious diseases. Journal of Infection and Chemotherapy 15:62-69

Niemz A, Ferguson TM, Boyle DS (2011) Point-of-care nucleic acid testing for infectious diseases. Trends in Biotechnology 29:240-250

Notomi T, Okayama H, Masubuchi H, Yonekawa T, Watanabe K, Amino N, Hase T (2000) Loop-mediated isothermal amplification of DNA. Nucleic Acids Research 28:e63

Piepenburg O, Williams CH, Stemple DL, Armes NA (2006) DNA detection using recombination proteins. Plos Biology 4:1115-1121

Pjescic I, Tranter C, Hindmarsh PL, Crews ND (2010) Glass-composite prototyping for flow PCR with in situ DNA analysis. Biomedical Microdevices 12:333-343

Poon LLM, Wong BWY, Ma EHT, Chan KH, Chow LMC, Abeyewickreme W, Tangpukdee N, Yuen KY, Guan Y, Looareesuwan S, Peiris JSM (2006) Sensitive and inexpensive molecular test for falciparum malaria: Detecting Plasmodium falciparum DNA directly from heat-treated blood by loop-mediated isothermal amplification. Clinical Chemistry 52:303-306

Seyrig G, Ahmad F, Stedtfeld RD, Tourlousse DM, Hashsham SA (2011). Simple, powerful, and smart: Using LAMP for low cost screening of multiple waterborne pathogens In Environmental Microbiology: Current Technology and Water Applications Caister Academic Press 103-125

Tarnok A (2008) SYTO dyes and histoproteins-myriad of applications. Cytometry A 73 A:477-479

Vincent M, Xu Y, Kong HM (2004) Helicase-dependent isothermal DNA amplification. Embo Reports 5:795-800

Yager P, Domingo GJ, Gerdes J (2008) Point-of-care diagnostics for global health. Annual Review of Biomedical Engineering 10:107-144

Yamazaki W, Taguchi M, Ishibashi M, Kitazato M, Nukina M, Misawa N, Inoue K (2008) Development and evaluation of a loop-mediated isothermal amplification assay for rapid and simple detection of Campylobacter jejuni and Campylobacter coli. Journal of Medical Microbiology 57:444-451

Yang MH, Kostov Y, Bruck HA, Rasooly A (2008) Carbon Nanotubes with Enhanced Chemiluminescence Immunoassay for CCD-Based Detection of Staphylococcal Enterotoxin B in Food. Analytical Chemistry 80:8532-8537

CHAPTER IV

4. DIGITAL LAMP FOR RAPID AND SENSITIVE GENETIC AMPLIFICATION OF GRAM-NEGATIVE AND GRAM-POSITIVE BACTERIA WITH NO SAMPLE PROCESSING

4.1 Introduction

Sample preparation is a key aspect in the implementation sample-in-answer-out gene analysis systems. Sample preparation methods to recover nucleic acids entails several steps depending on the sample being analyzed, but often includes cell enrichment, cell lysis and nucleic acid purification (Mariella 2008; Kim et al. 2009; Price et al. 2009). Enrichment/concentration of target cells becomes extremely important in the sensitive diagnosis of infectious disease agents due to their low concentrations in high amount of background (e.g., 200 human immunodeficiency virus particles in 1 mL of blood containing 5×10^9 red blood cells). Sample preparation techniques such as filtration (Mach and Di Carlo 2010), immuno-separation (Dharmasiri et al. 2010), and dielectrophoresis (Hu et al. 2005) for cell enrichment, and biochemical, thermal, electrical, and mechanical methods for cell lysis (Brown and Audet 2008), and silica-based solid-phase methods for nucleic acid separation and purification (Price et al. 2009) have been translated on microfluidic chips. Microfluidic chips (for sample preparation) are being integrated with nucleic acid amplification and detection modules for gene analysis systems with sample-in-answer-out capabilities (Easley et al. 2006). However, microfluidic-based sample preparation modules are limited by low nucleic acid extraction efficiency (50-80%) and high processing time (~1 h), affecting the sensitivity and total detection time of gene analysis systems (Grodzinski et al. 2003). As such, development of rapid gene analysis systems would require either the elimination of sample preparatory steps or improvements in their protocols.

Microfluidic PCR systems are known to carry out DNA amplification directly from bacterial cells (Kaigala et al. 2006; Atrazhev et al. 2010; Manage et al. 2011) by using polymerases which are less prone to inhibition (Kermekchiev et al. 2009; Matheson et al. 2010; Zhang et al. 2010). *Taq* polymerase, the enzyme commonly used to amplify nucleic acids in PCR is inhibited by a variety of compounds such as cell debris, hemoglobin, and humic acid (Abu Al-Soud and Radstrom 1998). Therefore, microfluidic PCR systems are often coupled with dedicated cell lysis and nucleic acid purification steps to remove cell debris and compounds that could inhibit DNA amplification (Easley et al. 2006; Witek et al. 2006; Park et al. 2011).

Loop-mediated isothermal amplification (LAMP) is a robust molecular method initially reported in 2000 and extensively been applied for the DNA/RNA-based amplification of a variety of pathogens (Notomi et al. 2000; Seyrig et al. 2011; Tourlousse et al. 2011). LAMP is highly sensitive, specific, and rapid, and most importantly, it is not affected by the presence of cell debris and compounds which typically inhibit PCR (Masaomi et al. 2003; Poon et al. 2006). LAMP is a promising method for nucleic acid amplification from bacterial cells at 63 ^{o}C. LAMP with bacterial cells (in conventional PCR vials) is performed with a separate heating of bacterial cells and mixing of cell lysate in the reaction solution. Direct heating of reaction solution above 80 ^{o}C deactivates *Bst* polymerase (Matovu et al. 2010). *In situ* LAMP is a modification of LAMP for DNA amplification directly from bacterial cells (Maruyama et al. 2003; Ye et al. 2011). *In situ* LAMP requires prior fixation and permeabilization of bacterial cells on a solid surface followed by LAMP reaction at 63 ^{o}C and fluorescence imaging of cells. Nucleic acids are amplified inside the cells by the inclusion of LAMP reaction components in the permeabilized cells. Due to the steps involved in sample processing, *in situ* LAMP is performed

in 3-4 h. DNA-based digital Polymerase chain reaction (Pohl and Shih 2004) and digital recombinase polymerase amplification (Shen et al. 2011) are performed for quantifying low concentrations of nucleic acids. Digital LAMP from bacterial cells would be more effective in target qualification, due to the elimination of upstream sample processing and the loss of nucleic acids associated with the processing.

To our knowledge, there is no report of a simple, sensitive, and rapid method for nucleic acid amplification directly from bacterial cells at a moderate temperature of 63 ^{o}C. Direct cell-based microfluidic LAMP would reduce the instrument complexity as compared to microfluidic PCR due to the isothermal nature of LAMP reaction. Direct cell-based LAMP without any sample processing is yet to be translated on microfluidic platform. Here we report an isothermal method for gene amplification directly from gram-negative (*Escherichia coli*) and gram positive (*Enterococcus faecalis*) bacterial cells at 63 ^{o}C with most probable number (MPN) approach leading to the concept of "digital LAMP". Real-time fluorescence loop-mediated isothermal amplification (RT_f-LAMP) assays were performed with bacterial cells, heat treated bacterial cells (95 ^{o}C for 5 min), and their purified genomic DNA templates on a commercial real-time PCR instrument. Gene amplification from viable bacterial cells was confirmed by performing propidium monoazide (PMA)-RT_f-LAMP assay with *E. faecalis* cells. Single cell-based RT_f-LAMP assays were also translated on polymeric microchips (microRT_f-LAMP) and monitored by a fluorescence imaging system, previously developed by our group (Ahmad et al. 2011). Single cell-level genetic amplification was performed by endpoint microRT_f-LAMP assays (10^5 cells to 0.01 cell) as digital LAMP. RT_f-LAMP assays (from 10^5 cells to single cell) of *E. coli*

(uidA gene) and *E. faecalis* (gelE gene) were successfully performed by directly incubating the cells at 63 ^{o}C without any prior processing. Threshold time values of RT_f-LAMP assays of bacterial cells, heat treated bacterial cells (95 ^{o}C for 5 min), and their purified genomic DNA templates were similar, implying that DNA could be amplified either by lysis or permeabilization of bacterial cells at 63 ^{o}C. PMA-LAMP results confirmed that DNA amplification was achieved with viable bacterial cells and not with the dead cells or extracellular DNA. MicroRT_f-LAMP assays provided signal-to-noise (SNR) ratio between 500- to 800, sensitivity of single cell, and detection time of approximately 20 min. MPN values from digital LAMP assays confirmed the genetic amplification were from single cell. Direct gene amplification from bacterial cells at 63 ^{o}C would eliminate the requirement of complex sample preparation steps, facilitating the development of sensitive, rapid, low-cost, and integrated point-of-care diagnostic systems.

4.2 Materials and methods

4.2.1 Bacterial cell and genomic DNA

E. faecalis (19433) cells were obtained from ATCC. *E. coli* K12 strain C3000 cells were graciously provided by Professor Joan B. Rose, Water Quality, Environmental, and Molecular Microbiology Laboratory at Michigan State University. Frozen stocks of *E. coli* and *E. faecalis* were resuspended in sterile Trypticase Soy Broth (TSB, 211768, BD, Sparks, MD). To revive the cells, these tubes were incubated at 37 ^{o}C in a shaker-incubator (New Brunswick Scientific, Edison, New Jersey) at 150 rpm for 12 h. Next, cultures were inoculated into 25 mL of TSB and incubated at 37 ^{o}C for 8-12 h to achieve mid-log phase. Bacterial cultures were placed overnight

in the refrigerator at 4 ^{o}C. Cultures were serially diluted in TSB and colony forming units of *E. coli* and *E. faecalis* were enumerated by plating 0.1 mL of dilutions of cultures on Trypticase Soy Agar (TSA, 211043, BD, Sparks, MD) plates. TSA plates were incubated at 37 ^{o}C for 12 h. Cell concentrations were approximately 1×10^{8} per mL for both the bacterial species. Strict aseptic techniques were followed throughout the experiments. Genomic DNA of *E. coli* strain K-12 (700926D) and *E. faecalis* strain V583 (700802D) was obtained from American Type Culture Collection (ATCC, Manassas, VA). Before use, dried genomic DNA was resuspended in nuclease-free sterile water (Fischer Scientific, Pittsburgh, PA).

4.2.2 LAMP primer design

LAMP primers were designed for β-D glucuronidase (uidA) and glutamate decarboxylase (gadA) genes of *E. coli* K-12 strain C3000, and gelatinase (gelE) gene of *E. faecalis* strain V583 respectively. Sequences of all primers are shown in the appendix. A set of six specific LAMP primers (F3, B3, FIP, BIP, LF and LB) were designed for each target by using Primer Explorer V4 (Eiken Chemicals Co., Tokyo, Japan). Primers were synthesized by Integrated DNA Technologies (IDT, Coralville, IA).

4.2.3 Microchip fabrication

Microchips with circular wells were fabricated with approximately 127 µm thick polyester film (8567K52, McMaster-Carr, Los Angeles, CA). A perforated steel sheet (10 cm × 12 cm) was gifted by Diamond Manufacturing Company, Wyoming, PA. The perforated sheet had 6600 holes, arranged in a straight line pattern, each having a diameter of 1 mm and hole-hole distance of 0.5 mm. Polyester was selected due to its low cost ($22 for 100 cm ×300 cm sheet)

and biocompatibility to LAMP reaction. A sheet of polyester was sandwiched between a perforated steel plate (Perforated Metals Plus, Charlotte, NC) and a piece of silicon rubber (70 A, McMaster-Carr, Los Angeles, CA), and preheated to 220 °C in a press (Carver press model 4386; Carver, Wabash, IN). An embossing pressure of 1000 lbs was applied for 3 min. The system was subsequently cooled to 105 °C while maintaining the embossing pressure. Microchip was then extracted from perforated sheet, rinsed with distilled water, and air-dried at 65°C in an oven. Microchip consisted of multiple circular wells with 1 mm diameter and 2 µL volume per well.

4.2.4 Experimental setup

Gene amplification and detection system was built by integrating light source, optical filters, thin film heater, and a CCD camera. Details of the fluorescence imaging system are provided in a previous publication (Ahmad et al. 2011). This system was slightly modified to obtain homogenous light for high throughput imaging. In the modified version, light emitting diode (LED) (05027-PM12, LED Supply) was replaced by a 525 nm LED array (LIU002; Thorlabs, Newton, New Jersey). LED array consists of 20 individual LEDs on a printed circuit board, providing homogeneously distributed light on larger area. Other components such as excitation filter (FF01-534/20-25, Semrock, Rochester, NY), emission filter (FF01-572/28-25, Semrock) filter, CCD camera with AutoStar Envisage imaging software (MEADE DSI Pro, Irvine, CA), and lens (16 mm, 15774, Deal Extreme), thermocouple (5SRTC-TT-T-40-36, Omega), pulse width modulator IC (DRV102T, Texas Instruments), USB DAQs (USB-DAQ 6009, National Instruments), thin film heater (HK5165R52.3L12, Minco, Minneapolis, MN), and

LabVIEW VI (developed in-house) were same as the previously reported system. The component cost of this experimental setup was approximately $1200.

4.2.5 RT_f-LAMP on commercial PCR instrument and on microchip

Reaction solution for RT_f-LAMP contained 1.6 µM each of FIP and BIP primer, 0.200 µM each of F3 and B3 primer, 0.8 µM each of LF and LB primer, 0.8 M betaine (Sigma, St Louis, MO), 1.4 mM of each dNTP (Invitrogen Corporation, Carlsbad, CA), 20 mM Tris-HCl (pH 8.8), 10 mM $(NH_4)_2SO_4$, 10 mM KCl, 8 mM $MgSO_4$, 8 mM Triton X-100, 0.64 units/µL of large fragment of *Bst* DNA polymerase (New England Biolabs Inc., Ipswich, MA), 0.2% Pluronic® F-68 (Invitrogen, Carlsbad, CA), 1 mg/ml bovine serum albumin (New England BioLabs), and 2 µM of Syto-82 (Invitrogen Corporation, Carlsbad, CA). Depending on the type of RT_f-LAMP assay (DNA or cell-based), LAMP solution was mixed with 1 µL of DNA solution (10^5 genomic DNA templates/ µL) or bacterial solution (10^5 cells/ µL) without any prior treatment. To examine the effect of heating on cell lysis, cell solutions were separately pre-heated at 95 ^oC for 5 min before mixing in the LAMP reaction solution. In another experiment, LAMP reaction solutions mixed with bacterial cells were preheated at 95 ^oC for 5 min to examine the effect of heating on *Bst* polymerase and on the performance of LAMP. To establish standard curves for quantitative analysis of *E. coli* and *E. faecalis*, RT_f-LAMP assays with 10-fold serial dilutions of bacterial cells (10^5 cells -1 cell) were prepared. RT_f-LAMP assays without any DNA template or bacterial cell were also prepared to serve as negative controls. Positive and negative LAMP controls with the volume of 25 µL were loaded in 0.2 mL PCR

tubes (VWR International, West Chester, PA) and incubated at 63 °C for 30-40 min on a commercial real-time PCR instrument (Chromo4™, Bio-Rad Laboratories, Hercules, CA). Fluorescence signals of the RT_f-LAMP assays were measured every minute in channel 2 (excitation wavelength range from 500-535 nm and emission wavelength range from 560-580 nm). RT_f-LAMP assays were performed in triplicate except 6 replicates for single cell dilution.

For single cell RT_f-LAMP assays on microchip, 1 µL of *E. coli* and *E. faecalis* solution (1 cell/ µL) was dispensed in each well (n=10) followed by 1 µL of LAMP solution. Wells were covered with mineral oil (Sigma, St. Louis, MO) during the reaction to avoid solution evaporation. Microchip was placed on the heating stage for incubation at 63 °C for 30 min and real-time imaging.

4.2.6 PMA-RT_f-LAMP assays with *E. faecalis* cells

In order to detect viable *E. faecalis* in the presence of dead cells and extracellular DNA templates in the cell solution, RT_f-LAMP assays were performed with DNA-modifying PMA dye. PMA stock solution (20 mM, Biotium Hayward, CA) was diluted to 500 µM in dimethyl sulfoxide. Approximately 9 µL of cell solutions (10^5 cells/µL) were placed in three PCR tubes (0.2 mL). The solution of the second tube was preheated at 95 °C for 5 min to lyse the cells. Solutions in the first and third tubes were not treated with heat. Approximately 1 µL of 500 µM PMA solution was mixed in the solutions of first and second PCR tubes to achieve PMA concentration of 50 µM. These two tubes were incubated in the dark for 20 min followed by

exposure with blue light (450 nm LED, LXML-PR01-0500, Ontario, Canada) for 15 min. Solution in the third tube was neither mixed with PMA nor exposed to the light. For RT_f-LAMP assays**,** 1 µL of each cell solution was mixed with 24 µl LAMP solutions and incubated at 63 ^{o}C for 30 min on a commercial PCR instrument. Solutions from these three tubes were streaked on TSA plates and incubated for 12 h at 37 ^{o}C.

4.2.7 Digital LAMP assays for most probable number calculation

In order to confirm the amplification from the single bacterial cell and to calculate most probable number (MPN), endpoint microLAMP assays were performed with serial dilutions of *E. coli* (gadA gene) and *E. faecalis* (gelE gene) from 10^5 cells to 0.01 cell for digital LAMP. Digital LAMP assay for gadA gene of *E. coli* was designed and tested for single cell-level sensitivity. Each of the 40 wells was dispensed with 1 µL of *E. coli* / *E. faecalis* dilution solution followed by 1 µL of LAMP solution. Five replicates of digital LAMP assays for each dilution were performed to match with the 5-tube MPN analysis. Wells were covered with mineral oil and the microchip was incubated at 63 ^{o}C for 40 min before imaging.

4.2.8 Fluorescence signal analysis

Opticon^{TM} software (Bio-Rad Laboratories, Hercules, CA) was used to extract the raw fluorescence signals of RT_f-LAMP assays on the commercial real-time PCR instrument. For microRT_f-LAMP assays, CCD imaged the microchips in time-lapse mode at every 30 s at an exposure time of 5 s. Imaging was stopped when the signals from the signals from the positive

wells reached to a plateau. A gain of 100 and an offset of 60 were used for CCD imaging. Images were saved in flexible image transport system format**.** CCD images were opened in Image J (National Institutes of Health, Bethesda, MD) and a microarray profile plugin (http://www.optinav.com/imagej.html) was applied to obtain fluorescence signals from the images. A microarray grid (circular wells with diameter of 1 mm) was used to extract the signals from the same pixel region of all the time lapse images. To calculate SNR values of RT_f-LAMP assays on the commercial real-time PCR instrument and on microchip, raw fluorescence signals were baseline corrected by subtracting the average fluorescence signals obtained in the first 3 min and dividing by their standard deviation. Average of the SNR from the triplicates was plotted with respect to amplification time. Tt was then defined as the time at which the SNR reached an arbitrary cut-off of 10 or higher. Tt values were calculated for individual LAMP reaction of triplicates and an average value of Tt is reported here. The error bars in the plots represented the standard deviations of the mean from three replicate experiments unless otherwise indicated. Data analysis and plotting was done with Microsoft Excel (Microsoft, Redmond, WA). Contrast of the images of single cell microRT_f-LAMP and endpoint microLAMP assays were modified for visual clarity. Modification in the image contrast would not change the fluorescence signal values.

4.3 Results and discussion

4.3.1 RT_f-LAMP assays from genomic DNA templates and bacterial cells

RT_f-LAMP assays with 10^5 genomic DNA copies and 10^5 bacterial cells of *E. coli* (uidA gene) and *E. faecalis* (gelE gene) were performed at 63 ^oC on a commercial PCR instrument. To

ensure bacterial cell lysis during the reaction, RT_f-LAMP assays were also performed with both the type of bacterial cells, separately preheated at 95 ^{o}C for 5 min. RT_f-LAMP assays were also performed, in which LAMP solution containing bacterial cells were preheated at 95 ^{o}C for 5 min to examine the effect of heating on the performance of *Bst* polymerase. RT_f-LAMP assays with genomic DNA templates and bacterial cells of *E. coli* (gram-negative) and *E. faecalis* (gram-positive) showed the DNA amplification at 63 ^{o}C (Figure 4.1). DNA amplification was also achieved from the RT_f-LAMP assays of bacterial cells, in which the bacterial cells were separately pretreated with heat (data not shown). No DNA amplification was achieved in the RT_f-LAMP assays of bacterial cells, in which the LAMP reaction solutions containing bacterial cells were pretreated with heat (data not shown). Negative controls did not show any increase in the SNR value during the reaction.

Gram-positive and gram-negative bacteria contain peptidoglycan layer, which is cross-linked with peptide bonds to provide the rigidity to the cell walls (Cabeen and Jacobs-Wagner 2005). Peptidoglycan layer in gram-positive microorganisms is thicker (15-80 nm) and more cross-linked than the gram-negative bacteria (~10 nm) resulting in more robust cell wall. LAMP assays have been reported with a number of prokaryotic and eukaryotic cells (Iwasaki et al. 2003). However, in all the cases, prior heating of sample containing bacterial cells at approximately 95 ^{o}C (3-10 min) for cell lysis and centrifugation to separate bigger cell debris were performed (Poon et al. 2006; Chen and Ge 2010). To our knowledge, this is the first demonstration of DNA amplification directly from bacterial cells (without any processing) at 63 ^{o}C.

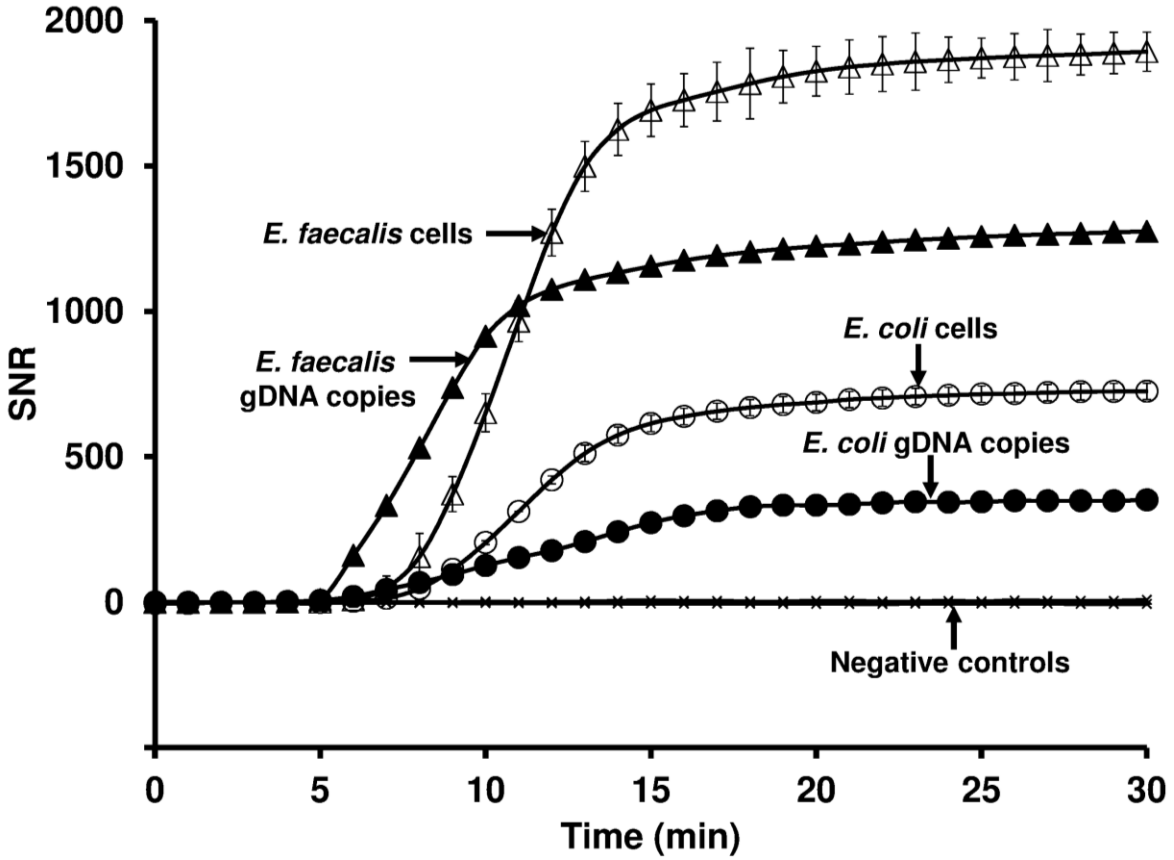

Figure 4.1 RT_f-LAMP assays of 10^5 genomic DNA copies and 10^5 cells of *E. coli* (uidA gene) and *E. faecalis* (gelE gene) at 63 ^oC on a commercial PCR instrument

Average SNR of bacterial cell assays were higher than genomic DNA-based assays. Also the average SNR from the cell assay of *E. faecalis* was higher than the cell assay of *E. coli*. For example, the highest average SNR from *E. coli* cell assay and genomic DNA assay were 725 and 352 respectively. The highest average SNR from *E. faecalis* cell assay and genomic DNA assay were 1893 and 1275 respectively. The highest average SNR from *E. faecalis* cell assay was 2.6-fold higher than *E. coli* cell assay. Although Syto-82 is a DNA interacting dye, higher SNR from bacterial cell assays than genomic DNA-based assays might be due to some interaction of Syto-82 dye with the cell membranes in addition to the genomic DNA. For another experiment, *E. coli*

growth was monitored in the presence of 2 µM Syto-82. Syto-82 was not appropriate for cell growth monitoring, but it showed a 2-fold higher fluorescence signal in the presence of *E. coli* cells than in water. Therefore, the interaction of Syto-82 dye with the cell membrane cannot be completely ruled out. Also higher SNR from *E. faecalis* cell assay than *E. coli* cell assay supports this hypothesis due to the thicker peptidoglycan layer in gram-positive, *E. faecalis* than gram-negative, *E. coli.* Higher standard deviations (SNR) in the cell assays than genomic DNA assays were observed, which might be due to non-specific interactions of Syto-82 with cell membranes.

Average Tt values of genomic DNA-based assays were slightly lower than bacterial cell assays. For example, the average Tt values of *E. coli* genomic DNA and cell assay were 6 min (SNR: 19.97) and 7 min (SNR: 13.89) respectively. And the average Tt values of *E. faecalis* genomic DNA and cell assay were 6 min (SNR: 161.1) and 7 min (SNR: 49.87) respectively. Also the average Tt values of the bacterial cells, which were preheated at 95 ^{o}C for 5 min were exactly the same as the cells without any preheating (date not shown). RT_f-LAMP assays containing bacterial cells, which were directly heated at 95 ^{o}C for 5 min, did not show any amplification. This was due to the fact that direct heating of LAMP reaction mixture at 95 ^{o}C deactivated *Bst* polymerase (Matovu et al. 2010).

Effect of temperature shock (from 50 ^{o}C to 70 ^{o}C) on the membrane permeability of a gram-negative (*E. coli*) and a gram-positive (*Deinococcus radiodurans*) was schematically studied by using flow cytometry (Baatout et al. 2005). An increase in the cell permeability of both the bacterial was observed at temperatures higher than 45 ^{o}C. Therefore, in our case,

incubation of cells at 63 ^{o}C might have increased the cell permeability leading to the inclusion of LAMP reaction components in the cells and DNA amplification inside the cells as *in situ* LAMP (Maruyama et al. 2003; Ye et al. 2011). The results showed that gene amplification was possible either by lysis or permeabilization of gram-negative and gram-positive bacterial cells at 63 ^{o}C. Genomic DNA assays were faster than cell assays by 1 min. In the genomic DNA assays, DNA templates were easily accessible to the LAMP reaction components. However, in cell assays, diffusion of LAMP reaction components inside the cells or their diffusion through cell debris might have slightly increased the Tt values.

4.3.2 RT_f-LAMP assays for quantitative analysis of *E. coli* and *E. faecalis* cells

To establish standard curves for quantitative analysis, RT_f-LAMP assays targeting uidA gene and gelE gene were performed on commercial PCR instrument (at 63 ^{o}C) with 10-fold serial dilutions of *E. coli* and *E. faecalis* respectively from 10^5 to 1 cell. Out of 6 positive controls of single cell assay of *E. coli* and *E. faecalis*, only 3 and 4 assays respectively showed the positive amplification. RT_f-LAMP assays of *E. coli* and *E. faecalis* showed a consistent increase in the SNR values reaching to a plateau in 15 min for 10^5 cells and between 20-30 min for higher dilutions. Tt values showed a consistent increment with respect to decreasing cell concentrations (Figure 4.2). Negative controls did not show any increase in the SNR throughout the reaction. For both the assays, standard deviations in the SNR values showed an increase with respect to decreasing cell concentrations. Additionally, standard deviations in the SNR values of the *E. faecalis* cell assays were higher than the *E. coli* cell assays. It could be attributed to the

higher non-specific interactions of Syto-82 with higher amount of cell membranes of *E. faecalis*. The standard curves for the RT_f-LAMP assays of both the bacterial cells were established by plotting the Tt values versus log of the number of cell (Figure 4.3). Cell-based RT_f-LAMP assays on commercial PCR instrument were quantitative and sensitive to single cell. Higher standard deviations in the average Tt values were observed for *E. faecalis* assay than *E. coli* assay. Correlation coefficients (R^2) of the fitted line were 0.98 and 0.97 for *E. coli* and *E. faecalis* assays respectively. Tt values of RT_f-LAMP assay from 10^5 cells to single cell of *E. coli* were from 8 min to 18.7 min respectively. And Tt values of RT_f-LAMP assay from 10^5 cells to single cell of *E. faecalis* were from 6.7 min to 13.3 min respectively. Faster amplification of the *E. faecalis* assay was due to rapidly increasing SNR values as compared to *E. coli* assay (Figure 4.1 and 4.2). Therefore, no preheating was needed for cell-based RT_f-LAMP assays i.e., LAMP can be performed by incubating the bacterial cells in the LAMP reagent mixture at 63 ^oC presumably because enough of the cells are lysed/permeabilized providing the access of genetic contents to the LAMP solution.

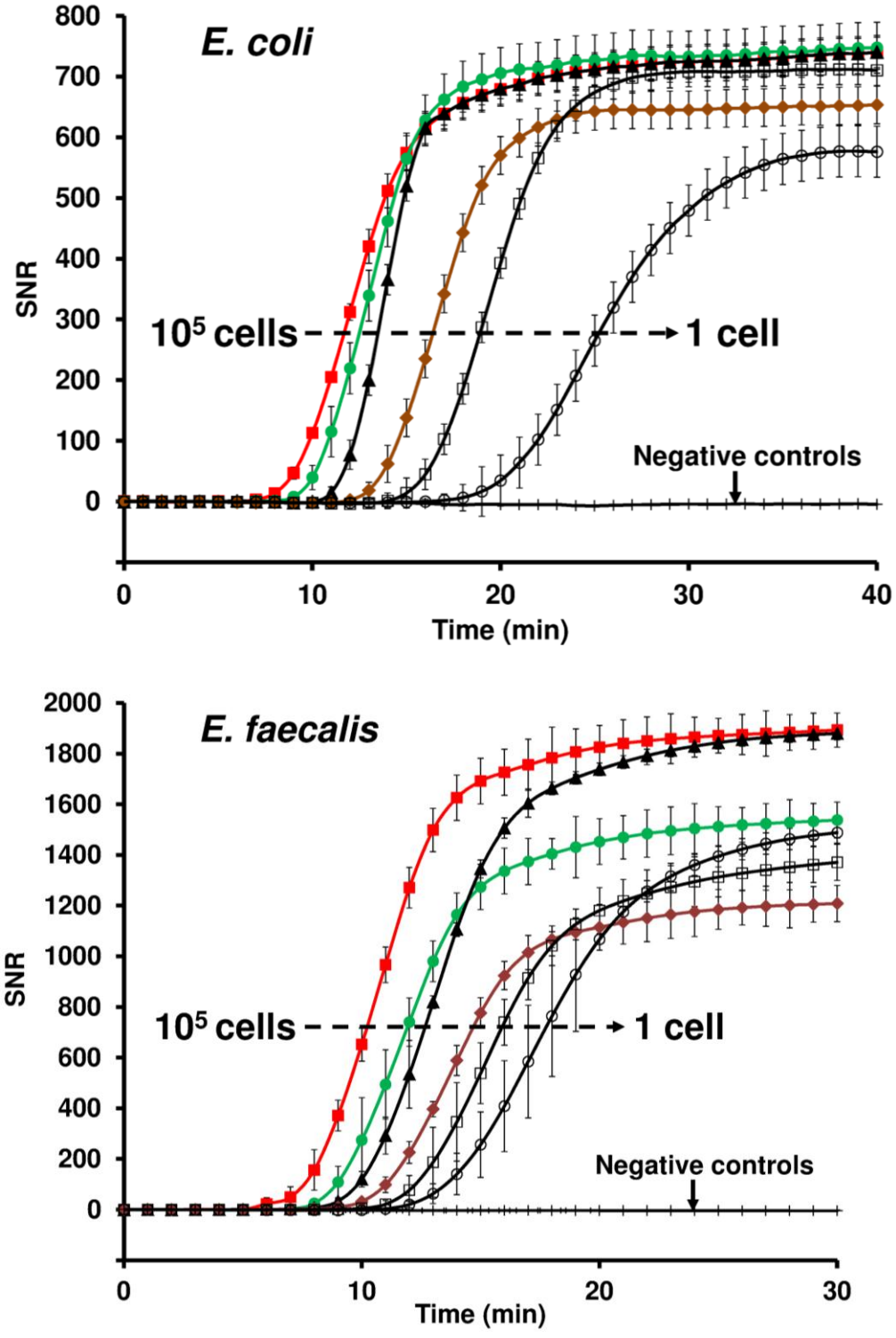

Figure 4.2 SNR verses amplification time of the dilution series of RT_f-LAMP assays of *E. coli* (uidA gene) and *E. faecalis* (gelE gene) cells from 10^5 cells to single cell on a commercial PCR instrument. For interpretation of the references to color in this and all other figures, the reader is referred to the electronic version of this dissertation.

4.3.3 Quantification of viable *E. faecalis* cells by PMA-RT$_f$-LAMP

RT$_f$-LAMP assays were performed with 10^5 *E. faecalis* (gelE gene) cells treated with PMA to confirm that the DNA amplification was only from viable cells and not from the dead cells or extracellular DNA in the solution (Figure 4.4). Differentiation of live and dead cells is a challenge in DNA-based molecular detection techniques (Girones et al. 2010). Prior treatment of pathogens with ethidium monoazide (EMA) (Nogva et al. 2003) and PMA (Nocker et al. 2007) is being applied to test cellular viability by using DNA-based molecular detection techniques.

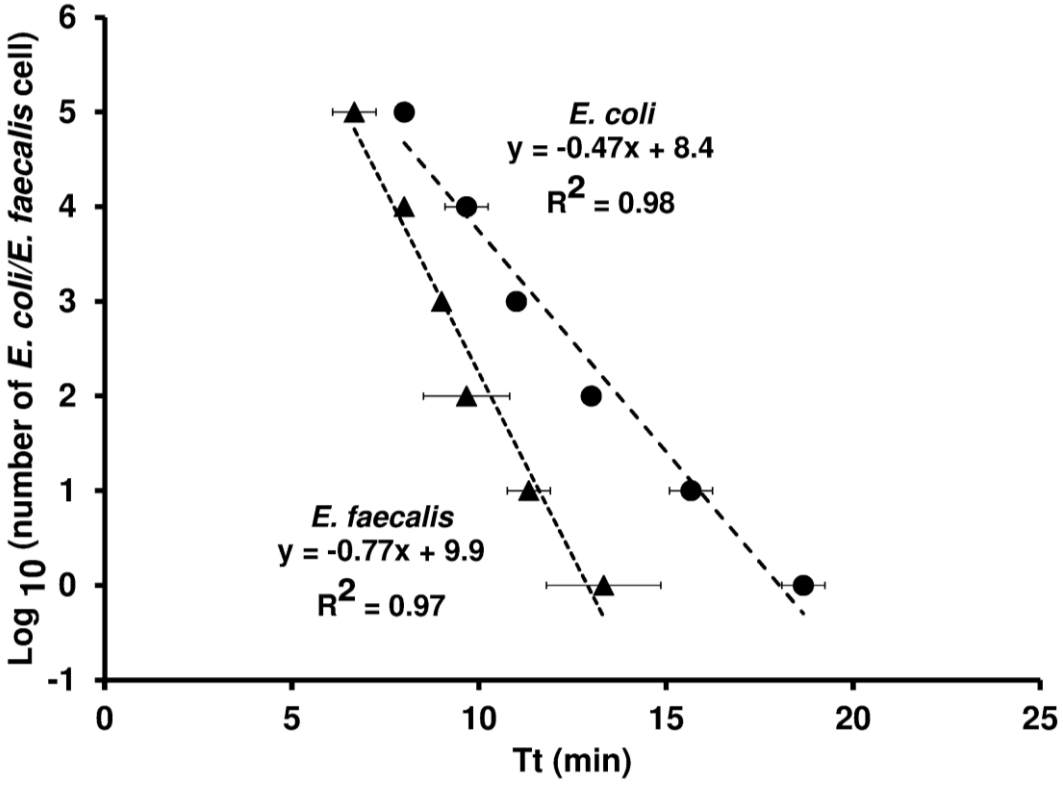

Figure 4.3 Standard curves of RT$_f$-LAMP assays of *E. coli* (uidA gene) and *E. faecalis* (gelE gene) cells on a commercial PCR instrument

EMA and PMA are photo-reactive dyes with high affinity for DNA. These dyes intercalate into double stranded DNA and forms covalent linkage upon exposure to blue light,

resulting into chemically modified DNA, which cannot be amplified by PCR or LAMP reactions. These dyes are designed to be cell-impermeable thus targeting only compromised or dead cells and extracellular DNA, without affecting the viable cells. Comparative investigations of membrane permeability characteristics of EMA and PMA have shown that EMA could penetrate the membranes of viable cells leading to cell loss (Nocker et al. 2006; Pan and Breidt 2007). However, due to higher molecular weight and higher positive charge of PMA than EMA, it remains membrane impermeant (Yanez et al. 2011). Compared to EMA, PMA has been shown to have greater success and non-lethal effects in identifying the viability of viruses (Parshionikar et al. 2010), bacteria (Nocker et al. 2009; Kralik et al. 2010; Chen et al. 2011; Liang et al. 2011), and protozoa (Sauch et al. 1991; Brescia et al. 2009) coupled with PCR, real-time PCR, and LAMP assays. Therefore, PMA-LAMP was selected to test the viability of *E. faecalis* cells. An optimum concentration 50 µM PMA was selected for this study as a range of concentrations from 30 to 50 µM was found to be effective in other studies (Pan and Breidt 2007; Vesper et al. 2008). *E. faecalis* cells treated with PMA were exposure to blue LED for 15 min for the PMA-DNA complex formation. A longer exposure time (15 min) with low-intensity LED was selected over a shorter exposure with brighter halogen lamp as heat generated by the halogen lamp has been reported to kill viable bacterial cells (Wang and Levin 2006; Vesper et al. 2008; Delgado-Viscogliosi et al. 2009).

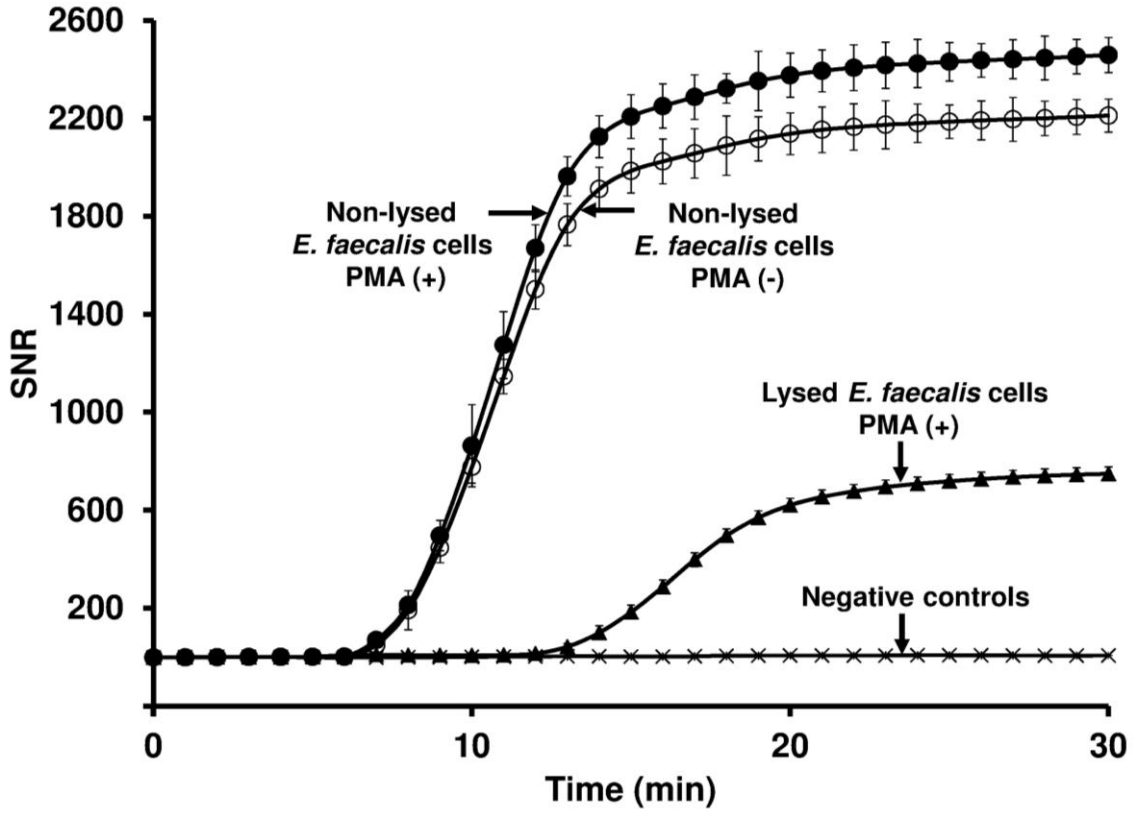

Figure 4.4 RT_f-LAMP assays of 10^5 *E. faecalis* non-lysed cells (with and without PMA treatment) and PMA treated lysed cells on a commercial PCR instrument

RT_f-LAMP assays of *E. faecalis* cells (non-lysed) with and without PMA treatment showed DNA amplification with the same Tt value of 7 min. SNR value (70.1) at Tt of non-PMA treated cells was higher than the SNR value (50) at Tt of PMA treated cells. Tt and the corresponding SNR of PMA treated lysed cells were 12 min and 14.5 respectively.

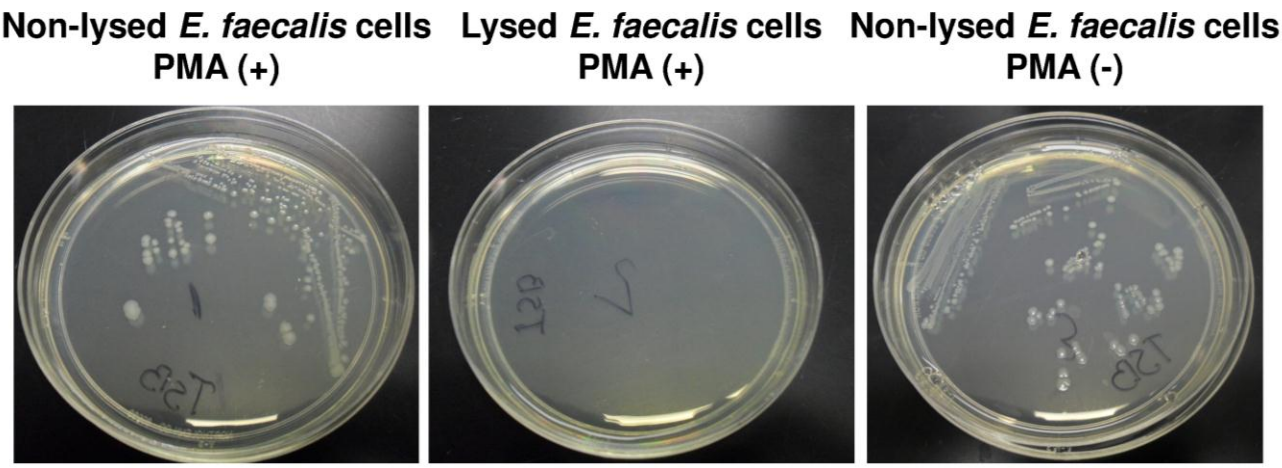

Figure 4.5 Colony forming units of non-lysed *E. faecalis* (with and without PMA treatment). No growth was observed from heat treated cells

Cell growth was only observed from the non-lysed cells solutions (with and without PMA treatment) (Figure 4.5). No cell growth was observed from the heat treated cell solution. RT_f-LAMP assays showed a drastic shift in the Tt value of PMA-treated lysed cells than PMA-treated non-lysed cells. A difference in Tt value of 5 min was observed, which corresponded to 4-log fold reduction in the cell concentration due to PMA treatment. No effect of PMA treatment was observed in RT_f-LAMP assays with non lysed cells (with and without PMA treatment). However, a slight lower SNR value of PMA treated cells than non-PMA treated cells might be due to death of few viable cells by the heat generated by LED light. Additionally, heat treatment (95 ^{o}C for 5 min) killed all the viable cells as observed by the lack of any cell growth on TSA plate (Figure 4.5). These results confirmed that the DNA amplification (Figure 4.1 and 4.2) was directly from viable bacterial cells rather than dead cells or extracellular DNA in solution.

4.3.4 MicroRT$_f$-LAMP assays of single cell of *E. coli* and *E. faecalis*

RT$_f$-LAMP assays were performed on polyester microchips and imaged with a CCD imaging system developed by our group (Ahmad et al. 2011) (Figure 4.6). Polyester material was compatible with LAMP reaction, as recently reported by our group (Stedtfeld et al. 2011). Also polyester was comparatively cheaper than cyclic olefin copolymer and no surface treatment of polyester was needed during/after microfluidic chip fabrication for performing LAMP, thus a cost effective and easy-to-use option.

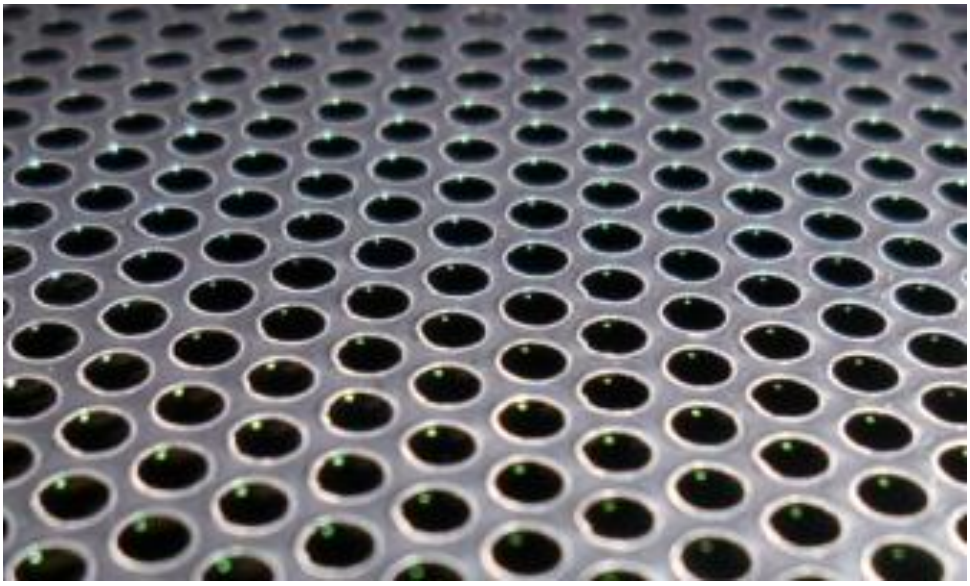

Figure 4.6 A polyester chip (2.5 cm × 2 cm) for microRT$_f$-LAMP assays. Each circular well was 1 mm in diameter with a volume of 2 µL. The circular wells were filled with food color

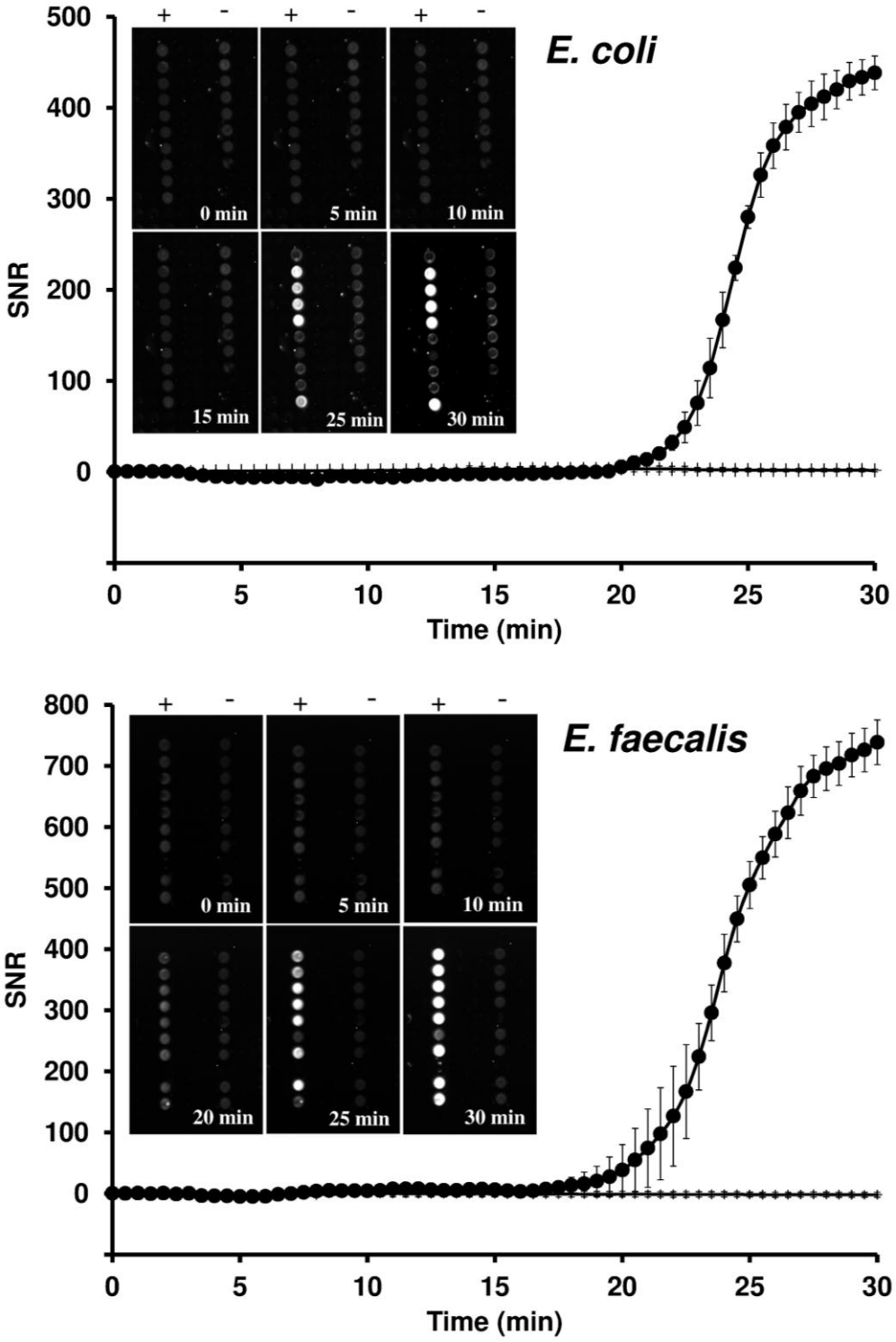

Figure 4.7 MicroRT$_f$-LAMP assays of single cell of *E. coli* (uidA gene) and *E. faecalis* (gelE gene). Inset showed the CCD time lapse images of microchip with 10 positive and 10 negative controls. The error bars represented the standard deviations of the mean from 5 and 8 positive replicates and 10 negative replicates for *E. coli* and *E. faecalis* respectively

MicroRT$_f$-LAMP assays with single cell of *E. coli* (uidA gene) and *E. faecalis* (gelE gene) were performed at 63 ^{o}C (Figure 4.7). MicroRT$_f$-LAMP assay of *E. coli* provided a maximum average SNR of 438 and an average Tt of 21 min respectively. And microRT$_f$-LAMP assay of *E. faecalis* provided a maximum average SNR of 738 and an average Tt of 17.5 min respectively. Due to dilution effect, only limited number of positive controls showed the DNA amplification. For example 5 and 8 positive amplifications were achieved out of 10 positive controls in *E. coli* and *E. faecalis* assays respectively. Negative controls did not show any increase in the SNR throughout the reaction. Higher SNR from *E. faecalis* assay than *E. coli* assay was consistent with the results from commercial PCR instrument. Additionally Tt values for *E. coli* and *E. faecalis* assay on microchip (5 s CCD exposure) was higher by 2.3 min and 4.2 min respectively than the assays on commercial PCR instrument. We had earlier demonstrated that increasing the CCD exposure time would reduce the Tt value of microRT$_f$-LAMP assays (Ahmad et al. 2011). However, in this case, reaction wells were covered with mineral oil to avoid evaporation. Due to the higher refractive index of mineral oil (1.5) than air (1.0), a portion of emitted photons from reaction wells might have been refracted from the oil-air interface, reducing the number of emission signals reaching to the CCD and increasing the Tt of cell-based microRT$_f$-LAMP assays. Also in this case, working distance between the CCD and the microchip was increased for image focusing, further reducing the incoming emission signals to the CCD. Tt could be further reduced by increasing the CCD exposure time from 5 s. However, increasing the CCD exposure time than 5 s would result into poor image contrast, reducing the image clarity.

4.3.5 Quantification of most probable number by digital LAMP

Digital LAMP assays were performed by targeting gadA gene and gelE gene with 10-fold serial dilutions of *E. coli* and *E. faecalis* respectively, from 10^5 cells to 0.01 cell. For each dilution, 5 replicates were performed to calculate the MPN concentrations of the assays by using the 10-fold dilution of 5-tube MPN analysis. As LAMP primers for gadA gene of *E. coli* were not tested earlier. Therefore, RT_f-LAMP assay from single *E. coli* cell was performed on a commercial PCR instrument at 63 ^oC to confirm the single-cell level sensitivity of the designed assay. The designed RT_f-LAMP assay of *E. coli* (gadA gene) was sensitive to single cell (Figure 4.8). This RT_f-LAMP assay showed slower amplification (Tt: 27 min) than the single cell assay designed for uidA gene. Therefore, for the MPN-based digital LAMP assays, microchips were incubated for 40 min before imaging.

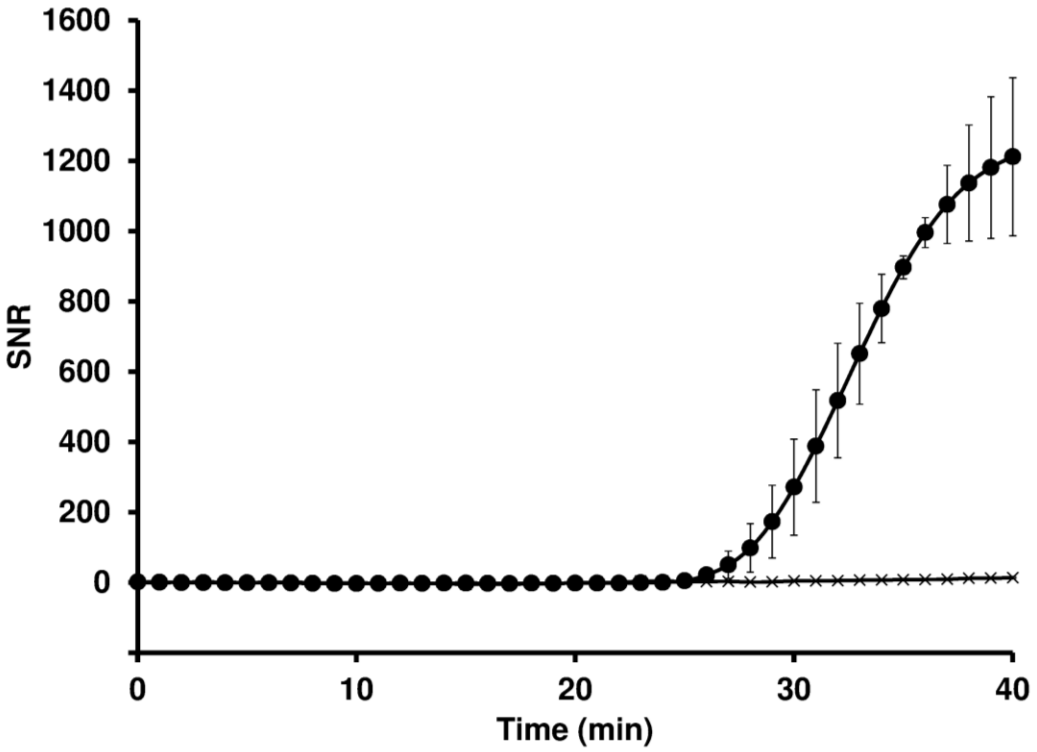

Figure 4.8 Single cell RT_f-LAMP assay of *E. coli* (gadA gene) on a commercial PCR instrument. Only two positive controls showed amplification out of six replicates. The error bars represented the standard deviations of the mean from two replicate experiments

MPN concentrations of single cell LAMP dilutions were quantified as per the statistical method of result rejection developed by Hurley and Roscoe and Taylor (Taylor 1962; Hurley and Roscoe 1983). The formula shown below was taken from the analysis of Hurley and Roscoe (Hurley and Roscoe 1983).

$$\sum_{i=1}^{k} \frac{d_i p_i v_i}{1-\exp\left(-d_i x v_i\right)} = \sum_{i=1}^{m} d_i n_i v_i$$

Here, k is the levels of dilution, n_i is the number of subsamples, p_i is the number of positive subsamples, d_i is the dilution factor, v_i is the volume of each subsample, and x is the estimated density of the microorganism.

The applied assumptions were that bacteria were distributed in the sample without any clustering and wells containing even a single viable bacterium would produce the growth/amplification. We have also assumed that the MPN values at the microscale volume would be consistent with the milliliter volume as used in the developed method. The result rejection method is based on that if the dilutions provide all the positive results, the calculation would include only the most diluted samples. If the dilutions provide all the negative results, calculation would include only the most concentrated samples.

Digital LAMP assay of gadA gene of *E. coli* showed amplification from 10^5 cells to single cell (Figure 4.9). However, only 2 out of 5 positive controls wells containing single cell showed amplification. No amplification was observed with the highest dilutions of 0.1 and 0.01 cell. Based on the 5-well MPN analysis [5 2 0], average MPN concentration of single cell dilution was 0.49 cell ($p = 0.05$) per 2 µL of reaction volume. Similarly, Digital LAMP assay of gelE gene of *E. faecalis* showed amplification from 10^5 cells to single cell (Figure 4.10). However, only 3 out of 5 positive controls wells containing single cell showed amplification. No amplification was observed with the highest dilutions of 0.1 and 0.01 cell. Based on the 5-well MPN analysis [5 3 0], average MPN of single cell dilution was 0.79 cell ($p = 0.05$) per 2 µL of reaction volume. The results implied that the digital LAMP assays had large dynamic range and single cell-level sensitivity.

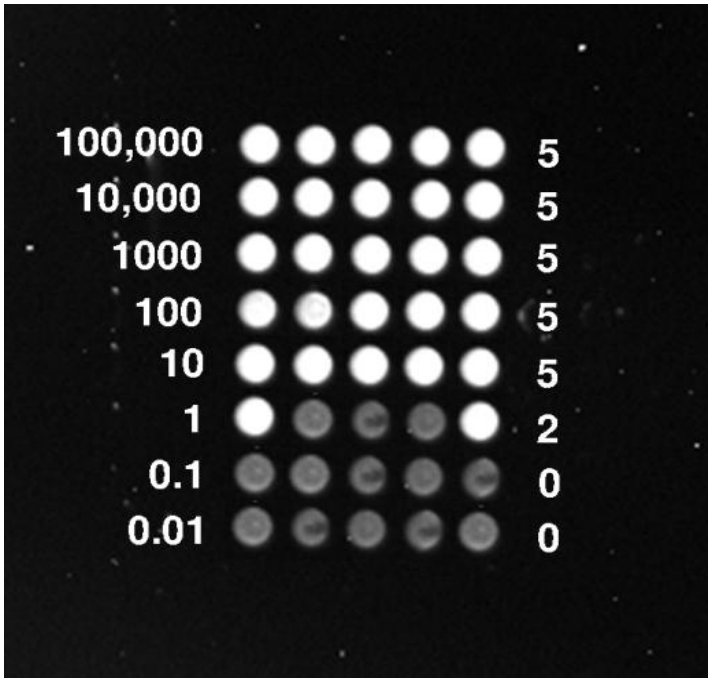

Figure 4.9 Digital LAMP image for *E. coli* (gadA gene) dilutions. Cell number per well (left) and number of positive reaction (right) were shown in the image

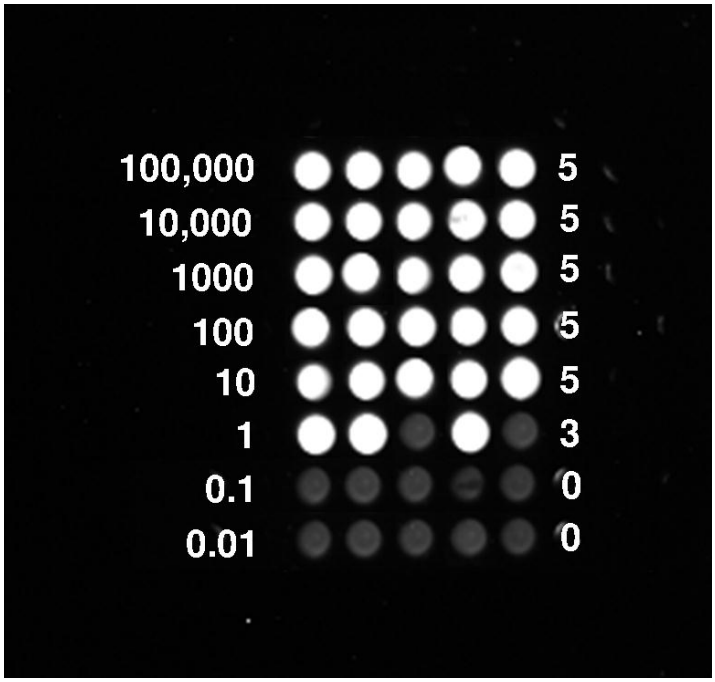

Figure 4.10 Digital LAMP image for *E. faecalis* (gel E gene) dilutions. Cell number per well (left) and number of positive reaction (right) were shown in the image

This approach of digital LAMP would be highly useful for the detection of extremely low concentration of target cells in higher reaction volume. Digital PCR and digital recombinase polymerase amplification assays based on DNA amplification have already been reported, which relies on the readout of high throughput reaction wells (positive/negative) at the end of reaction (Pohl and Shih 2004; Shen et al. 2011). MPN analysis is generally performed by using culture-based approaches, e.g., broth/agar dilution, which takes 10-12 h for the results (Evans et al. 1981; Rompre et al. 2002; Kinzelman et al. 2003). Digital LAMP could be used for the rapid bacterial enumeration by gene amplification from cells, thus has the potential to replace the MPN-based analysis.

4.4 Conclusions

RT_f-LAMP assays for rapid and sensitive gene amplification directly from *E. coli* and *E. faecalis* bacterial cells (without any sample processing) were developed. PMA-LAMP was performed to test the viability of *E. faecalis*, which also confirmed that DNA amplification was only from the bacterial cells. RT_f-LAMP assays of single bacterial cell were also translated on microchips. DNA amplification from single cell-level digital LAMP assays was confirmed by MPN analysis. LAMP from bacterial cells at a temperature of 63 ^{o}C might be due to the cell lysis or increased cell permeability at this temperature leading to DNA amplification. Direct DNA amplification from bacterial cells at this moderate temperature would eliminate any sample processing steps and reduce the complexity of gene analysis instruments. This work would be helpful towards the simple, sensitive, and rapid integrated gene analysis system with sample-in-answer-out capability.

REFERENCES

4.5 References

Abu Al-Soud W, Radstrom P (1998) Capacity of nine thermostable DNA polymerases to mediate DNA amplification in the presence of PCR-Inhibiting samples. Applied and Environmental Microbiology 64:3748-3753

Ahmad F, Seyrig G, Tourlousse DM, Stedtfeld RD, Tiedje JM, Hashsham SA (2011) A CCD-based fluorescence imaging system for real-time loop-mediated isothermal amplification-based rapid and sensitive detection of waterborne pathogens on microchips. Biomedical Microdevices 13:929-937

Atrazhev A, Manage DP, Stickel AJ, Crabtree HJ, Pilarski LM, Acker JP (2010) In-Gel Technology for PCR Genotyping and Pathogen Detection. Analytical Chemistry 82:8079-8087

Baatout S, De Boever P, Mergeay M (2005) Temperature-induced changes in bacterial physiology as determined by flow cytometry. Annals of Microbiology 55:73-80

Brescia CC, Griffin SM, Ware MW, Varughese EA, Egorov AI, Villegas EN (2009) Cryptosporidium propidium monoazide-PCR, a molecular biology-based technique for genotyping of viable cryptosporidium oocysts. Applied and Environmental Microbiology 75:6856-6863

Brown RB, Audet J (2008) Current techniques for single-cell lysis. Journal of the Royal Society Interface 5:S131-S138

Cabeen MT, Jacobs-Wagner C (2005) Bacterial cell shape. Nature Reviews Microbiology 3:601-610

Chen SY, Ge BL (2010) Development of a toxR-based loop-mediated isothermal amplification assay for detecting vibrio parahaemolyticus. BMC Microbiology 10:1-9

Chen SY, Wang F, Beaulieu JC, Stein RE, Ge BL (2011) Rapid detection of viable salmonellae in produce by coupling propidium monoazide with loop-mediated isothermal amplification. Applied and Environmental Microbiology 77:4008-4016

Delgado-Viscogliosi P, Solignac L, Delattre JM (2009) Viability PCR, a culture-independent method for rapid and selective quantification of viable legionella pneumophila cells in environmental water samples. Applied and Environmental Microbiology 75:3502-3512

Dharmasiri U, Witek MA, Adams AA, Osiri JK, Hupert ML, Bianchi TS, Roelke DL, Soper SA (2010) Enrichment and detection of Escherichia coli O157:H7 from water samples using an antibody modified microfluidic chip. Analytical Chemistry 82:2844-2849

Easley CJ, Karlinsey JM, Bienvenue JM, Legendre LA, Roper MG, Feldman SH, Hughes MA, Hewlett EL, Merkel TJ, Ferrance JP, Landers JP (2006) A fully integrated microfluidic genetic analysis system with sample-in-answer-out capability. Proceedings of the National Academy of Sciences of the United States of America 103:19272-19277

Evans TM, Waarvick CE, Seidler RJ, Lechevallier MW (1981) Failure of the most-probable-number technique to detect coliforms in drinking-water and raw water-supplies. Applied and Environmental Microbiology 41:130-138

Girones R, Ferrus MA, Alonso JL, Rodriguez-Manzano J, Calgua B, Correa AD, Hundesa A, Carratala A, Bofill-Mas S (2010) Molecular detection of pathogens in water - The pros and cons of molecular techniques. Water Research 44:4325-4339

Grodzinski P, Yang J, Liu RH, Ward MD (2003) A modular microfluidic system for cell-preconcentration and genetic sample preparation. Biomedical Microdevices 5:303-310

Hu XY, Bessette PH, Qian JR, Meinhart CD, Daugherty PS, Soh HT (2005) Marker-specific sorting of rare cells using dielectrophoresis. Proceedings of the National Academy of Sciences of the United States of America 102:15757-15761

Hurley MA, Roscoe ME (1983) Automated statistical analysis of microbial enumeration by dilution series. Journal of Applied Bacteriology 55:159-164

Iwasaki M, Yonekawa T, Otsuka K, Suzuki W, Nagamine K, Hase T, Tatsumi K, Horigome T, Notomi T, Kanada H (2003) Validation of the loop-mediated isothermal amplification method for single nucleotide polymorphism genotyping with whole blood. Genome Letters 2:119-126

Kaigala GV, Huskins RJ, Preiksaitis J, Pang XL, Pilarski LM, Backhouse CJ (2006) Automated screening using microfluidic chip-based PCR and product detection to assess risk of BK virus-associated nephropathy in renal transplant recipients. Electrophoresis 27:3753-3763

Kermekchiev MB, Kirilova LI, Vail EE, Barnes WM (2009) Mutants of Taq DNA polymerase resistant to PCR inhibitors allow DNA amplification from whole blood and crude soil samples. Nucleic Acids Research 37:e40

Kim J, Johnson M, Hill P, Gale BK (2009) Microfluidic sample preparation: cell lysis and nucleic acid purification. Integrative Biology 1:574-586

Kinzelman J, Ng C, Jackson E, Gradus S, Bagley R (2003) Enterococci as indicators of Lake Michigan recreational water quality: Comparison of two methodologies and their impacts on public health regulatory events. Applied and Environmental Microbiology 69:92-96

Kralik P, Nocker A, Pavlik I (2010) Mycobacterium avium subsp paratuberculosis viability determination using F57 quantitative PCR in combination with propidium monoazide treatment. International Journal of Food Microbiology 141:S80-S86

Liang NJ, Dong J, Luo LX, Li Y (2011) Detection of viable salmonella in lettuce by propidium monoazide real-time PCR. Journal of Food Science 76:M234-M237

Mach AJ, Di Carlo D (2010) Continuous scalable blood filtration device using inertial microfluidics. Biotechnology and Bioengineering 107:302-311

Manage DP, Morrissey YC, Stickel AJ, Lauzon J, Atrazhev A, Acker JP, Pilarski LM (2011) On-chip PCR amplification of genomic and viral templates in unprocessed whole blood. Microfluidics and Nanofluidics 10:697-702

Mariella R (2008) Sample preparation: the weak link in microfluidics-based biodetection. Biomedical Microdevices 10:777-784

Maruyama F, Kenzaka T, Yamaguchi N, Tani K, Nasu M (2003) Detection of bacteria carrying the stx2 gene by in situ loop-mediated isothermal amplification. Applied and Environmental Microbiology 69:5023-5028

Masaomi I, Toshihiro Y, Kimihiko O, Wataru S, Kentaro N, Tetsu H, Ke-Ita T, Tsuneyoshi H, Tsugunori N, Hidetoshi K (2003) Validation of the loop-mediated isothermal amplification method for single nucleotide polymorphism genotyping with whole blood Genome Letters 2:119-126

Matheson CD, Gurney C, Esau N, Lehto R (2010) Assessing PCR inhibition from humic substances. The Open Enzyme Inhibition Journal 3:38-45

Matovu E, Kuepfer I, Boobo A, Kibona S, Burri C (2010) Comparative detection of trypanosomal DNA by loop-mediated isothermal amplification and PCR from flinders

technology associates cards spotted with patient blood. Journal of Clinical Microbiology 48:2087-2090

Nocker A, Cheung CY, Camper AK (2006) Comparison of propidium monoazide with ethidium monoazide for differentiation of live vs. dead bacteria by selective removal of DNA from dead cells. Journal of Microbiological Methods 67:310-320

Nocker A, Mazza A, Masson L, Camper AK, Brousseau R (2009) Selective detection of live bacteria combining propidium monoazide sample treatment with microarray technology. Journal of Microbiological Methods 76:253-261

Nocker A, Sossa-Fernandez P, Burr MD, Camper AK (2007) Use of propidium monoazide for live/dead distinction in microbial ecology. Applied and Environmental Microbiology 73:5111-5117

Nogva HK, Dromtorp SM, Nissen H, Rudi K (2003) Ethidium monoazide for DNA-based differentiation of viable and dead bacteria by 5 '-nuclease PCR. Biotechniques 34:804-813

Notomi T, Okayama H, Masubuchi H, Yonekawa T, Watanabe K, Amino N, Hase T (2000) Loop-mediated isothermal amplification of DNA. Nucleic Acids Research 28:e63

Pan Y, Breidt F (2007) Enumeration of viable Listeria monocytogenes cells by real-time PCR with propidium monoazide and ethidium monoazide in the presence of dead cells. Applied and Environmental Microbiology 73:8028-8031

Park S, Zhang Y, Lin S, Wang T, Yang S (2011) Advances in microfluidic PCR for point-of-care infectious disease diagnostics. Biotechnology Advances 29:830-839

Parshionikar S, Laseke I, Fout GS (2010) Use of propidium monoazide in reverse transcriptase PCR To distinguish between Infectious and noninfectious enteric viruses in water samples. Applied and Environmental Microbiology 76:4318-4326

Pohl G, Shih LM (2004) Principle and applications of digital PCR. Expert Review of Molecular Diagnostics 4:41-47

Poon LLM, Wong BWY, Ma EHT, Chan KH, Chow LMC, Abeyewickreme W, Tangpukdee N, Yuen KY, Guan Y, Looareesuwan S, Peiris JSM (2006) Sensitive and inexpensive molecular test for falciparum malaria: Detecting plasmodium falciparum DNA directly

from heat-treated blood by loop-mediated isothermal amplification. Clinical Chemistry 52:303-306

Price CW, Leslie DC, Landers JP (2009) Nucleic acid extraction techniques and application to the microchip. Lab on a Chip 9:2484-2494

Rompre A, Servais P, Baudart J, de-Roubin MR, Laurent P (2002) Detection and enumeration of coliforms in drinking water: current methods and emerging approaches. Journal of Microbiological Methods 49:31-54

Sauch JF, Flanigan D, Galvin ML, Berman D, Jakubowski W (1991) Propidium Iodide as an Indicator of Giardia Cyst Viability. Applied and Environmental Microbiology 57:3243-3247

Seyrig G, Ahmad F, Stedtfeld RD, Tourlousse DM, Stedtfeld RD, Hashsham SA (2011). Simple, powerful, and smart: Using LAMP for low cost screening of multiple waterborne pathogen. In K. Sen & N. J. Ashbolt (Eds.), Environmental Microbiology: Current Technology and Water Applications: Caister Academic Press 103–125

Shen F, Davydova EK, Du WB, Kreutz JE, Piepenburg O, Ismagilov RF (2011) Digital isothermal quantification of nucleic acids via simultaneous chemical initiation of recombinase polymerase amplification reactions on slipchip. Analytical Chemistry 83:3533-3540

Stedtfeld RD, Tourlousse DM, Seyrig G, Ahmad F, Tiedje JM, Hashsham SA (2011) Gene-Z: A device for point-of-care genetic testing using a smartphone. Submitted to Lab on a Chip

Taylor J (1962) The estimation of numbers of bacteria by tenfold dilution series. Journal of Applied Microbiology 25:54-61

Tourlousse DM, Ahmad F, Stedtfeld RD, Seyrig G, Tiedje JM, Hashsham SA (2011) A polymer microfluidic chip for quantitative detection of multiple water- and foodborne pathogens using real-time fluorogenic loop-mediated isothermal amplification. Submitted to Biomedical Microdevices

Vesper S, McKinstry C, Hartmann C, Neace M, Yoder S, Vesper A (2008) Quantifying fungal viability in air and water samples using quantitative PCR after treatment with propidium monoazide (PMA). Journal of Microbiological Methods 72:180-184

Wang SS, Levin RE (2006) Discrimination of viable Vibrio vulnificus cells from dead cells in real-time PCR. Journal of Microbiological Methods 64:1-8

Witek MA, Llopis SD, Wheatley A, McCarley RL, Soper SA (2006) Purification and preconcentration of genomic DNA from whole cell lysates using photoactivated polycarbonate (PPC) microfluidic chips. Nucleic Acids Research 34:e74

Yanez MA, Nocker A, Soria-Soria E, Murtula R, Martinez L, Catalan V (2011) Quantification of viable Legionella pneumophila cells using propidium monoazide combined with quantitative PCR. Journal of Microbiological Methods 85:124-130

Ye YX, Wang B, Huang F, Song YS, Yan H, Alam MJ, Yamasaki S, Shi L (2011) Application of in situ loop-mediated isothermal amplification method for detection of Salmonella in foods. Food Control 22:438-444

Zhang Z, Kermekchiev MB, Barnes WM (2010) Direct DNA amplification from crude clinical samples using a PCR enhancer cocktail and novel mutants of Taq. Journal of Molecular Diagnostics 12:152-161

CHAPTER V

5. RAPID AND SENSITIVE DETECTION OF THE GROWTH OF ESCHERICHIA COLI AND ANTIBIOTIC SUSCEPTIBILITY TESTING ON MICROCHIP

5.1 Introduction

Gold standard methods for antibiotic susceptibility testing (AST) rely upon culture-based approaches, e.g., broth/agar dilution and disk diffusion, which are simple and inexpensive (Bauer et al. 1966; Stalons and Thornsberry 1975). AST for faster growing microorganisms such as *Escherichia coli* is performed in 12 -18 h, which increases to 4-6 weeks for slow growing *Mycobacterium* species (Limb et al. 1993). These conventional methods are labor intensive and time consuming to permit same-day diagnosis which delays treatment and increase the risk of inappropriate use of antibiotics (Jorgensen and Ferraro 2009). Towards the automation and rapid AST, techniques those measure the bacterial density such as fluorescence (Kim et al. 2010; Joyce et al. 2011; Sun et al. 2011), optical density (Arora et al. 2009; Chen et al. 2010; Meyer et al. 2011), and micromechanical oscillation (Gfeller et al. 2005) or their activity such as bioluminescence (Hattori et al. 1998) and radioactive CO_2 release (Deblanc et al. 1972) in microfluidic or microtiter plate formats are being developed. Although the detection times of these techniques are in hours, they require a number of processing/measurement steps in their protocols, further delaying the results. Additionally, these techniques are not suitable for point-of-care AST due to the application of expensive detectors such as spectrophotometer, fluorescence microscope, and cantilever.

Bacterial growth monitoring through fluorescence detection can be used for rapid and low-cost AST by combining disposable microchips, low-cost and sensitive photon detectors, and highly fluorogenic membrane staining styryl or Fei Mao (FM) dyes. FM dyes contain two

lipophilic tails for partial insertion into the cell membranes and a core containing two aromatic rings connected with a double bond for generating fluorescence (Gaffield and Betz 2006; Wu et al. 2009). They provide high fluorescence in the hydrophobic environment i.e., in the presence of the cellular membranes and remain non-fluorescent otherwise. FM dyes have been extensively applied for staining prokaryotic (Joyce et al. 2011), eukaryotic (Vida and Emr 1995), and plant cells (Bolte et al. 2004). A variant of FM dye, FM5-95 can be useful for fluorescence imaging with simple optical filters and detectors due to the huge difference between the excitation and emission maxima (Stokes shift of 174 nm). Application of FM5-95 dye for the fluorescence microscope-based growth monitoring of *Mycobacterium* species reduced the detection time to 7 h from 4-6 weeks (Joyce et al. 2011). However, to our knowledge there is no report of real-time monitoring of bacterial growth or AST through fluorescence detection of FM5-95 dye on microfluidic platform.

Here, the real-time growth monitoring of *E. coli* at 37 ^{o}C in the presence of a membrane intercalating FM dye, by using a low-cost microchip and CCD imaging system is reported. Various concentrations of FM5-95 dye (1 µg/mL to 50 µg/mL) and two different CCD exposure times (1 s and 10 s) were tested towards the rapid detection of *E. coli* growth. A combination of 20 µg/mL FM5-95 dye and 10 s of CCD exposure time provided the detection of 10^4 *E. coli* in only 1 h. Highest concentration of FM5-95 (50 µg/mL) inhibited the *E. coli* growth. Sensitivity of the cell growth assay was tested with the dilution series of *E. coli* from 10^4 to 1 cell. The assay was sensitive to single cell with a detection time of 5 h. Antibiotic sensitivity of ampicillin and tetracycline on this *E coli* strain was tested. MIC values of ampicillin and tetracycline were 16 µg/mL and 1.6 µg/mL respectively, which were also consistent with the literature values. This

method would be useful for high throughput, rapid and real-time monitoring of bacterial growth for their AST.

5.2 Methods and materials

5.2.1 Microchip fabrication

Microchip with circular wells was fabricated with polyester film. Microchip consisted of multiple circular wells with 1 mm diameter and 2 µL volume per well. Detailed information about microchip fabrication process is provided in Chapter IV.

5.2.2 Fluorescence imaging system and signal acquisition

Fluorescence imaging system was built by integrating light source, optical filters, thin film heater, and a CCD camera. Detailed information about the fluorescence imaging system is provided in Chapter IV and also in a previous publication (Ahmad et al. 2011). In this modified system, emission filter (FF01-534/20-25) was replaced with another emission filter (FF01-747/33-25, Semrock, Rochester, NY) suitable for FM5-95 dye. Also the heater was maintained at 37 ^{o}C. For real-time monitoring of *E. coli* growth and AST, microchips were manually imaged with the CCD at every 5 min till the first 20 min. After 20 min, images were taken at every 20 min for 4-5 h. Light emitting diode was turned on before imaging and then turned off to avoid any quenching of FM5-95 dye by the constant light illumination. CCD gain of 100, offset of 60, and exposure times of 1 s and 10 s were used for imaging. Images were saved in flexible image transport system format**.** CCD images were opened in Image J (National Institutes of Health, Bethesda, MD) and a microarray profile plugin (http://www.optinav.com/imagej.html) was

applied to obtain fluorescence signals from the images. A microarray grid (circular wells with diameter of 1 mm) was used to extract the signals from the same pixel region of all the images.

5.2.3 Bacterial cell and genomic DNA

E. coli K12 strain C3000 cells were graciously provided by Professor Joan B. Rose, Water Quality, Environmental, and Molecular Microbiology Laboratory at Michigan State University. Frozen stock of *E. coli* was resuspended in Trypticase Soy Broth (TSB, 211768, BD, Sparks, MD) followed by the incubation at 37 ^{o}C in a shaker-incubator (New Brunswick Scientific, Edison, New Jersey) at 150 rpm for 12 h. Broth culture was further inoculated in 25 mL of sterile TSB and incubated at 37 ^{o}C for 8-12 h to achieve mid-log phase. Broth culture was placed overnight in the refrigerator at 4 ^{o}C. Broth culture was serially diluted in sterile TSB and colony forming units of *E. coli* were enumerated by plating 0.1 mL of their dilutions on Trypticase Soy Agar (TSA, 211043, BD, Sparks, MD) plates. TSA plates were incubated at 37 ^{o}C for 12 h before counting of cell colonies. The concentration of *E. coli* cells in the broth culture was approximately 1×10^{8} colony forming units/mL. Strict aseptic techniques were followed throughout the experiments.

5.2.4 Bacterial growth and AST on microchip

Styryl dye, FM5-95, (N-(3-trimethylammoniumpropyl)-4-(6-(4-(diethylamino) phenyl) hexatrienyl) pyridinium dibromide) was purchased from Molecular Probes (T23360, Invitrogen, Carlsbad, CA). A stock concentration of 1000 µg/mL of FM5-95 dye was prepared in sterile water and stored at 4 ^{o}C. The overnight broth culture of *E. coli* was diluted to approximately

100-fold in 50 µL fresh TSB to a concentration of 5 $\times 10^3$ cells/µL. Broth culture of *E. coli* was mixed with appropriate amounts of FM5-95 dye solution to prepare cell solutions with dye concentrations of 50 µg/mL, 20 µg/mL, 10 µg/mL, 5 µg/mL, and 1 µg/mL. A negative control (5 $\times 10^3$ cells/µL in TSB without any dye) was also prepared. To establish standard curve for quantitative analysis, 10-fold dilutions of *E coli* broth culture (10^4 cells to 1 cell) with 20 µg/mL FM5-95 dye were prepared. Negative controls containing 20 µg/mL FM5-95 dye in TSB were also prepared.

Ampicillin (A0166-25G, Sigma Aldrich, St. Louis, MO) and tetracycline (T7660-5G Sigma Aldrich, St. Louis, MO) were dissolved in sterile water. Stock solutions of ampicillin (50 mg/mL) and tetracycline (10 mg/mL) were filtered through a 0.22-µm nitrocellulose filters (Millipore, Billerica, MA) and stored at 4 ^{o}C and -20 ^{o}C respectively. *E. coli* broth cultures with 20 µM FM5-95 dye (50 µL; 5 $\times 10^3$ cells/µL) were mixed with appropriate amounts of ampicillin to the final concentrations of 32 µg/mL, 16 µg/mL, 8 µg/mL, 4 µg/mL, 2 µg/mL, and 1 µg/mL. And *E. coli* broth cultures with 20 µM FM5-95 dye (50 µL; 5 $\times 10^3$ cells/µL) were mixed with appropriate amounts of tetracycline to the final concentrations of 2.5 µg/mL, 2 µg/mL, 1.5 µg/mL, 1.2 µg/mL, 1 µg/mL, 0.5 µg/mL, and 0.1 µg/mL. Negative controls were free from any antibiotic and only contained 5 $\times 10^3$ *E. coli* cells/µL and 20 µM FM5-95 dye in TSB.

Approximately 2 µL of broth culture of *E. coli* (1×10^4 cells) containing appropriate amount of dye and or antibiotic was dispensed in each well of the microchip. Each assay was performed in quadruplicate. Wells were covered with mineral oil (Sigma, St. Louis, MO) during

the incubation to avoid the solution evaporation. Afterwards microchip was placed on the heating stage for incubation at 37 ^{o}C for 4-5 h and real-time CCD-based imaging.

5.2.6 Fluorescence signal analysis

To calculate SNR values of real-time bacterial growth and microAST, raw fluorescence signals were baseline corrected by subtracting the average fluorescence signals obtained in the first 15 min and dividing by their standard deviation. Tt was then defined as the time at which the SNR reached an arbitrary cut-off of 20 or higher. Average of the SNR from the quadruplicate was plotted with respect to amplification time. Tt values were calculated for individual reactions of quadruplicate and an average value of Tt is reported here. The error bars in the plots represented the standard deviations of the mean from four replicate experiments unless otherwise stated. Data analysis and plotting was done with Microsoft Excel (Microsoft, Redmond, WA).

5.3 Results and discussion

5.3.1 Real-time fluorescence monitoring during *E. coli* growth

Microchip-based growth of *E. coli* (1×10^{4} cells) in the presence of FM5-95 was monitored in real-time by measuring the fluorescence signals by a CCD imaging system. To investigate the effect of dye concentration on the cell growth and the resulting fluorescence signals, increasing concentrations of dye from 1 µg/mL to 50 µg/mL were applied. FM5-95 dye has a maximum excitation and emission peak at 560 nm and 734 nm respectively, with a high Stokes shift of 174 nm. By applying an appropriate emission filter, background light could be minimized to the detector for highly sensitive detection. Another advantage is the low intrinsic background from FM5-95 dye. Approximately 40 µM (23 µg/mL) of FM5-95 was found to be

optimum, when compared against a variety of styryl dyes towards their brightness and affinity for liposomal membrane (Wu et al. 2009). We have also included a higher concentration of FM5-95 dye (50 µg/mL) in this study to investigate its effect on *E. coli* growth. Two different CCD exposure times (1 s and 10 s) were applied during imaging to enhance the collection of photons/fluorescence signals as observed in our microRT$_f$-LAMP assays (Ahmad et al. 2011). The overall goal was to reduce the detection time of *E. coli* growth by optimizing the dye concentration and the CCD exposure time. Fluorescence signals were measured at every 5 min for the first 20 min (then every 20 min) to have a lower standard deviation of the mean of signal values in the first 15 min. The measured fluorescence signals were converted into SNR values to apply the cut-off (SNR≥20) for the calculation of Tt values. Higher SNR values were achieved due to the lower standard deviation of the mean of signal values in the first 15 min.

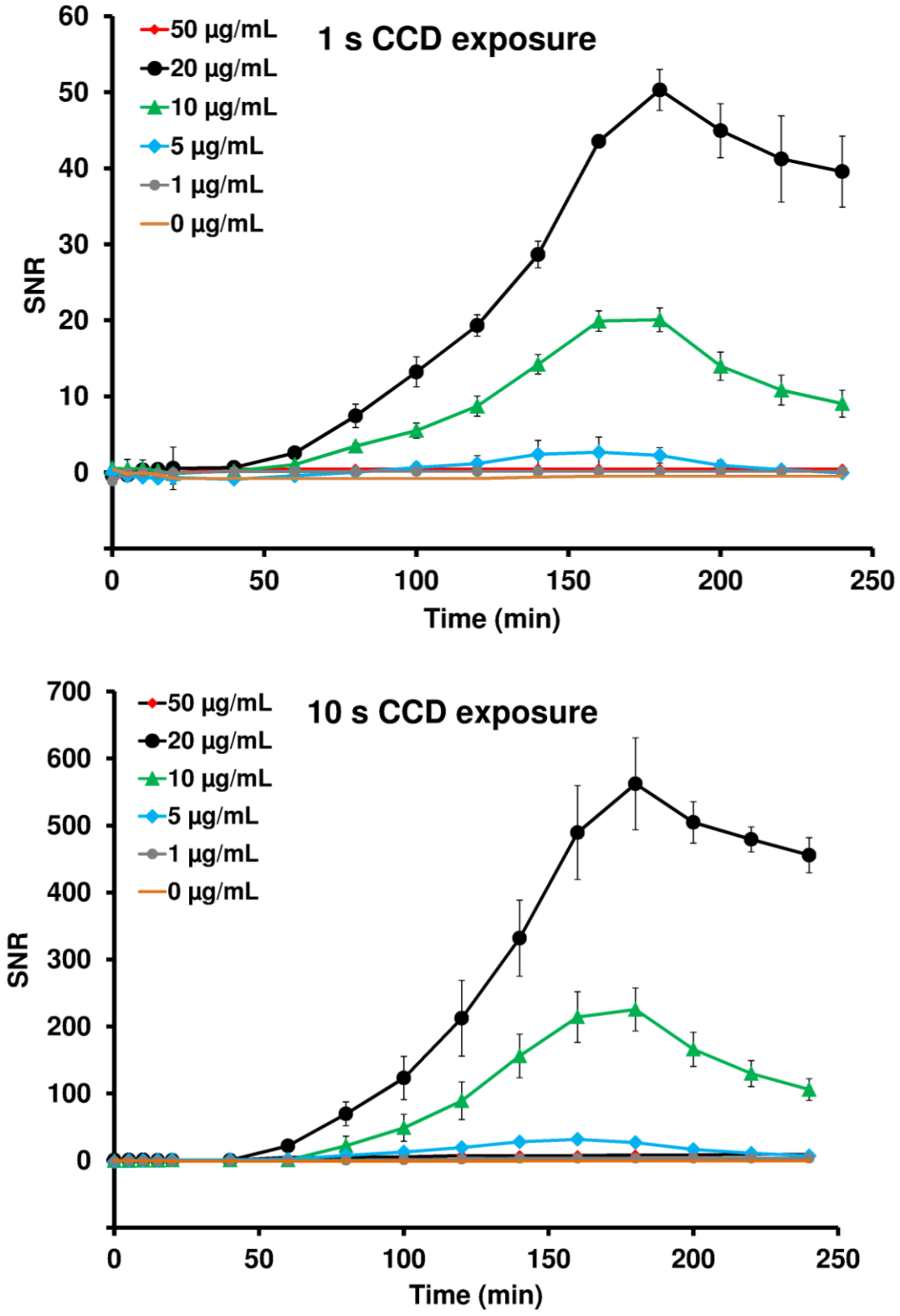

Figure 5.1 Real-time fluorescence growth curves of *E. coli* with various concentrations of FM5-95 dye at 1 s and 10 s of CCD exposure times.

E. coli growth curves showed a consistent increase in the average SNR values with respect the dye concentration and incubation time (Figure 5.1). Fluorescence-based growth curves exhibited a lag, exponential, and stationary phase similar to real-time optical density-based measurement of *E. coli* growth in microchip (Arora et al. 2009). With the CCD exposure time of 1 s, *E. coli* with the dye concentrations of 20 µg/mL, 10 µg/mL, and 5 µg/mL showed an increment in SNR values during the incubation time. The increase in the SNR values with 1 µg/mL dye was relatively lower than higher dye concentrations. The same trend of SNR increase during the *E. coli* growth with these dye concentrations was also observed with 10 s of CCD exposure time. However, no increment in the SNR values was observed with the 50 µg/mL dye, for both the exposure times. Also the negative controls did not show any increment in the SNR values during the incubation time. With the CCD exposure time of 1 s, the maximum SNR values for the 20 µg/mL, 10 µg/mL, and 5 µg/mL dye concentrations were 50.31 ± 2.7, 20.09 ± 1.6, and 2.66 ± 1.9 respectively. And with the CCD exposure time of 1 s, the maximum SNR values for the 20 µg/mL, 10 µg/mL, and 5 µg/mL dye concentrations were 562.31 ± 68.7, 225.45 ± 31.9, and 31.73 ± 6.16 respectively. SNR values with the 10 s of exposure time were approximately 11-fold higher than the 1 s of exposure time. Our observations were consistent with other reports demonstrating the improvements in the SNR values with the increasing CCD exposure times (Yang et al. 2008; Pjescic et al. 2010). Faster increase in the SNR values would reduce the Tt values leading to faster detection of *E. coli* growth as microRT$_f$-LAMP assays (Ahmad et al. 2011).

Lack of increase in the SNR values with 50 µg/mL dye might be due to the *E. coli* growth inhibition with such a high dye concentration. In other study, imaging of real-time growth of *Mycobacterium smegmatis* on thin agar film was performed with a 10-fold lower FM5-95

concentration of 2 µg/mL (Joyce et al. 2011). Also, a maximum concentration of 23 µg/mL of FM5-95 was applied in the liposomal affinity study (Wu et al. 2009). FM5-95 dye has been commonly applied for staining cellular membranes of a variety of microorganisms with dye concentrations ranging from 1 µg/mL to 5 µg/mL (Veach et al. 2004; Adams et al. 2011; Sass et al. 2011; Willemse et al. 2011). However, cell membrane staining with FM5-95 would not require the cells to be alive for the endpoint imaging applications. Application of the lower concentration of FM5-95 dye in the live cell imaging of acid fast gram-positive microorganisms might be due to the dye-based cell growth inhibition (Joyce et al. 2011). Dye-based growth inhibition of multiple gram-positive and gram-negative microorganisms with a number of fluorogenic dyes including, orange II, sudan II, tetrazolium dyes has been reported (Fung and Miller 1973; Ullrich et al. 1996; Pan et al. 2011). However, no systematic study on the inhibitory effect of styryl dyes, including FM5-95 is currently available. Growth inhibition might be due to higher interaction between the FM5-95 and cell membrane *E. coli*, leading to the inclusion of dye inside the cells (Bolte et al. 2004). However, this hypothesis was not confirmed in this study.

5.3.2 Effect of FM5-95 dye concentration and CCD exposure time on the Tt value of *E. coli* growth on microchip

The effect of FM5-95 dye concentrations (1 µg/mL to 20 µg/mL) and two different CCD exposure times (1 s and 10 s) on the Tt values was investigated (Figure 5.2). Tt values were calculated based on the SNR≥20. A higher cut-off of SNR (≥20) was applied, as fluorescence signals/SNR in these cell assays showed a drastic increase at the starting of exponential phase (e.g., SNR <2 to ≥20), especially with 10 s of exposure time. With the CCD exposure time of 1 s, Tt values for 20 µg/mL and 10 µg/mL dye concentrations were 106.67 ± 18.9 min and 133.33 ± 18.9 respectively. Tt for 5 µg/mL dye concentration was not included in the analysis as the SNR

with this dye concentration did not increase above the cutoff value. With the CCD exposure time of 10 s, Tt values for 20 µg/mL, 10 µg/mL, and 5 µg/mL dye concentrations were 60 ± 0.0, 80 ± 11.5, and 100 ± 0.0 respectively. The analysis showed that the Tt values were dependent on both the dye concentration and the CCD exposure time. Additionally, the fastest detection of *E. coli* (1×10^4 cells) growth in 60 min was possibly with a combination of 20 µg/mL FM5-95 dye and 10 s of CCD exposure time.

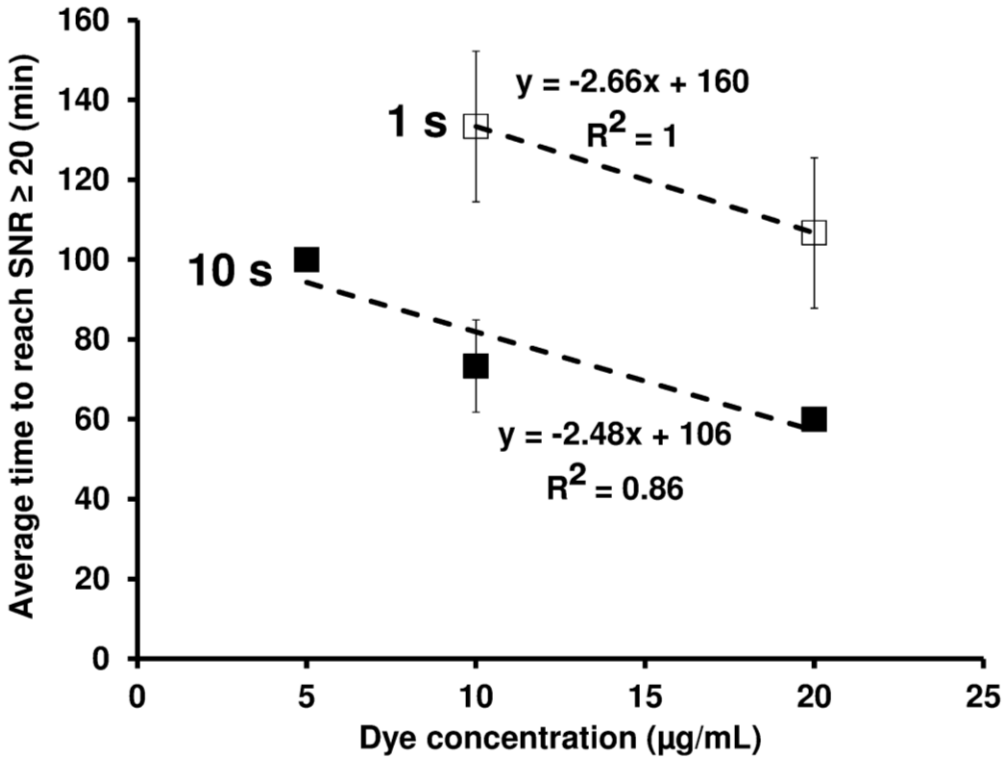

Figure 5.2 Comparison of *E. coli* (1×10^4 cells) growth detection times (SNR cut-off ≥ 20) with various concentrations of FM5-95 dye measured with 1 s and 10 s of CCD exposure times.

5.3.3 Quantitative analysis of *E. coli* dilution series on microchip

To establish standard curve for quantitative analysis, real-time growth assays of 10^4 to 1 cell of *E. coli* with 20 µg/mL FM5-95 dye were monitored by the CCD imaging system at an

exposure time of 10 s. Real-time growth curves showed consistent increase in the SNR values during the incubation time (Figure 5.3). Fluorescence-based growth curves showed a lag phase, exponential phase, and stationary phase for all the assays except single cell assay. Higher incubation time of single cell than 320 min was needed to obtain the complete growth curve. No increment in the SNR values was observed in the negative controls. Maximum average SNR values showed a decreasing trend with respect to the decreasing cell number in the assay. The maximum SNR values for the assays with 10^4, 10^3, 10^2, 10, and 1 cell (s) were 590.3 ± 25.4, 470.4 ± 15.6, and 301.2 ± 15.6, 256.8 ± 16.6, and 165.6 ± 14.6 respectively. Out of 4 positive controls of single cell assay, only 2 replicate showed the increase in fluorescence signals during the incubation time of 5 h. That might be due to the dilution effect in single cell assay. Tt values of the assays were calculated by applying the SNR cutoff value of ≥20. Tt values of assays with 10^4, 10^3, 10^2, 10, and 1 cell(s) were 60 ± 0.0, 120 ± 0.0, 173.3 ± 11.5, 246.7 ± 11.5, and 306.7 ±23.1 respectively. The standard curve for growth assay was established by plotting the logarithmic values of the number of cell versus the Tt values. *E. coli* growth was quantitative and showed the single cell-level sensitivity. Correlation coefficient (R^2) of the fitted line was 0.99.

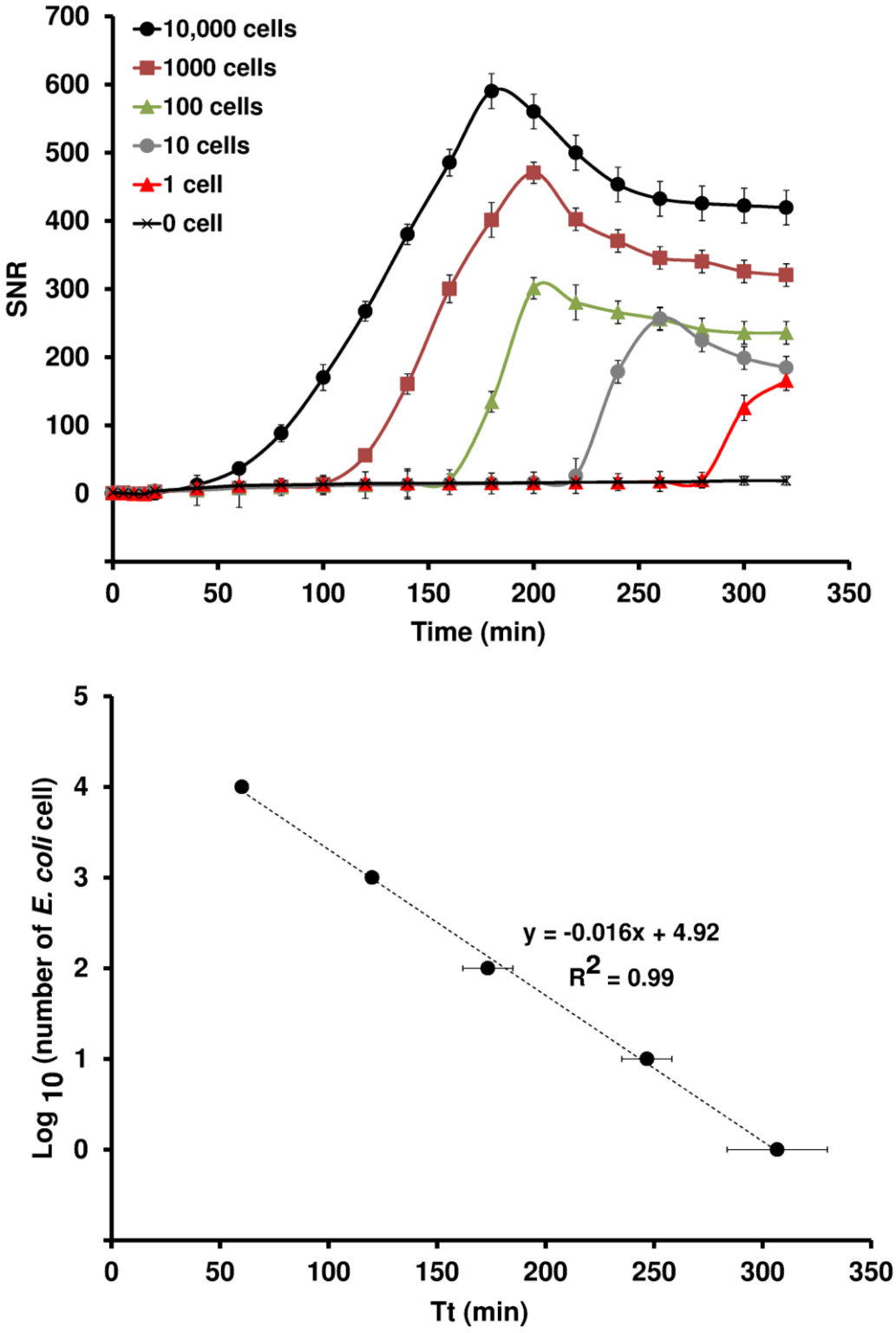

Figure 5.3 Real-time fluorescence growth curves of the dilution series of *E. coli* (1×10^4 cells to 1 cell) with 20 µM FM5-95 dye and the standard curve. For single cell dilution, the error bars represent the standard deviations of the mean only from 2 replicates

Standard growth curve was used for the calculation of the generation time of *E. coli* C3000 strain by the formula applied for the growth rate as measured by the increase in the cell density/optical density with respect to the incubation time . A negative sign was applied as the Tt values were decreasing with respect to decreasing cell number in the assay. Here, k is the growth rate, N is the number of cell in the lowest dilution, No is the number of cells in the highest dilution, and t and t_o are the Tt values for lowest and highest dilutions respectively.

$$k = - (\ln N - \ln N_o) / (t - t_o)$$

In our case, the numbers of cell(s) in the lowest and highest dilutions were 10^4 and 1 and their respective Tt values 306.7 min and 60 min were respectively. Therefore the growth rate and generation time of *E. coli* C3000 strain was 0.037 min^{-1} and 27 min respectively. Generation time of 27 min for this *E. coli* C3000 strain was earlier reported based on the optical density-based measurement (Hsu 1968).

5.3.4 Ampicillin and tetracycline susceptibility testing of *E. coli* in microchip

Real-time growth of *E. coli* (1×10^4 cells) was monitored in the microchip in the presence of two different antibiotics, ampicillin (0 to 32 µg/mL) and tetracycline (0 to 2.5 µg/mL), to examine their inhibitory effect on cell growth. *E. coli* growth in the presence of 20 µg/mL FM5-95 dye were monitored by the CCD imaging system with 10 s exposure time under varying concentrations of ampicillin and tetracycline. Ampicillin and tetracycline were selected in this study due to their different modes of inhibition on microbial growth (Figure 5.4).

Ampicillin belongs to the penicillin group of β-lactum antibiotics, which acts an inhibitor for transpeptidase enzyme required for cell wall synthesis, leading to microbial cell lysis

(Campolirichards and Brogden 1987). Tetracycline belongs to the family of polyketides also called protein synthesis inhibitor, which interacts with the 30S ribosome preventing the binding of aminoacyl-t-RNA to the ribosomal acceptor site, eventually ceasing the microbial growth (Chopra and Roberts 2001). Both the antibiotics have been found to be effective against a wide range of gram-positive and gram-negative bacteria, including *E. coli* (Chopra et al. 1963; Chopra and Roberts 2001).

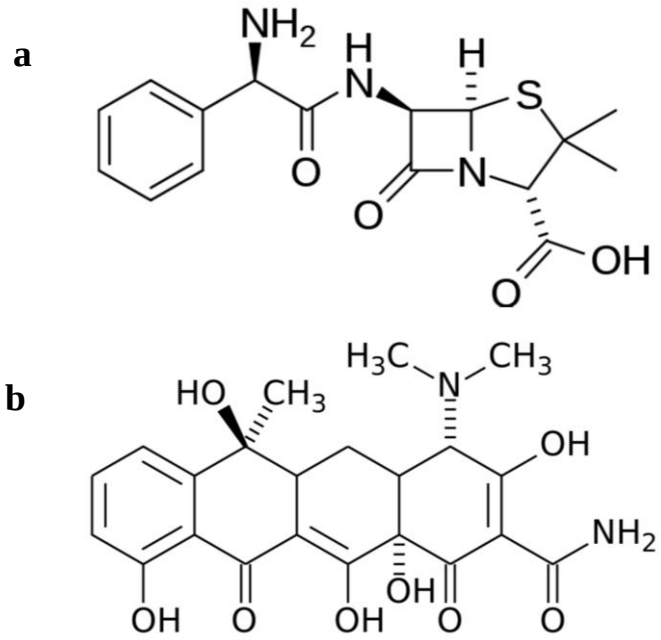

Figure 5.4 Chemical structures of (a) ampicillin and (b) tetracycline

Real-time *E. coli* growth curves showed a consistent decrease in the average SNR values with respect the increasing dye concentrations (Figure 5.5). The maximum SNR values of the growth curves with ampicillin concentrations of 1 µg/mL, 2 µg/mL, 4 µg/mL, 8 µg/mL, 16 µg/mL, and 32 µg/mL were 407.8 ± 25.4, 300.5 ± 15.0, 221.2 ± 15.0, 121.5 ± 20.2, 35.62 ± 6.46, and 16.6 ± 6.45 respectively. The maximum SNR values of the growth curves with tertacycline concentrations of 0.1 µg/mL, 0.5 µg/mL, 1 µg/mL, 1.2 µg/mL, 1.5 µg/mL, 2 µg/mL, and 2.5

µg/mL were 490.33 ±25.4, 300.5 ± 15.0, 160.4 ± 15.0, 115.55 ± 15.2, 35.58 ± 7.24, 15.56 ± 6.45, and 15.50 ± 7.24 respectively. The maximum SNR values of the growth curves of negative controls (with any antibiotic) were 578.30 ± 20.4 and 590.33 ± 25.7 respectively. These SNR values were consistent with the maximum SNR value of 562.31 ± 68.7 for the *E. coli* growth with 20 µg/mL FM5-95 dye and 10 s of CCD exposure time (Figure 5.1). The only difference between the *E. coli* growth curves were different slope/rate of growth with the specific type of antibiotic and their concentrations.

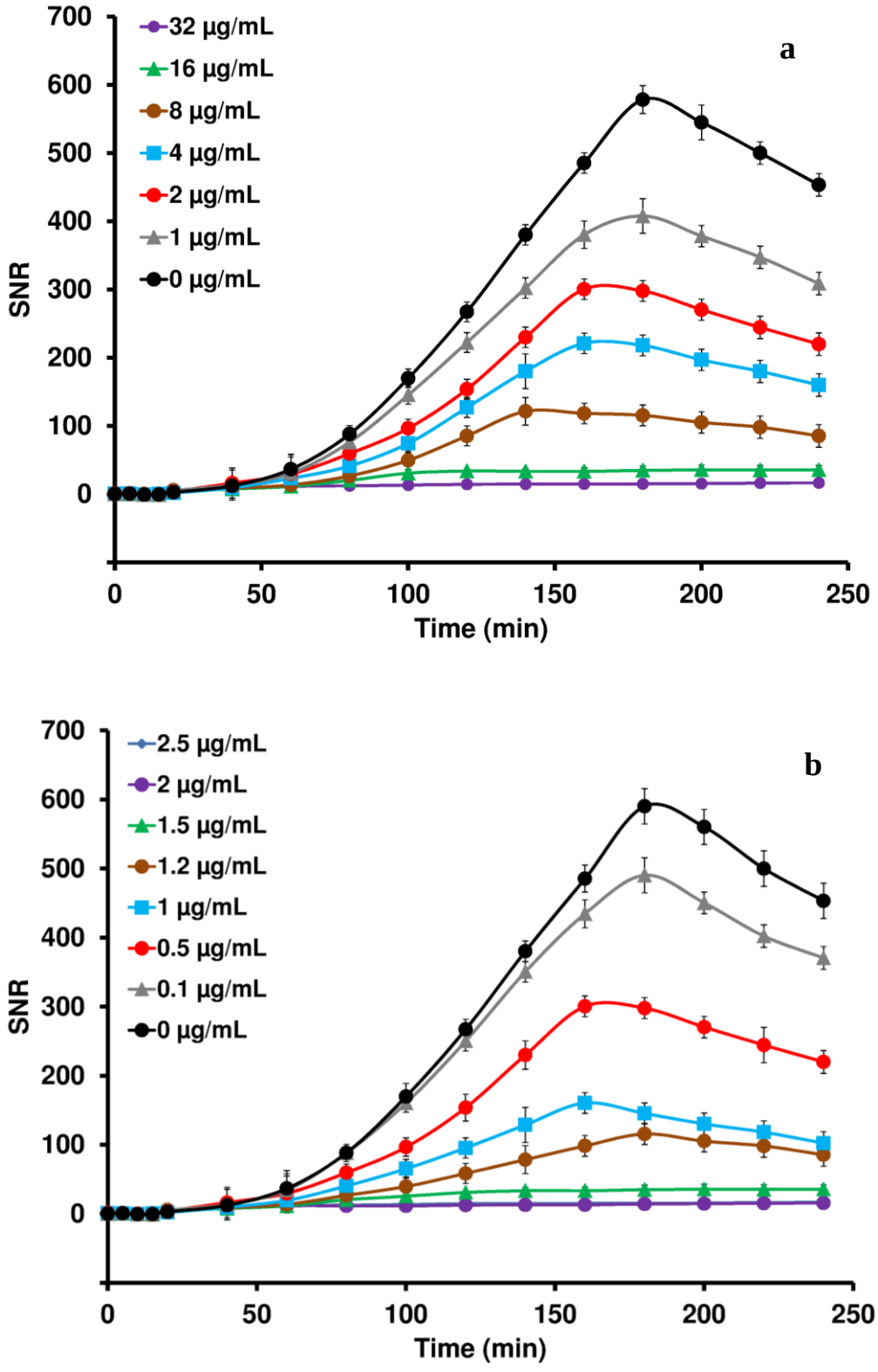

Figure 5.5 Real-time fluorescence growth curves of 1 $\times 10^4$ cells of *E. coli* (with 20 µg/mL FM5-95 dye) and increasing concentrations of (a) ampicillin and (b) tetracycline

5.3.5 Determination of MIC values of ampicillin and tetracycline for *E. coli* on microchip

Quantitative evaluation of the inhibitory effects of ampicillin and tetracycline on *E. coli* (1×10^4 cells) was performed on the microchip. For that, average slopes of the linear portion of the ampicillin/tetracycline treated growth curves during the exponential phase were calculated. Data was normalized by dividing the average growth rate with the average slope of the ampicillin/tetracycline free growth curve (Figure 5.6) (Fesenko et al. 2005; Sun et al. 2011). Normalized growth rates of *E. coli* with ampicillin concentrations of 1 µg/mL, 2 µg/mL, 4 µg/mL, 8 µg/mL, 16 µg/mL, and 32 µg/mL were 0.89 ± 0.1, 0.60 ± 0.09, 0.35 ± 0.05, 0.13 ± 0.04, 0.08 ± 0.03, 0.06 ± 0.02 respectively. Normalized growth rates of *E. coli* with tetracycline concentrations of 0.1 µg/mL, 0.5 µg/mL, 1 µg/mL, 1.2 µg/mL, 1.5 µg/mL, 2 µg/mL, and 2.5 µg/mL were 0.91 ± 0.1, 0.75 ± 0.09, 0.31 ± 0.09, 0.20 ± 0.09, 0.07 ± 0.03, 0.05 ± 0.02, and 0.04 ± 0.02 respectively. The trend showed that the growth rate(s) of *E. coli* decreased drastically up to a particular concentration of antibiotic(s) and then became linear (constant) for higher concentration of antibiotic(s). However, a faster decline in the growth rate of *E. coli* was observed with ampicillin as compared to tetracycline. Therefore, ampicillin exerts more acute inhibition effect on *E. coli* C3000 than tetracycline.

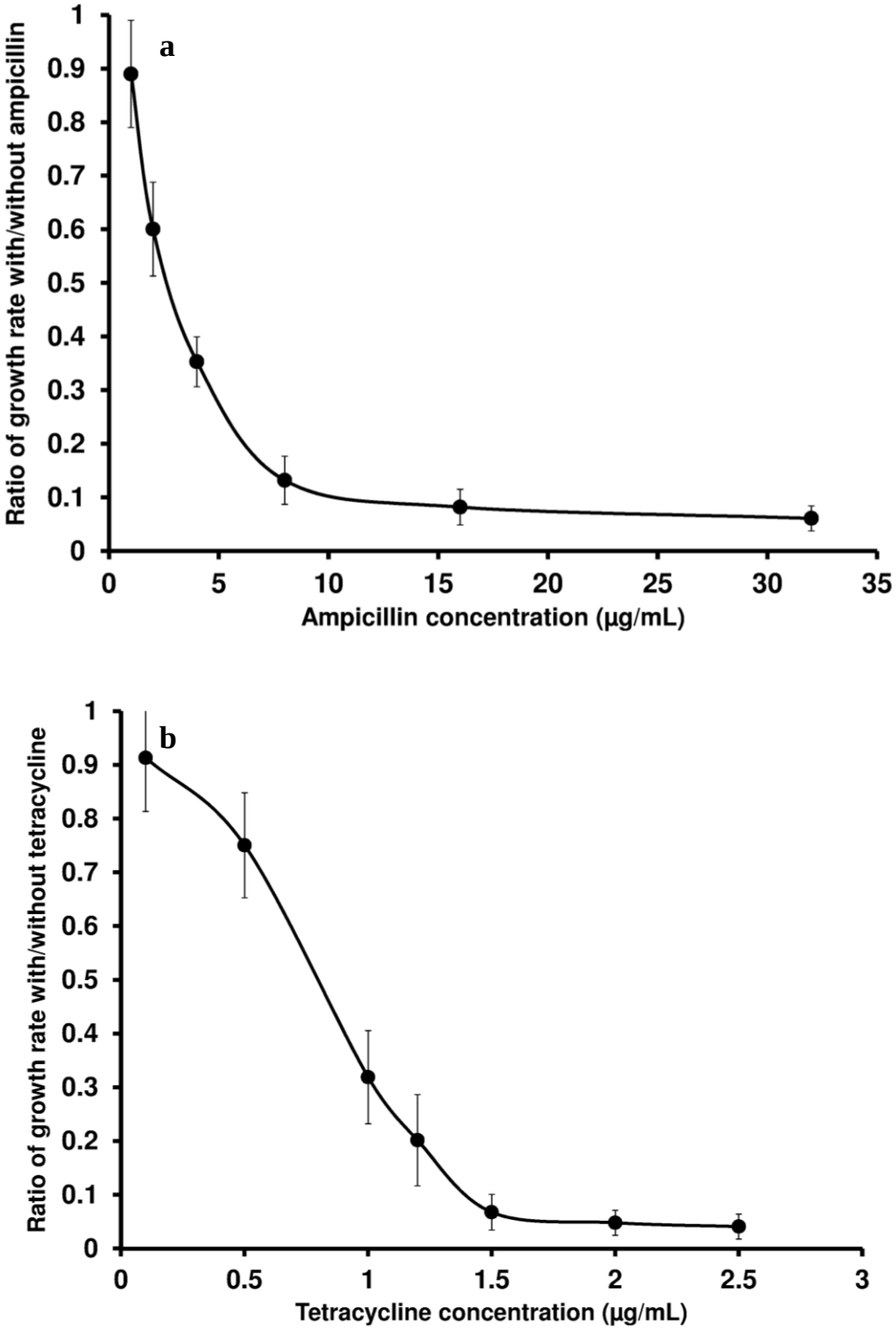

Figure 5.6 Ratio of the growth rates of 1 $\times 10^4$ cells of *E. coli* (with 20 μg/mL FM5-95 dye) with and without (a) ampicillin and (b) tetracycline

MIC values of ampicillin and tetracycline were calculated by extrapolating the linear portion of the growth rate to the antibiotic concentration. The calculated MIC values of ampicillin and tetracycline for *E. coli* C3000 were 16 µg/mL and 1.6 µg/mL respectively. Inhibitory effects of ampicillin (Chen et al. 2010) and tetracycline (Sun et al. 2011) on other *E. coli* strains are being evaluated in microfluidic platforms. The inhibition effect on *E. coli* growth in the presence of these two antibiotics and their MIC values, as observed in our case, was similar to other reports.

5.4 Conclusions

Microchip-based real-time fluorescence monitoring of *E. coli* growth in the presence of a novel dye, FM5-95 by using the CCD imaging system was performed. Concentration and CCD exposure time was optimized for the rapid *E. coli* growth detection in 1 h. *E. coli* growth assay was sensitive to single cell and required a low volume of 2 µL. Effect of *E. coli* growth inhibition in the presence of antibiotics were studied. Microchip-based MIC values were found to be in consistent with the values reported in literature. This real-time, rapid, and sensitive method of cell growth monitoring could be extended for the AST of microorganisms in high throughput microchips by applying low-cost CCD imaging system.

REFERENCES

5.5 References

Adams DW, Wu LJ, Czaplewski LG, Errington J (2011) Multiple effects of benzamide antibiotics on FtsZ function. Molecular Microbiology 80:68-84

Ahmad F, Seyrig G, Tourlousse DM, Stedtfeld RD, Tiedje JM, Hashsham SA (2011) A CCD-based fluorescence imaging system for real-time loop-mediated isothermal amplification-based rapid and sensitive detection of waterborne pathogens on microchips. Biomedical Microdevices 13:929-937

Arora S, Lim CS, Foo JY, Sakharkar MK, Dixit P, Liu AQ, Miao J-M (2009) Microchip system for monitoring microbial physiological behavior under drug influences. Journal of Engineering in Medicine 223:777-786

Bauer AW, Kirby WMM, Sherris JC, Turck M (1966) Antibiotic susceptibility testing by a standardized single disk method. American Journal of Clinical Pathology 45:493-496

Bolte S, Talbot C, Boutte Y, Catrice O, Read ND, Satiat-Jeunemaitre B (2004) FM-dyes as experimental probes for dissecting vesicle trafficking in living plant cells. Journal of Microscopy 214:159-173

Campolirichards DM, Brogden RN (1987) Sulbactam Ampicillin - A review of Its antibacterial activity, pharmacokinetic properties, and therapeutic use. Drugs 33:577-609

Chen CH, Lu Y, Sin MLY, Mach KE, Zhang DD, Gau V, Liao JC, Wong PK (2010) Antimicrobial susceptibility testing using high surface-to-volume ratio microchannels. Analytical Chemistry 82:1012-1019

Chopra I, Roberts M (2001) Tetracycline antibiotics: Mode of action, applications, molecular biology, and epidemiology of bacterial resistance. Microbiology and Molecular Biology Reviews 65:232-260

Chopra SL, Dale DG, Blackwood AG (1963) Effect of ampicillin on E. coli of swine origin. Canadian Journal of Comparative Medicine and Veterinary Science 27:223-&

Deblanc HJ, Wagner HN, Charache P (1972) Automatic radiometric measurement of antibiotic effect on bacterial growth. Antimicrobial Agents and Chemotherapy 22:360-&

Fesenko DO, Nasedkina TV, Prokopenko DV, Mirzabekov AD (2005) Biosensing and monitoring of cell populations using the hydrogel bacterial microchip. Biosensors & Bioelectronics 20:1860-1865

Fung DYC, Miller RD (1973) Effect of dyes on bacterial growth. Applied Microbiology 25:793-799

Gaffield MA, Betz WJ (2006) Imaging synaptic vesicle exocytosis and endocytosis with FM dyes. Nature Protocols 1:2916-2921

Gfeller KY, Nugaeva N, Hegner M (2005) Micromechanical oscillators as rapid biosensor for the detection of active growth of Escherichia coli. Biosensors & Bioelectronics 21:528-533

Hattori N, Nakajima MO, O'Hara K, Sawai T (1998) Novel antibiotic susceptibility tests by the ATP-bioluminescence method using filamentous cell treatment. Antimicrobial Agents and Chemotherapy 42:1406-1411

Hsu YC (1968) Propagation or Elimination of Viral Infection in Carrier Cells. Bacteriological Reviews 32:387-399

Jorgensen JH, Ferraro MJ (2009) Antimicrobial susceptibility testing: a review of general principles and contemporary practices. Clinical Infectious Diseases 49:1749-1755

Joyce G, D. RB, Williams KJ (2011) A modified agar pad method for mycobacterial live-cell imaging. BMC Research Notes 4:1-4

Kim KP, Kim YG, Choi CH, Kim HE, Lee SH, Chang WS, Lee CS (2010) In situ monitoring of antibiotic susceptibility of bacterial biofilms in a microfluidic device. Lab on a Chip 10:3296-3299

Limb DI, Wheat PF, Spencer RC, Harris GS, Rayner AB, Watt B (1993) Comparison of techniques for antimicrobial susceptibility testing of mycobacteria. Journal of Clinical Pathology 46:403-407

Meyer MT, Roy V, Bentley WE, Ghodssi R (2011) Development and validation of a microfluidic reactor for biofilm monitoring via optical methods. Journal of Micromechanics and Microengineering 21:1-10

Pan HM, Feng JH, Cerniglia CE, Chen HZ (2011) Effects of Orange II and Sudan III azo dyes and their metabolites on Staphylococcus aureus. Journal of Industrial Microbiology & Biotechnology 38:1729-1738

Pjescic I, Tranter C, Hindmarsh PL, Crews ND (2010) Glass-composite prototyping for flow PCR with in situ DNA analysis. Biomedical Microdevices 12:333-343

Sass P, Josten M, Famulla K, Schiffer G, Sahl HG, Hamoen L, Brotz-Oesterhelt H (2011) Antibiotic acyldepsipeptides activate ClpP peptidase to degrade the cell division protein FtsZ. Proceedings of the National Academy of Sciences of the United States of America 108:17474-17479

Stalons DR, Thornsberry C (1975) Broth-dilution method for determining the antibiotic susceptibility of anaerobic bacteria. Antimicrobial Agents and Chemotherapy 7:15-21

Sun P, Liu Y, Sha J, Zhang ZY, Tu Q, Chen P, Wang JY (2011) High-throughput microfluidic system for long-term bacterial colony monitoring and antibiotic testing in zero-flow environments. Biosensors & Bioelectronics 26:1993-1999

Ullrich S, Karrasch B, Hoppe HG, Jeskulke K, Mehrens M (1996) Toxic effects on bacterial metabolism of the redox dye 5-cyano-2,3-ditolyl tetrazolium chloride. Applied and Environmental Microbiology 62:4587-4593

Veach RA, Liu DY, Yao S, Chen YL, Liu XY, Downs S, Hawiger J (2004) Receptor/transporter-independent targeting of functional peptides across the plasma membrane. Journal of Biological Chemistry 279:11425-11431

Vida TA, Emr SD (1995) A new vital stain for visualizing vacuolar membrane dynamics and endocytosis in yeast. Journal of Cell Biology 128:779-792

Willemse J, Borst JW, de Waal E, Bisseling T, van Wezel GP (2011) Positive control of cell division: FtsZ is recruited by SsgB during sporulation of Streptomyces. Genes & Development 25:89-99

Wu Y, Yeh FL, Mao F, Chapman ER (2009) Biophysical characterization of styryl dye-membrane interactions. Biophysical Journal 97:101-109

Yang MH, Kostov Y, Bruck HA, Rasooly A (2008) Carbon nanotubes with enhanced chemiluminescence immunoassay for CCD-based detection of staphylococcal enterotoxin B in food. Analytical Chemistry 80:8532-8537

CHAPTER VI

6. CONCLUSIONS AND FUTURE PERSPECTIVES

6.1 Conclusions

Culture-based gold standard methods for pathogen/resistance identification are labor intensive and time consuming resulting into delayed diagnosis of pathogens and increase in mortality and morbidity. Molecular methods have tremendous potential for addressing the global threat of infectious diseases due to their rapidity, sensitivity, and accuracy. However, due to their high cost and complexity, molecular methods are currently used in centralized laboratories. Therefore, a need exists for a simplified and low-cost platform, on which genetic and cellular-based molecular assays could be performed with similar speed, sensitivity, and accuracy as commercially available systems. Microfluidic PCR systems are being developed and applied for gene amplification and detection of a variety of pathogens. However, due to the need for thermal cycling and the associated high thermal mass, microfluidic PCR systems are slow. Decreasing the thermal mass and increasing the heating/cooling rates leads to faster gene amplification. However, that would increase the power consumption and the complexity of the microfluidic PCR systems. An additional limitation of microfluidic PCR systems is the inhibition of commonly used *Taq* polymerase in the presence of cell debris and a variety of other chemicals. Therefore, completely integrated microfluidic PCR systems (for sample-in-answer-out capability) require dedicated cell lysis, and nucleic acid purification steps, which increases the total detection time. Compared to PCR, isothermal nucleic acid amplification methods have not extensively translated on microfluidic platforms. Translation of loop-mediated isothermal amplification (LAMP) on microfluidic platform is promising due to i) moderate incubation

temperature leading to simplified heating and low power consumption, ii) high amount of amplification products, which can be detected either by simple detectors, iii) direct genetic amplification from bacterial cells due to the superior tolerance to substances that typically inhibit PCR, iv) high specificity, sensitivity up to single copy, and rapid detection in 10-20 min.

Towards the development of a simplified system to perform the rapid detection of bacterial pathogens and their antibiotic susceptibility, the following key tasks were accomplished:

1. Developed low-cost polymeric microchips with cyclic olefin copolymer and polyester and a CCD-based imaging system.
2. Validated microRT$_f$-LAMP assays of 12 virulence genes of 6 diarrheal pathogens on microchip by using a CCD imaging system. Applied Syto-82 dye and CCD exposure time control for reducing the Tt of microRT$_f$-LAMP by 10 to 50-fold as compared to commercial PCR instrument.
3. Developed digital LAMP assays for genetic amplification directly from gram-negative and gram-positive bacterial cells at 63 ^{o}C without any sample processing.
4. Developed real-time fluorescence-based cell growth assays on microchip by using a novel cell membrane intercalating dye, FM5-95, for rapid and sensitive detection of *E. coli* growth and antibiotic susceptibility testing in 1-2 h.

To our knowledge, the strategies used to reduce the Tt values of microRT$_f$-LAMP assays and cell growth/microAST method by applying novel fluorogenic dyes and CCD exposure time

control, and direct gene amplification from bacterial cells at 63 ^{o}C are novel. These developments could be easily extended for the rapid testing of pathogens in clinical, environmental, agricultural, and biodefense applications.

6.2 Future perspectives

In this project, it was shown that gene amplification could be performed directly from gram-negative and gram-positive bacterial cells in digital format. Also assays for bacterial cell growth monitoring and AST were developed. Both the assays digital LAMP and AST were performed separately in this project. However, in future, both the assays will be combined on single high throughput microfluidic chip for simultaneous detection of pathogens and their antibiotic susceptibility.

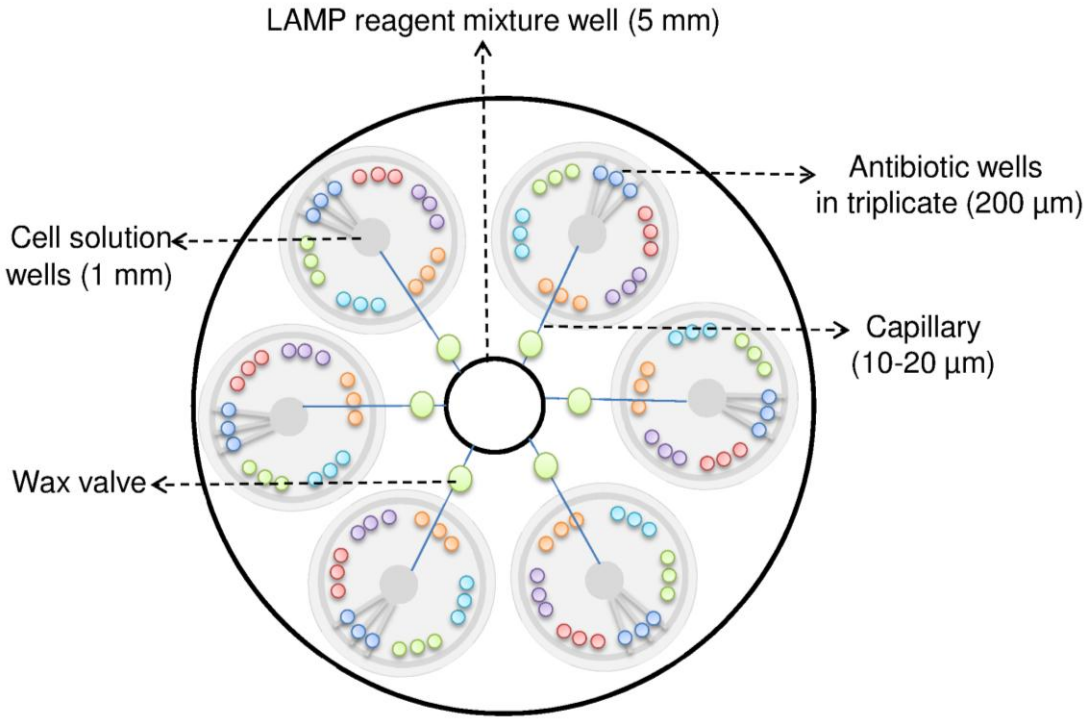

Figure 6.1 Conceptual picture a microfluidic chip for integrated AST and digital LAMP

High throughput microfluidic chip will be fabricated by using a low-cost CO_2 laser cutter capable of prototyping high resolution microstructures in polymeric microchips. Microfluidic chip will have 6 circular patterns containing 18 wells in each circle connected through capillaries. Also, all the 6 circular patterns will be connected to a central well through capillaries, which will be initially blocked by wax (melting temperature of 65 ^{o}C). These 6 circular wells will be used for AST testing (against a variety of antibiotics, as shown below) and then subsequently for digital LAMP from six individual clinical samples containing diarrheal pathogens.

Organism	Drug
Salmonella enterica	Children: Ceftriaxone Adults: Ciprofloxacin
Vibrio cholerae	Tetracyclin Doxycycline Norfloxacin Ciprofloxacin Furazolidone
Escherichia coli (diarrheal)	Ciprofloxacin Rifaximin
Shigella spp.	Children: Azithromycine or Ceftriaxone Adults: Ciprofloxacin or Oflaxin
Campylobacter jejuni	Fluoroquinolones Macrolides
Borrelia burgdorferi	doxycycline, Amoxicillin Cefuroxime axetil

APPENDICES

APPENDICES

Table A1.1 Nucleotide sequences of the designed LAMP primers

Target	Primer	Sequence (5'-3')
C. parvum hsp70	F3	ACAACTCCATCTGTTGTGG
	B3	GCATCCCCATTATCAGCC
	FIP	CAGTGTTTTCTGGGTTTGTGATTGCTTTTTCTGAAGATGGGCAG
	BIP	TTACGCAACAAAGAGGCTAATTGGTTATATGGTAAAATTCCCTGTTCC
	LF	TTGCAACTTCACCAACCAATCT
	LB	AGAAGGTACGAAGAAGAAGCAATC
C. parvum gp60	F3	ACGCAGAAGGCAGTCAAGA
	B3	ACCACACTTCAATGTCGCAG
	FIP	GGAAGCAGCACTAGTTTGGCCAACTGAAGCTTCTGGTAGCCA
	BIP	TCCAGCTCAAAGTGAAGGCGCGGGGTACCTTCTCCGAACC
	LF	TCACTACCTTCCTCTTCAGAACC
	LB	TGCGGCACTTCATTTGTAATGT
S. enterica invA	F3	GAAGCGTACTGGAAAGGGAA
	B3	TCAACAATGCGGGGATCTG
	FIP	ATGATGCCGGCAATAGCGTCACAGCCAGCTTTACGGTTCCT
	BIP	GATGACCCGCCATGGTATGGATACCATCACCAATGGTCAGC
	LF	TGATAAACTTCATCGCACCGTC
	LB	TTRTCCTCCGCTCTGTCTAC
S. enterica phoB	F3	GCCATTCCACATCGAAGAGGT
	B3	ATGAGAACATCAATGGTATGGC
	FIP	GGCGTGAGAGATCCACCTGGAATGCGCCGTAATAGCGGTC
	BIP	CACCATTATGGAAACGCTTATCCGCCGGATACAGCTGAAGCATC
	LF	CAGGTGATCAACATCCCGCC
	LB	CGGTAAAGTGGTCAGCAAAGAT
C. jejuni cdtA	F3	CCCCACCTTTAACTAGAACAA
	B3	GCCAAATCCTTTGCTATCGA

Table A1.1
(cont'd)

	FIP	CGCAGGGCGATTTTCAAAAATTAAACAATAATGCAGYAAA TGGGAT
	BIP	TTAACCATTTTAGGCCCTAGCGGCAAATCCAATTTCCTTGT GCT
	LF	GCTTCGTCTTTAAAGYGAGGATTG
	LB	AGCAGCTTTAACGGTTTGGG
C. jejuni 0414	F3	GCAAGACAATATTATTGATCGC
	B3	CTTTCACAGGCTGCACTT
	FIP	ACAGCACCGCCACCTATAGTAGAAGCTTTTTTAAACTAGG GC
	BIP	AGGCAGCAGAACTTACGCATTGAGTTTGAAAAAACATTCT ACCTCT
	LF	CTAGCTGCTACTACAGAACCAC
	LB	CATCAAGCTTCACAAGGAAA
E. coli O157:H7 eaeA	F3	AGCTCTAACAATGTACAGCT
	B3	AGTTGCAGTTCCTGAAACA
	FIP	GTCTTATCCGCCGTAAAGTCCGCCGTTCTGTCGAATGGTC
	BIP	CTAAAGCGGATAACGCCGATACCCAGGGACATTAGCCTGA G
	LF	CCCAACCTGGTCGACAACTT
	LB	ATTACTTATACCGCGACGGTGAA
E. coli O157:H7 stx2	F3	GAGATATCGACCCCTCTTG
	B3	AATCTGAAAAACGGTAGAAAGT
	FIP	TCCACAGCAAAATAACTGCCCAACATATATCTCAGGGGAC CA
	BIP	GATGTCTATCAGGCGCGTTTTGCCGTATTAACGAACCCGG
	LF	TGTGGTTAATAACAGACACCGATG
	LB	ACCATCTTCGTCTGATTATTGAGC
V. cholerae ctxA	F3	TCGGGCAGATTCTAGACC
	B3	GTGGGCACTTCTCAAACT
	FIP	TTGAGTACCTCGGTCAAAGTACTTCCTGATGAAATAAAGC AGTCA
	BIP	TCAACCTTTATGATCATGCAAGAGGGGAAACATATCCATC ATCGTG

Table A1.1
(cont'd)

	LF	CCTCTTGGCATAAGACCACC
	LB	AACTCAGACGGGATTTGTTAGG
V. cholerae toxR	F3	CGAGTGGAAACGGTTGAAGA
	B3	AGGGGAAGTAAGACCGCTAT
	FIP	GCACACTGCTTGAYTCTGCGTACGAAAGCGAAGCTGCTCAT
	BIP	AGCCACTGTAGTGAACACACCGTCGATTCCCCAAGTTTGGAG
	LF	ACAGATTCTGGCTGAGAGATGTC
	LB	CAGCCAGCCAATGTTGTGAC
L. pneumophila dotA	F3	GTCAAGCAACCTGATCT
	B3	TGCCGCAATCAAAATCCT
	FIP	CCA TCATGGAATTGTTGACAAATCCTAATCCTCAACGACAGTCTG
	BIP	GCCAGGTCAACCAGGAATAAAACGCTTCATATAATAAAG CGACGT
	LF	GAGGACAATGGCCCACTCA
	LB	CGTTGACCTTTGCCAATCTGA
L. pneumophila lepB	F3	TCTTTACGTTGATGAACTAGC
	B3	AAGTTGAAAGTATTAGGGTCTAC
	FIP	AGAGCAAACAGATTAGGGGTGCCATCACGTGTGAAGCCAA
	BIP	ATAGCGGTGGTGAAGCGATTGTAAATAGGCGGCGCAAT
	LF	TGTCTATTCTTTCTTTTGCCCAGAC
	LB	CACGGACATGCCTTTGTTCC
E. coli uidA	F3	CKGTAGAAACCCCAACCCG
	B3	AWACGCAGCACGATACGC
	FIP	TAACGCGCTTTCCCACCAACGGCCTGTGGGCATTCAGTC
	BIP	TAACGATCAGTTCGCCGATGCACTGCCCAACCTTTCGGTAT
	LF	TCCACAGTTTTCGCGATCCA
	LB	ACGTCTGGTATCAGCGCGAAGT
E. coli gadA	F3	GCTGTTCTGCTGGGCAATA

Table A1.1
(cont'd)

	B3	CGGGATACACCCTGTACGA
	FIP	GTCGCGGCTTCGAAATGGACTTTTCGGGTGATCGCTGAGA
	BIP	GCATCACCACGATGTCGGTGGTCTCTGAACGTCTGCGTCT
	LF	AGACTACAAAGCCTCCCTGAAATA
	LB	CTTCACCGCCGAGAGTGA
E. faecalis gelE	F3	GTTGATGAACAACATCCAGA
	B3	CATTCAACGCACCTGATTG
	FIP	CGTTTTTCCTGTTGGTGTACTTGTTTGCTTATGACAATGCTTTTTGG
	BIP	GCTTCCTCTTTAGATGTAGTTGGTCTAAATATTCTAAACCGGCAGT
	LF	CCATAACGCATTGCTTTTCCATC
	LB	CATGAAATGACACATGGTGTAACGG